2021

Cardiac Arrest and Global Ischemia Reperfusion Injury: Role of mitochondria and Cannabinoid Receptor 2 signaling.

Jennifer L. Bradley
Virginia Commonwealth University

www.manaraa.com

Cardiac Arrest and Global Ischemia Reperfusion Injury: Role of mitochondria and Cannabinoid Receptor 2 signaling.

A dissertation submitted in partial fulfillment of the requirements for the degree of Doctor of Philosophy at Virginia Commonwealth University

by

Jennifer Leigh Bradley
Master of Science, Virginia Commonwealth University, 2016
Bachelor of Art, Berea College, 2006

Director: Wanchun Tang, MD, MCCM, FAHA, FNAI
Affiliate Professor, Department of Microbiology and Immunology
Professor, Emergency Medicine

Virginia Commonwealth University
Richmond, VA
February, 2021

Acknowledgement

The author wishes to thank several people. I thank Dr. Gail Christie for accepting me to the MBG program for my MS and PhD. She was always available to guide and listen and for that I am truly thankful. I greatly appreciate Dr. Michael McVoy's mentorship throughout my PhD. He has been invaluable as a mentor for this process and next steps. I would like to thank my advisor, Dr. Wanchun Tang, and the Deputy Directors of the Weil Institute, Dr. Joseph Ornato and Dr. Mary Ann Peberdy, for allowing me to work on my PhD part-time while working as a Research Manager. I am grateful for their guidance and knowledge. I would also like to thank the members of my graduate committee: Dr. Martin Mangino, Dr. Xianjun Fang, Dr. Huiping Zhou and Dr. Gea-Ny Tseng for their time and guidance. Dr. Martin Mangino was always available to answer my questions, to provide a platform for scientific discussion and was instrumental with allowing Jad Khoraki to help me with VF induction for my *in vivo* studies. Dr. Huiping Zhou and her student, Yanyan Wang, taught me cell culture technique for RAW 264.7 macrophage cells and provided me with a crash course in Prism. Dr. Gea-Ny Tseng and her laboratory members collaborated with the Weil Institute and prepared heart whole tissue lysates for proteomic analysis completed by Poochon Scientific LLC. I am also thankful for our Co-Corresponding author, Dr. Edward Lesnefsky, for providing his laboratory and Jeremy's time to teach Xianfei Ji and me how to isolate mitochondria, for guiding me through manuscript preparation and review and for completing the ETC assay with the help of his technician Rabiya Shabman. My peers throughout this process have been invaluable in sharing their knowledge, time and technique. I would especially like to thank Apparao Kummarapurugu, Shuo Zheng, Jeremy Thompson, Ria Fyffe-Friel and Jad Khoraki. Karen Lo, a summer medical student volunteer, graciously created the potential role of WIN55 in S100A8/A9 mediated inflammation in IR injury figure. Lastly, I would like to thank my family for enduring all that accompanies a graduate education. My husband and daughter provided encouragement, support and understanding throughout. Many people have supported me during my journey and I am indebted for everyone's time and support.

Dedicated to family members that have passed on due to heart disease.

Table of Contents

Chapter

iii

List of Tables **Page**

viii

x

List of Abbreviations

µg	microgram
µL	microliter
µm	micrometer
µM	micromolar
2-AG	2-arachidonoylglycerol
AC	adenylate cyclase
ACA	asphyxial cardiac arrest
ADP	adenosine diphosphate
AEA	Arachidonoyl ethanolamide or anamide
ATP	adenosine triphosphate
ANOVA	analysis of variance
BBB	blood brain barrier
BM	brain mitochondria
Breg	B regulatory
BSA	bovine serum albumin
CA	cardiac arrest
CB_1	cannabinoid receptor 1
CB_2	cannabinoid receptor 2
CBF	cerebral blood flow
CO	cardiac output
COX	cyclooxygenase
COMICA	characterization of mitochondrial injury after cardiac arrest
CPP	coronary perfusion pressure
CPR	cardiopulmonary resuscitation
CRC	calcium retention capacity
CypD	cycophilin D
DAMPs	damage-associated molecular patterns
DMEM	Dulbecco's modified eagle medium
DNA	deoxyribonucleic acid
EF	ejection fraction
eCB	endocannabinoid
ECG	electrocardiogram
ECS	endocannabinoid system
ETC	electron transport chain
$ETCO_2$	end-tidal carbon dioxide
ELISA	enzyme-linked immunosorbent assay
FiO2	fraction of inspired oxygen
HR	heart rate

xi

Hz	hertz
ICU	intensive care unit
IFM	interfibrillar mitochondria
Ig	immunoglobulin
IHCA	in-hospital cardiac arrest
IL1β	interleukin 1β
IL6	interleukin 6
IL10	interleukin 10
IRAKs	IL1R-associated kinases
IR	ischemia reperfusion
kDa	kilodalton
LPS	lipopolysaccharide
LC/MS-MS	liquid chromatography tandem mass spectrometry
LDL	low-density lipoprotein
MAP	mitogen-activated protein
MAP	mean aortic pressure
MAPK	mitogen-activated protein kinase
MB	methylene blue
MCAO	middle cerebral artery occlusion
mA	milliamp
mL	milliliter
min	minute
MPI	myocardial performance index
MPTP	mitochondrial permeability transition pore
NaCl	sodium chloride
NADH	nicotinamide adenine dinucleotide
NADPH	nicotinamide adenine dinucleotide phosphate
NFƘB	nuclear factor ƘB
NFR	NADH-ferricyanide reductase
ng	nanogram
NLRP3	NLR family pyrin domain containing 3
NO	nitric oxide
O_2^-	superoxide
OHCA	out-of-hospital cardiac arrest
OXPHOS	oxidative phosphorylation
PAGE	polyacrylamide gel electrophoresis
PBS	phosphate buffered saline
pg	picogram
post-CA	post-cardiac arrest
PCAS	post-cardiac arrest syndrome
ROS	reactive oxygen species

RAGE	receptor for advanced glycation end products
ROSC	return of spontaneous circulation
RNA	ribonucleic acid
rpm	revolutions per minute
rRNA	ribosomal ribonucleic acid
SCA	sudden cardiac arrest
SCD	sudden cardiac death
SD	standard deviation
SDS	sodium dodecyl sulfate
SSM	subsarcolemmal mitochondria
TTM	targeted temperature management
Tregs	regulatory T cells
TLR	toll-like receptor
TMB	3,3',5,5'-Tetramethylbenzidine
TMPD	N,N,N',N' tetramethyl p-phenylenediamine
TNFα	tumor necrosis factor α
TRAF6	TNFR-associated factor 6
VF	ventricular fibrillation
VFCA	ventricular fibrillation cardiac arrest
WIN55	WIN55, 212-2

Abstract

Cardiac Arrest and Global Ischemia Reperfusion Injury: Role of mitochondria and Cannabinoid Receptor 2 signaling.

By Jennifer Leigh Bradley

A dissertation submitted in partial fulfillment of the requirements for the degree of Doctor of Philosophy at Virginia Commonwealth University

Virginia Commonwealth University, 2021

Director: Wanchun Tang, MD, MCCM, FAHA, FNAI
Affiliate Professor, Department of Microbiology and Immunology
Professor, Emergency Medicine

Sudden cardiac arrest is a major public health challenge in the United States with very poor outcomes. Current advanced cardiac life support therapies with cardiopulmonary resuscitation, defibrillation, and medications save less than 5% of victims despite substantial evidence that many of these lives could be saved with improved resuscitation protocols including the expanded use of hypothermia. Clinically, no effective treatment other than targeted temperature management is utilized. We have previously demonstrated that WIN55, 212-2 (WIN55), a non-selective cannabinoid CB_1/CB_2 receptor agonist, induced hypothermia when administered immediately following resuscitation with significantly improved post-resuscitation myocardial and cerebral function and duration of survival. We further demonstrated that the hypothermia effect of WIN55 is mediated through CB_1 receptors.

However, the results of our previous studies indicated that the beneficial effect of WIN55 on myocardial and cerebral function and duration of survival may not be solely due to its

hypothermic effect. The overall objective of this study is to determine if cardiac arrest causes mitochondrial dysfunction and increased plasma concentrations of TNFα, IL6 and IL10. Intramuscular Administration of SR141716A (CB_1 antagonist) before ventricular fibrillation + cardiopulmonary resuscitation followed by infusion of WIN55 5 min after return of spontaneous circulation will prohibit the release of inflammatory mediators caused by cardiac arrest via the CB_2 receptor.

We explored the effects of cardiac arrest on mitochondria populations and heart whole tissue lysate proteomics utilizing the Weil Institute's *in vivo* rat model of cardiac arrest and cardiopulmonary resuscitation. We have discovered that brain mitochondria are more sensitive to global ischemia compared to heart mitochondria. Additionally, complex I is the most sensitive electron transport chain complex to ischemic injury and is a major control point of the rate of oxidative phosphorylation following cardiac arrest and cardiopulmonary resuscitation. Preservation of brain mitochondrial activity and function during cardiac arrest may enhance outcomes and recovery.

A recent article focusing on acute myocardial infarction was able to link S100A8 and S100A9 gene upregulation during ischemia and reperfusion and revealed this caused mitochondrial dysfunction in cardiomyocytes. S100A8 and S100A9 protein expression levels were upregulated in rat LV Apex epicardium whole tissue lysate from animals that experienced global ischemia reperfusion injury via cardiac arrest and cardiopulmonary resuscitation. Further studies are necessary to confirm S100A8 and S100A9 proteins increase expression in brain and heart tissue samples after cardiac arrest and cardiopulmonary resuscitation.

Testing WIN55 as a possible pharmacologic tool, *in vitro* results indicated that WIN55 was anti-inflammatory. Therefore, we moved to *in vivo* studies with intramuscular administration

of SR141716A (CB$_1$ antagonist) before ventricular fibrillation + cardiopulmonary resuscitation followed by infusion of WIN55 5 min after return of spontaneous circulation. After treatment, plasma concentrations of TNFα, IL6 and IL10 were decreased at return of spontaneous circulation 4hrs. One possible mechanism to drive down proinflammatory cytokine release is binding CB$_2$. WIN55 could be a novel pharmacologic tool against cardiac arrest as it can induce hypothermia and it has ant-inflammatory effects. Further studies are needed to determine mechanism of action for anti-inflammatory effects as peroxisome proliferator-activated receptors are also cannabinoid targets.

CHAPTER 1: Introduction and Literature Review

I.   **Cardiac Arrest**
      A. **Epidemiology and Disease Spectrum**

Cardiac arrest (CA) is a major public health problem with substantial morbidity and mortality. It is the cessation of cardiac mechanical activity, as confirmed by the absence of signs of circulation (1). CA is characterized by severe and generalized ischemia that persists during the resuscitation efforts and reverses only after restoration of spontaneous circulation (ROSC) (2). An operational definition of sudden cardiac arrest (SCA) is unexpected CA that results in attempts to restore circulation (1). If resuscitation attempts are unsuccessful, this situation is referred to as sudden cardiac death (SCD). In the United States, any-mention sudden cardiac death (SCD) mortality in 2017 was 379, 133 (1). Over the past 5 decades, the strategy of cardiopulmonary resuscitation (CPR) has been focused on early defibrillation, better and more effective chest compression, and more recently, post-resuscitation management including therapeutic hypothermia. However, the current outcomes of CPR are disappointing, which yield a functional survival rate of only 8.2% (1). Circulatory failure and myocardial dysfunction resulting from CA largely contribute to morbidity and mortality after initially successful CPR (3). Out-of-hospital cardiac arrest (OHCA) is a significant cause of death and disability in adults with 356,461 reported "EMS-worked" cases per year in the United States (1).

      B. **Ischemia Reperfusion Injury**

Ischemia is an imbalance between the oxygen demand of the tissue and the oxygen delivery that it receives. Oxygen delivery could be simple diffusion or the heart delivering oxygen conductively (oxygen through blood flow). Whenever oxygen delivery does not match demand, technically it is ischemia. Ischemia is a condition where energy expenditure outpaces energy production. For aerobic cells ischemia is a critical change in the oxygen demand to delivery ratio (4). Ischemia Reperfusion (IR) injury is a complex process, which involves several

17

interrelated factors, including a decrease in cellular adenosine triphosphate (ATP) levels, accumulation of hydrogen ions, calcium overload, and production of reactive oxygen species (ROS) (5). Cerebral and myocardial tissue suffers from IR injury even after successful CPR (6, 7). The destructive effects of IR arise from the acute generation of ROS subsequent to reoxygenation, which inflicts direct tissue damage and initiates a chain of deleterious cellular responses leading to inflammation, cell death, and eventually organ failure (8). The cessation (ischemia) and restoration (reperfusion) of cerebral blood flow (CBF) after CA induce inflammatory processes that can result in additional brain injury (9). Post-cardiac arrest (post-CA) ischemia induces neurodegeneration, cerebral edema and impaired cerebrovascular autoregulation within the brain (10). This phenomenon is reflected in 2004 epidemiological data that shows brain injury as the leading cause of death post-CA, accounting for 68% and 23% of OHCA and in-hospital cardiac arrest (IHCA) deaths (10).

Post-arrest myocardial dysfunction includes the development of low cardiac output (CO) or ventricular systolic or diastolic dysfunction (7). The pathophysiology involves cardiovascular IR injury and cardiovascular toxicity from excessive levels of inflammatory cytokine activation, among other contributing factors (7). There is an almost instant inflammatory response where interleukins are produced by affected tissues and the endothelial cells of the local capillary vasculature (11). Chemical signaling results in white blood cells being attracted to affected areas and attaching themselves to the endothelial lining of the capillaries, resulting in capillary blockage and further ischemia (11). It is recognized that cells can be programmed to die by cellular signaling mechanisms via the processes of apoptosis and autophagy.

C. Mitochondrial Dysfunction

Neurologic and myocardial dysfunction after successful resuscitation is prominent and mitochondrial dysfunction is a key determinant of poor outcomes (9, 12-16). Neurons and

18

cardiomyocytes, two high energy-consuming organs, are enriched with mitochondria and are highly sensitive to IR injury (17). The central nervous system receives almost a third of the CO (9). Morbidity and mortality after initially successful CPR can be attributed to immediate and delayed effects of reperfusion in the central nervous and cardiovascular systems (18). The principal role of mitochondria is to generate cellular energy (ATP) by the mitochondrial electron transport chain (ETC) through oxidative phosphorylation (OXPHOS). An adequate amount of energy by mitochondria is crucial for neuronal excitability and survival. In addition, mitochondria are critically involved in the regulation of cell death via apoptosis, autophagy and necroptosis (14, 19).

Mitochondrial dysfunction is one hallmark of IR injury, which induces neuronal death (9, 20). During the ischemic phase, OXPHOS is inhibited by lacking oxygen, causing low levels of adenosine triphosphate (ATP) and cellular acidification secondary to the diverging of glycolytic pyruvate to lactate (21). Upon reperfusion, the rapid re-establishment of OXPHOS induces several mitochondrial events such as ROS generation, H+ leaking, mitochondrial Ca^{2+} overload and the release of cell-death inducing protein cytochrome *c* (21).

Ultrastructural and functional injury occurs early in and progresses during ischemia (22). Mitochondrial morphological dynamics are relevant to IR injury (23, 24). Under physiological conditions, the removal of damaged or dysfunctional mitochondria is mediated by mitophagy, a mitochondrial-selective subtype of autophagy that involves sequestration and subsequent fusion of mitochondrial contents with lysosomes containing degradative enzymes (25, 26). This process allows maintenance of mitochondrial homeostasis; however, in the context of major cellular stress like that of IR or heart failure, mitochondrial DNA leak out from damaged and necrotic cardiomyocytes into the cytoplasm and extracellular space (26, 27). Mitochondrial DNA serves

as the damage-associated molecular patterns (DAMPs) that can activate several pro-inflammatory pathways, such as toll-like receptor (TLR) on immune cells such as circulating neutrophils and macrophages, leading to the formation of inflammatory cytokines TNFα and IL6 (Figure *1*) (28-30). Mitochondrial DNA has also been shown to activate inflammasome complexes, which are responsible for recruiting active caspase-1 and converting pro-IL1β and proIL18 into their bioactive forms IL1β and IL18 (25, 31). Mitochondrial damage from cardiovascular events like IR thus appear to have major downstream effects on the development of inflammation, which may, in turn, influence the severity of the ischemic insult.
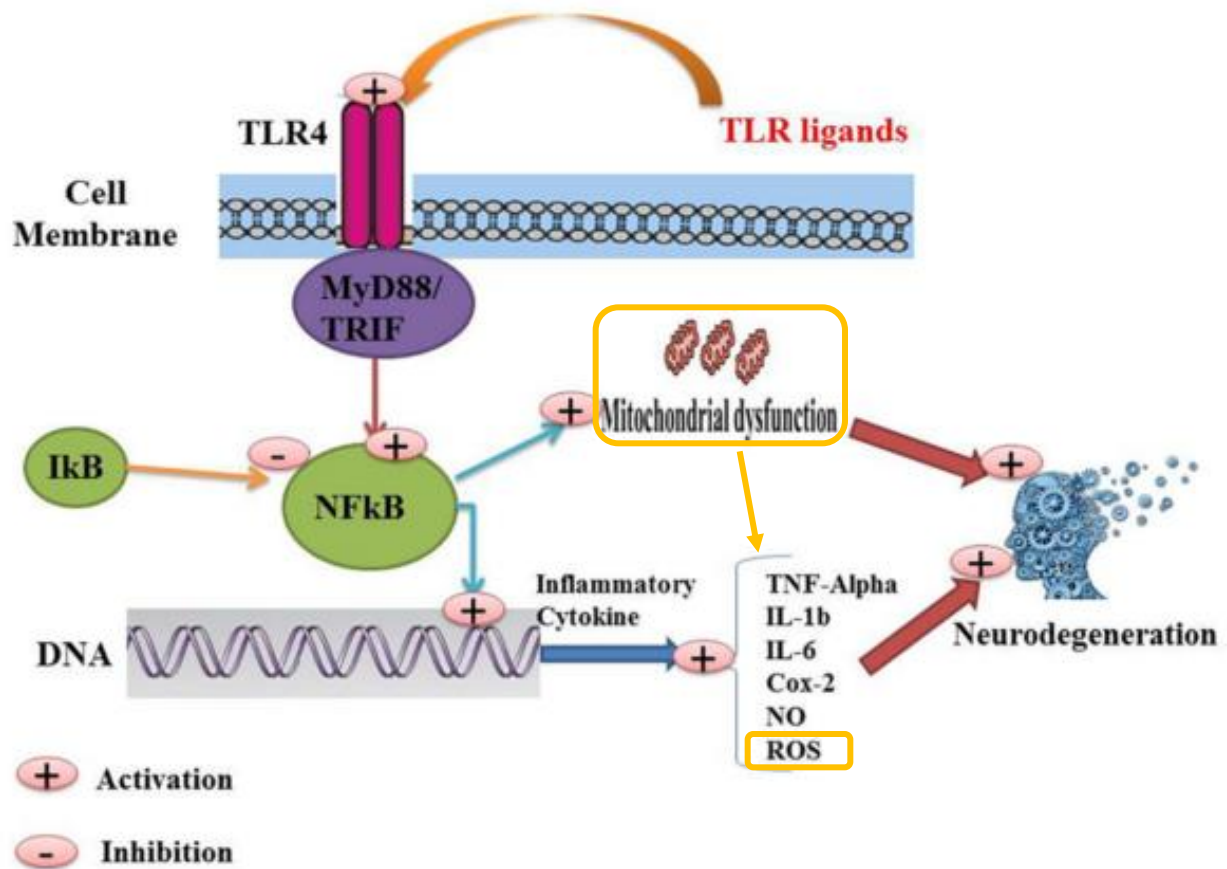
Figure 1. Role of TLR in production of inflammatory mediators. Adapted from (29).

An experiment with a mitochondrial protective agent (SS31) demonstrates improved

cardiac contractility and ejection fraction (EF) with lower levels of inflammatory cytokines

TNFα and IL1β (32). Translational studies have yielded similar results. Levels of circulating

cell-free mitochondrial DNA were found to be a more accurate prognostic marker in CA patients

(33). Additionally, in the COMICA study, higher serum levels of mitochondrial injury marker,

cytochrome c, were seen in post-CA patients compared to controls. Even higher levels were seen

in non-survivors versus survivors (34). Neurological outcomes in post-CA have not been as

extensively studied. However, anti-inflammatory studies in a rat model of cerebral IR yielded

comparable results with reduced cerebral infarct sizes, improved neurobehavioral scores and

21

lower levels of oxidative stress following treatment (35). Based on these findings, further research into agents that can attenuate the pro-inflammatory pathway in mitochondrial dysfunction could prove to be crucial in improving functional and mortality outcomes associated with IR.

Recognition of potential mitochondrial-driven pathology in IR has led to growing interest in investigating the relationship between mitochondrial injury and functional outcomes following SCA and IR. An imbalance in mitochondrial dynamics contributes to brain injury after cardiac arrest. Thus, targeting mitochondria is a promising neuroprotective strategy (36). Activation of the mitochondrial permeability transition represents a major mechanism of IR injury. A CB_2 receptor agonist (JWH133) protected mitochondria against IR injury and reduced apoptosis through inhibition of apoptotic protein released from the mitochondrial permeability transition pore (MPTP) (37). Administration of the cannabinoid agonist WIN 55,212-2 after hypoxia ischemia in fetal lambs reduces brain injury, diminishing both apoptosis and mitochondrial dysfunction (38).

D. Post Cardiac Arrest Syndrome

Whole-body ischemia and reperfusion due to CA and subsequent ROSC constitute post-CA syndrome (PCAS) (39). PCAS is a combination of post-cardiac brain injury, circulatory dysfunction, systemic IR response and persistent precipitating pathology proposed by Nolan et al. in 2008 (40-42). Binks et al. state PCAS can be divided into four phases 1) immediate post-arrest (occurs in the first 20 minutes following ROSC 2) early post-arrest (occurs between 20 minutes and 6 to 12 hours after ROSC) 3) intermediate (between 6 to 12 hours and 72 hours) 4) recovery (extends from 3 days and beyond) (43). Management of PCAS patients includes complex and multidisciplinary interventions. Early and intensive management should be focused on hemodynamic stability and neurologic recovery (42).

22

PCAS is most notably characterized by profound IR injury. Due to CA being an extreme of shock states, oxygen delivery is dramatically reduced during an arrest event, leading to profound tissue hypoxia (44). Depending on the cause of the arrest and severity of PCAS, many patients will require multiple organ support (45). Treatment received during this post-resuscitation period influences the overall outcome significantly, particularly quality of neurological recovery (45). Although CA impacts all organ systems, its impact is most profound on the neurological system as brain tissue is exquisitely sensitive to lack of oxygen (46). Post-CA anoxic brain injury is a major cause of morbidity and mortality, and is responsible for two thirds of intensive care unit (ICU) deaths in the post-CA period (47). Post–CA myocardial dysfunction also contributes to a low survival rate after in- and out-of-hospital CA. However, preclinical and clinical evidence indicates that this phenomenon is both responsive to therapy and potentially reversible (10).

Successful resuscitation from CA is usually characterized by the development of an IR syndrome of the body that may enhance cerebral and cardiac damage (41). The main determinant of this syndrome is a generalized activation of inflammatory reactions resulting in symptoms similar in many aspects to those of sepsis (48). Inflammatory responses play pivotal roles in the pathophysiology of cerebral and cardiac damage after CA/CPR (48-51). Systemic inflammation promotes disorders in the macro-circulation and micro-circulation and increases vascular permeability promoting protein extravasation and edema formation in the tissues, due to metabolic imbalance, leucocyte activation, endothelial toxicity and impairment of mitochondrial respiratory chain activity (40, 52).

Management of the post–CA patient is complex, and addresses multiple key issues simultaneously: diagnosing and treating the etiology, minimizing hypoxic brain injury, addressing sequelae of global IR injury, and managing cardiovascular dysfunction (53). Global

23

cerebral ischemia induced by CA and followed by reperfusion triggers a multitude of processes that ultimately result in neuroinflammatory responses with activation of glial cells, release of proinflammatory cytokines, and delayed neuronal death (54). Levels of TNFα and IL6 were shown to be strongly associated with the severity of PCAS, mortality rate, and neurologic outcomes (54). The severity of this syndrome will vary with the duration and cause of CA (45).

II.   Role of Inflammatory Mediators in Cardiac Arrest
A. Pro-inflammatory mediators (Tumor Necrosis Factor α and interleukin 6)

Inflammatory responses play a pivotal role in the pathophysiology of brain and heart damage after CA/CPR, which leads to neuronal death, myocardial dysfunction, and apoptosis (55-57). Systemic and central nervous system (CNS) levels of various cytokines including tumor necrosis factor (TNF)α, interleukin (IL)1, IL6, IL8, IL10, and others are increased after CA (50, 51). One definitive mechanism of cerebral IR injury is inflammation. It is characterized by the activation of glial cells, influx of peripheral immune and inflammatory cells, high concentrations of ROS and release of pro-inflammatory mediators, including cytokines and adhesion molecules (58). The most studied cellular sources of ROS within the heart include cardiomyocytes, endothelial cells, and neutrophils (59). One function of cytokines is to change the physiological state of cells and the way they respond to environmental stimuli (60). TNFα induces inflammation, activates vascular endothelium, orchestrates the tissue recruitment of immune cells and promotes tissue destruction (60). Inflammation is a protective response of the host to infections and tissue damage, characterized by a series of reactions, including vasodilation and recruitment of immune cells and plasma proteins to the site of infection or tissue injury (61).

Normally, inflammation is beneficial to the host and can be resolved in a timely manner; however, deregulated inflammatory responses can cause excessive or long-lasting tissue damage, contributing to the development of acute or chronic inflammatory diseases (61). Increased

24

release of DAMP molecules and cellular dysfunction in activated microglia and astrocytes contribute to ischemia-induced cytotoxic and pro-inflammatory cytokine generation, and ultimately to delayed death of neurons (58). TNFα has been shown to play an important role in the pathogenesis of neurological diseases (62). It has been demonstrated that the brain and innate immune system are engaged in bidirectional cross-talk. The cerebral inflammatory cascade comprises an increase of neutrophil recruitment and peripheral macrophage infiltration, activation and migration of microglia, also known as brain macrophages and release of pro-inflammatory stimuli within the brain. When an ischemic event occurs, the normally immune-privileged brain environment collapses, DAMP molecules released by cellular injury can be recognized as invader to induce the activation of toll like receptors and triggers the activation process of nuclear factor ƙB (NFƙB), which is linked to the transcription of numerous proinflammatory genes (58).

In the central nervous system, TNF is produced primarily by microglia and astrocytes in response to a wide range of pathological processes, including infection, inflammatory disease, ischemia and traumatic injury (63).This leads to neurologic damage. Cerebral injury is correlated to the abundant synthesis of inflammatory cytokines during CA and RES. In the brain, cytokines are not only produced by the cells of the immune system, but are also expressed in resident brain cells including neurons and glia. Neuroinflammation can continue for days and months, which contributes to neurological damage that ultimately determines the impaired recovery following CA/CPR (58). Increasing evidence reveals that suppressing the inflammatory process facilitates neuroprotection and has the potential for use in the clinical treatment of cerebral IR damage regarding CA (58).

25

Post-resuscitation myocardial dysfunction has been ascribed to post-ischemic stunning, the pathobiology of which has been well described in models of global and regional myocardial ischemia and reperfusion (64). Tumor necrosis factor (TNF) has been implicated in the pathogenesis of a number of cardiovascular diseases, including atherosclerosis, myocardial infarction, heart failure, myocarditis and cardiac allograft rejection, and vascular endothelial cell responses to TNF may underlie vascular pathology in many of these conditions (63). TNFα increases during the early post-resuscitation period and may play a role in post-resuscitation myocardial dysfunction (64). Niemann et al. show the time courses of LV systolic and diastolic dP/dt and TNFα are significantly negatively correlated. TNFα concentration is a statistically significant predictor of systolic dP/dt, with higher TNF concentrations being associated with decreased left ventricular systolic function (64). Hemodynamic effects of TNFα are characterized by decreased contractility, reduced EF, decreased systemic vascular resistance, hypotension, and biventricular dilation. TNFα is believed to exert its myocardial depressant effect by disrupting calcium homeostasis or calcium sensitivity and the normal myocardial contraction relaxation cycle (64).

Cardiotoxicity is primarily attributed to TNF-induced cardiomyocyte apoptosis (60).The inflammatory response after ROSC is characterized by polymorphonuclear leukocyte activation, adhesion molecule expression, reactive oxygen species (ROS) production from inducible nitric oxide synthase (iNOS), and release of cytokines such as TNFα and interleukin 6 (IL6) (7). IL6 represents a keystone cytokine in infection, cancer and inflammation, in which it drives disease progression or supports the maintenance of immunological reactions (65). An enormous repertoire of biological functions can be attributed to the cytokine IL6, establishing IL6 as a pleiotropic cytokine and a major player in health and disease (66). Soluble ambient IL6 is

26

available during massive inflammation (66). Baseline IL6 was a good predictor of in-hospital mortality and poor functional outcome. It was associated with mortality in multivariable analysis (51). IL6 has context-dependent pro- and anti-inflammatory properties and is regarded as a prominent target for clinical intervention (65).

Cytokine production is also altered by stress. Increased production of TNFα, IL6 and IL1β contributes to the acute-phase reaction and hypermetabolic response that accompanies overwhelming infection , hemorrhage, injury and surgery (64). These stress-activated cytokines all have the potential to produce cardiac decompensation when in sufficiently high concentrations (64). The effects of stress-activated cytokines extend beyond the myocardium.

B. S100A8 and S100A9

S100A8 and S100A9, also known as myeloid-related protein 8 (MRP8) and MRP14 respectively, are DAMPs that belong to the S100 family. Both are constitutively expressed in neutrophils, monocytes and dendritic cells. However, they can also be intensely upregulated upon the onset of trauma, infection, stress and other inflammatory processes (67-70). Under physiological conditions they can exist as homodimers, but under inflammatory states they preferentially form heterodimers with each other (S100A8/A9) because the heterodimeric structure confers increased resistance to the protease-rich environment of inflammation (71). Additionally, S100A8 and S100A9 contain a characteristic helix-loop-helix motif with charged amino acid residues, giving them a high affinity for divalent ions such as calcium (69).

Therefore, they are calcium-binding proteins that have been implicated as key modulators in the development of inflammation (67). Together, these features allow S100A8 and S100A9 to achieve functional diversity both intracellularly and extracellularly (69). They are able to exhibit both intracellular and extracellular effects on various cells of the innate immune system and have therefore become a point of interest for therapeutic intervention (*Figure 2*) (67, 70).

27
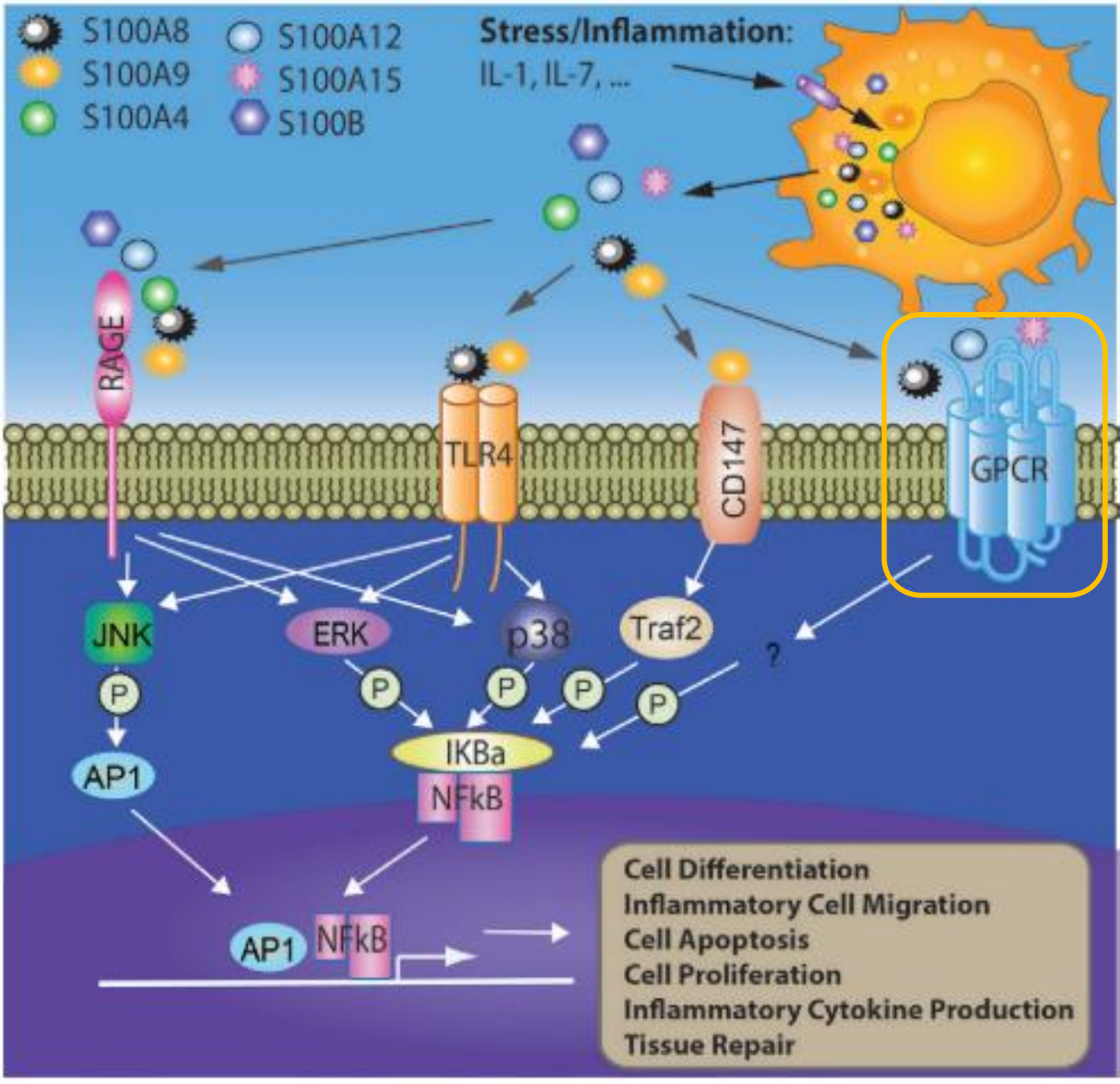
Figure 2. Involvement of S100 proteins in stress and inflammation. Adapted from (70)

Intracellular S100A8/A9 is best known for the ability to regulate trans endothelial migration of leukocytes (72). Transmigration is primarily achieved through extensive remodeling of the cytoskeletal structures which, in turn, is controlled by elevation of intracellular calcium levels and specific protein phosphorylation (72). As S100A8 and S100A9 are the major calcium-binding proteins expressed in neutrophils and monocytes, it has been demonstrated that calcium-

28

induced S100A8/A9 complexes promote microtubule polymerization via direct interaction with tubulin (72).

Extracellular S100A8 and S100A9 function primarily as DAMP molecules after being released from damaged or activated cells. The exact secretion mechanism remains unknown; however, it appears to require monocytic activation of both protein kinase C and the receptor for advanced glycation end products (RAGE) pathways (73, 74). Once released, S100A8/A9 exerts its effects through two different innate immune receptors: TLR4 and RAGE (67). Upon binding to TLR4 on phagocytes, S100A8/A9 triggers the MyD88-dependent pathway, where MyD88 recruits and activates IL1R-associated kinases (IRAKs) and TNFR-associated factor 6 (TRAF6). This, in turn, causes a downstream signaling cascade, ultimately leading to loss of inhibition of transcription factors NF-kB and AP-1. These factors can then translocate the nucleus and induce expression of pro-inflammatory cytokines such as TNFα, IL6 and IL8 (*Figure 3*) (69). Similarly, binding to RAGE results in subsequent activation of JNK and JAK-STAT signaling (75). Effects are under investigation but appear to inhibit anaerobic glycolysis in myocardium in the setting of ischemia (76). Overall, S100A8/A9 serves as a key modulator in the early stages of inflammation and can have a profound impact on long-term severity of inflammatory diseases.
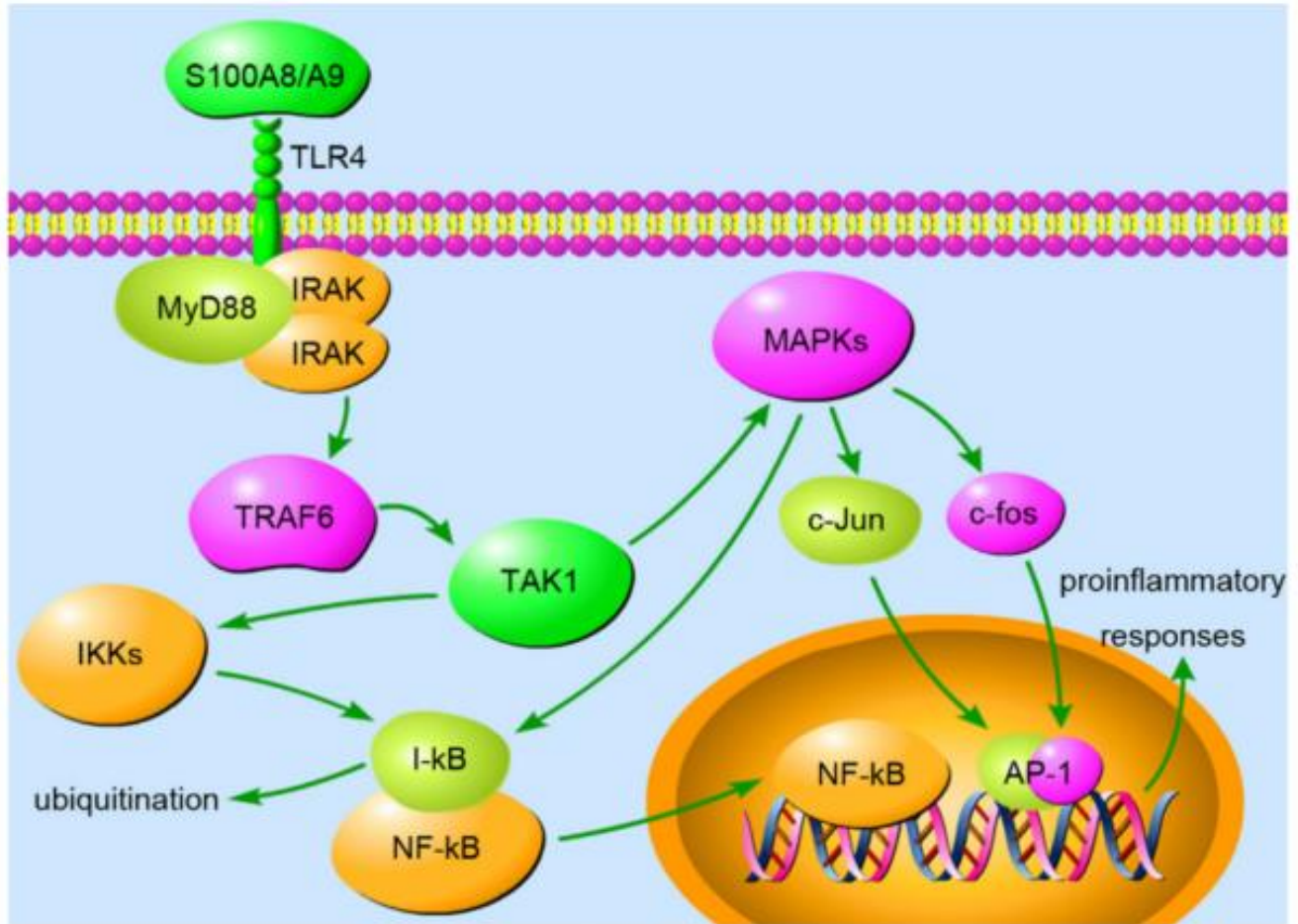
Figure 3. S100A8/A9 effects through TLR4 (77).

C. Anti-inflammatory mediators (interleukin 10)

Anti-inflammatory cytokines, such as IL10, have been shown to inhibit the LPS-induced

production of pro-inflammatory cytokines (78). IL10 is a secondary cytokine released by

leukocytes or endothelial cells following stimulation by IL1β and TNFα (51). IL6 might also

contribute to the regulation of inflammation by inducing IL10-producing B regulatory (Breg)

cells (66). Zhang et al show an elevated level of IL-10 attenuates LPS-induced activation of NF-

κB, JNK, ERK and p38MAPK, which results in reduced production of TNFα and IL6 (78).

Understanding the role of IL10 in the regulation of metabolic processes is essential both for

deciphering how IL10 acts to control inflammatory responses and for discovering key molecular

controlling processes involved in the resolution of inflammation (79). IL10 production was first

described in T_H2 cells where its expression accompanies that of the T_H2 type cytokines IL4, IL5 and IL13 (80).

In the absence of IL-10 signaling, macrophages accumulate damaged mitochondria in a mouse model of colitis and inflammatory bowel disease, which results in dysregulated activation of the NLRP3 inflammasome and production of IL-1β (79). The absence of IL10 leads to ROS production from accumulated mitochondria (79). Various cell types can express IL-10, which makes IL10 regulation challenging (80). IL10 might act to reverse the metabolic program associated with inflammatory response (79).

III. Cannabinoids
A. Endocannabinoid System (ECS)

The psychoactive properties of marijuana have been known for thousands of years, however, the biological basis of the effects of marijuana and its bioactive ingredients, collectively called cannabinoids, has unfolded in the last few decades (81, 82). Since 1998, the use of cannabis for medical purposes has become legal in 29 states (according to state, but not federal law) in the USA, and numerous countries have also opted to legalize marijuana for medicinal use (83). Cannabinoid compounds are being extensively studied for therapeutic potential. Although there is an abundance of information on the role of cannabinoids in the central and peripheral nervous systems, their role in the cardiovascular system is more complex (84). Cannabinoids and their synthetic and endogenous analogs are best known for prominent psychoactive properties, however, their cardiovascular effects were recognized as early as the 1960's (85). Cannabinoids are highly lipophilic molecules that have been shown to alter the functional activities of immune cells *in vitro* and *in vivo*. The term "exogenous cannabinoid" has been applied to cannabinoids that are extracted from the marijuana plant *cannabis sativa* or are

synthesized in the laboratory (86). WIN55,212-2 (WIN55) is an exogenous cannabinoid (*Figure 4*).
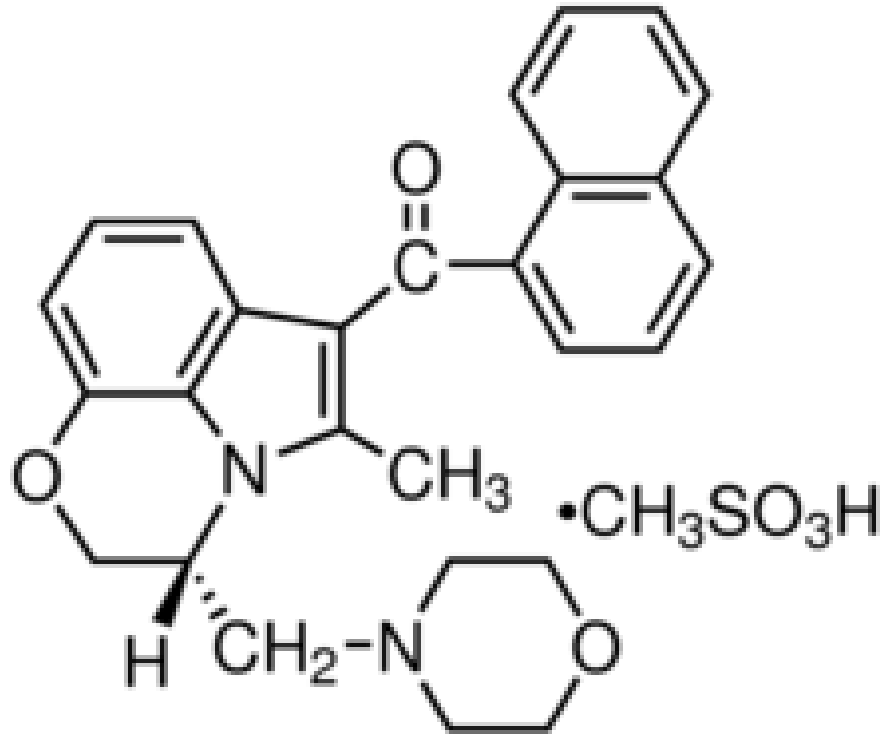
Figure 4. WIN55 is a full agonist for CB$_1$ and CB$_2$ (87)

Cannabinoids modulate inflammation through multiple pathways (88). They have been reported to have immunosuppressive activity and alter macrophage functions (89). It has been reported that, under pathological conditions, cannabinoids can avoid mitochondrial dysfunction, thus inhibiting apoptotic signaling (38) .Cannabinoids were shown *in vivo* and *in vitro*, to exert their immunosuppressive properties through 4 main pathways: induction of apoptosis, inhibition of cell proliferation, inhibition of cytokines, and chemokine production and induction of regulatory T cells (tregs) (90). Distinct phytocannabinoids may activate immune cells by receptor-mediated as well as by non-receptor mediated modes (91).Cannabidiol inhibits IL1, IL12, TNF-α and interferon-gamma cytokine release by peripheral blood mononuclear cells, and

32

enhances production of the Th2-associated cytokines, IL4 and IL10 (90). The ECS, which comprises specific cannabinoid receptors, endogenous ligands (endocannabinoids), and synthetic and degradative pathways, is a new therapeutic target in a variety of disorders, such as inflammation and tissue injury, including the cardiovascular system (37).

B. Cannabinoid Receptors

Endocannabinoids (eCBs) act locally in a paracrine or autocrine manner by activating cannabinoid receptors (83). The endocannabinoid signaling system has emerged as an important target for therapeutic drug development, although the design of receptor-selective ligands has remained a challenge (92). Endocannabinoids may limit hepatic injury by modulating the expression of adhesion molecules and the infiltration and activation of inflammatory cells by CB_2 dependent mechanisms, which is consistent with the emerging role of CB_2 receptors in regulating microglial cell function and neuroinflammation (8). The discovery of cannabinoid receptors that mediate the action of THC and synthetic cannabinoids, precipitated the search for the endogenous ligands that bind these receptors. Arachidonoyl ethanolamide or anamide (AEA) and 2-arachidonoylglycerol (2-AG) represent the primary endogenous ligands that bind and activate CB_1 and CB_2 (91).

These cannabinoid receptors belong to the G-protein coupled receptor family and play a key role in downstream intracellular regulation of apoptosis and inflammation (82). Both receptors have seven transmembrane domains, are coupled to inhibitory G proteins, and are linked to signaling cascades that may involve adenylyl cyclase and cAMP, mitogen-activated protein (MAP) kinase, and the regulation of intracellular calcium (91). Cannabinoid receptors signal via $G_{i/o}$-protein-dependent pathways to inhibit adenylyl cyclase and modulate ion-channel function, but also activate mitogen-activated protein kinases (p44/42 MAPKs, p38, ERK, and JNK) or ceramide signaling, and can also engage G-protein-independent pathways via β-arrestins

(*Figure 5*) (83). Saroz et al. recently reported CB_2 activation induces simultaneous $G_{\alpha i}$ and $G_{\alpha s}$ (G protein-stimulating adenylate cyclase) coupling, which produces a delayed cAMP flux in human primary leukocytes (93, 94). The cannabinoid system with its receptors (CB_1 and CB_2), provides neuroprotection against cerebral and spinal cord ischemia-reperfusion (IR) injuries (95). During ischemic injury, endocannabinoids accumulate, cannabinoid receptors are up-regulated, and treatment with cannabinoid agonists (either endocannabinoids or phytocannabinoids/synthetic cannabinoids) protects neurons against damage resulting from ischemic stroke (96).
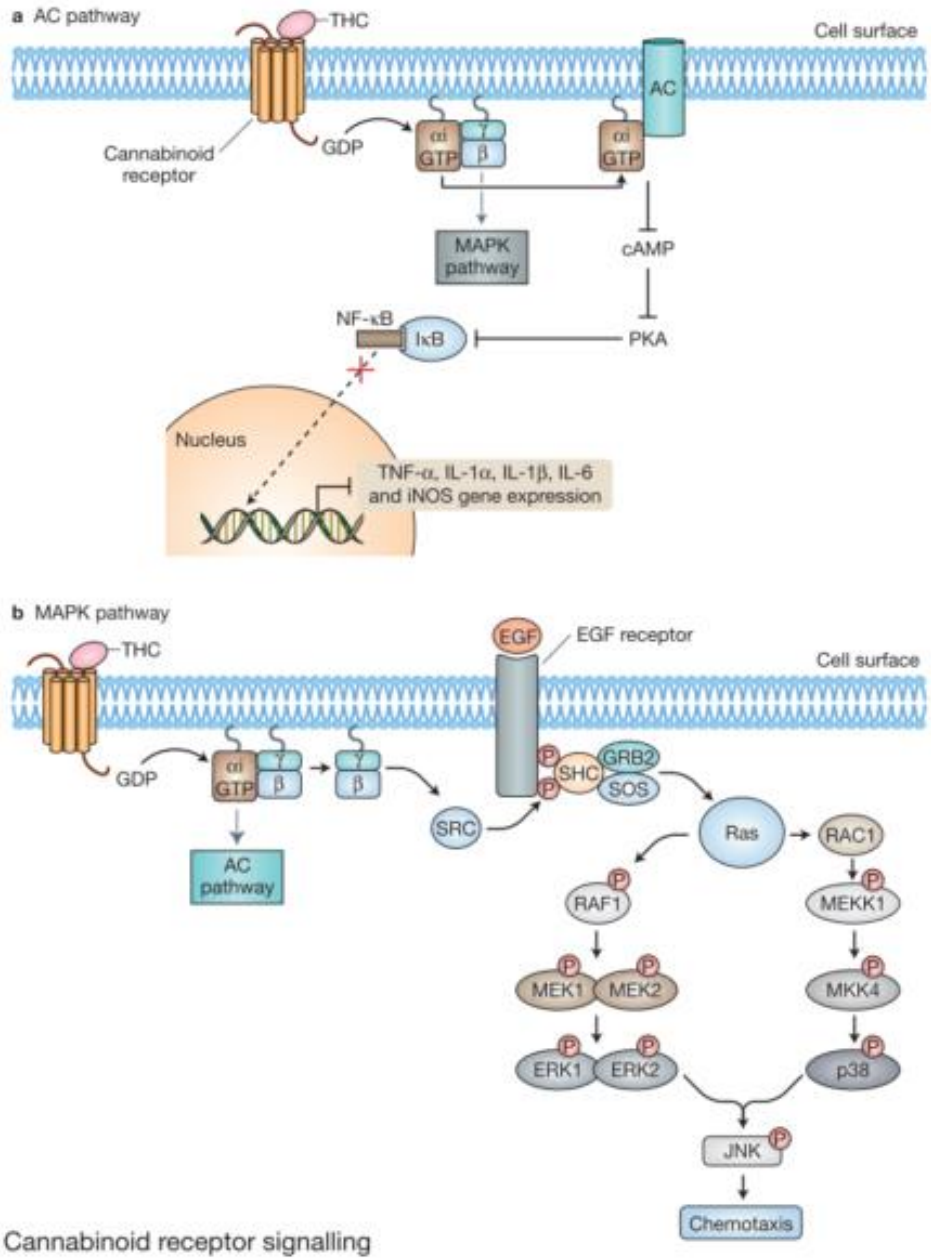
Figure 5. Cannabinoid receptor signaling (a) The adenylate cyclase (AC) pathway. $G_{\alpha i}$ signaling downregulates the pro-inflammatory immune response via adenylate cyclase. CB_2 couples predominantly to $G_{\alpha i/o}$, resulting in adenylyl cyclase inhibition (b) The mitogen-activated protein kinase (MAPK) pathway. CB_2 $_{\beta\gamma}$subunit mediated activation of the MAPKs extracellular regulated kinase (ERK1/2), p38 and janus-kinase (JNK)(86, 97). The CB_2 receptor is coupled with $G_{\alpha i/o}$ and $G_{\alpha q}$ (G protein-activating phospholipase C and G protein-increasing cytosolic Ca^{2+}) (94).

In the cardiovascular system, cannabinoid receptors are located in the myocardium,

vascular endothelial and smooth muscle cells, as well as circulating blood cells (83). Both CB_1

35

and CB_2 receptor signaling modulate remote ischemic preconditioning-induced cardio protection (98). Endocannabinoids overproduced during various forms of IR injury have been proposed to protect against myocardial IR injury and to contribute to the ischemic preconditioning effect of endotoxin, heat stress, or brief periods of ischemia, while these lipid mediators may also mediate the cardiovascular dysfunction in these pathologies (99).

In a whole animal model of myocardial IR injury induced by coronary occlusion/reocclusion in anesthetized mice, the protective role of CB_2 but not CB_1 receptor activation was determined (8). Cannabinoid receptor 2 could potentially mediate protection against the four phases after resuscitation (thought to occur depending on the degree and duration of organ ischemia): 1. first 24hours after the event-a microcirculatory dysfunction from the multifocal hypoxia leads to rapid release of toxic enzymes and free radicals into the cerebrospinal fluid and blood; 2. 1 to 3 days- cardiac function and systemic function improve, but intestinal permeability increases predisposing the patient to sepsis syndrome leading to multiple organ dysfunction syndrome; 3. Days after cardiac arrest-a serious infection may occur, and the patient declines rapidly, and; 4. The patient eventually dies (48). "Myocardial stunning" classically defined as temporary mechanical dysfunction persisting after episodes of ischemia and reperfusion with the absence of irreversible histological damage is also responsive to therapeutic initiatives, namely inotropic therapy or even antioxidants or calcium antagonists for implementing prevention strategies (100).

In addition to the cell-surface cannabinoid receptors, there is growing evidence that the intracellular peroxisome proliferator-activated receptors (PPARs) are cannabinoid targets (101). There are other non-CB_1/CB_2 receptors—such as GPR55, GPR119 and TRPV1 that are phylogenetically unrelated to the CB_1 or CB_2 receptors but have the ability to respond to

36

endocannabinoids (102). PPARγ is a nuclear hormone receptor that regulates gene expression as a ligand-activated transcription factor and, in the central nervous system, is expressed on oligodendrocytes and astrocytes as well as neurons in multiple brain areas (103). WIN55 has been reported to reduce inflammation in murine brain ECs through PPARγ, independent of CB_1 and CB_2. This mechanism needs further exploration (104) as nuclear transcription factors play an important role in the regulation of initiation and resolution of the inflammatory process (*Figure 6*) (105). Direct binding of PPARs and the indirect effect of these receptors stimulate production of antioxidant enzymes and inhibit NFkβ (105). Activated PPARγ with endogenous or synthetic ligands can not only directly combine with the p50/p65 dimer and form a new complex that downregulates the NFkβ signaling pathway but also upregulate the expression of IkBα and indirectly inhibit the transcriptional activity of NFkβ (106).
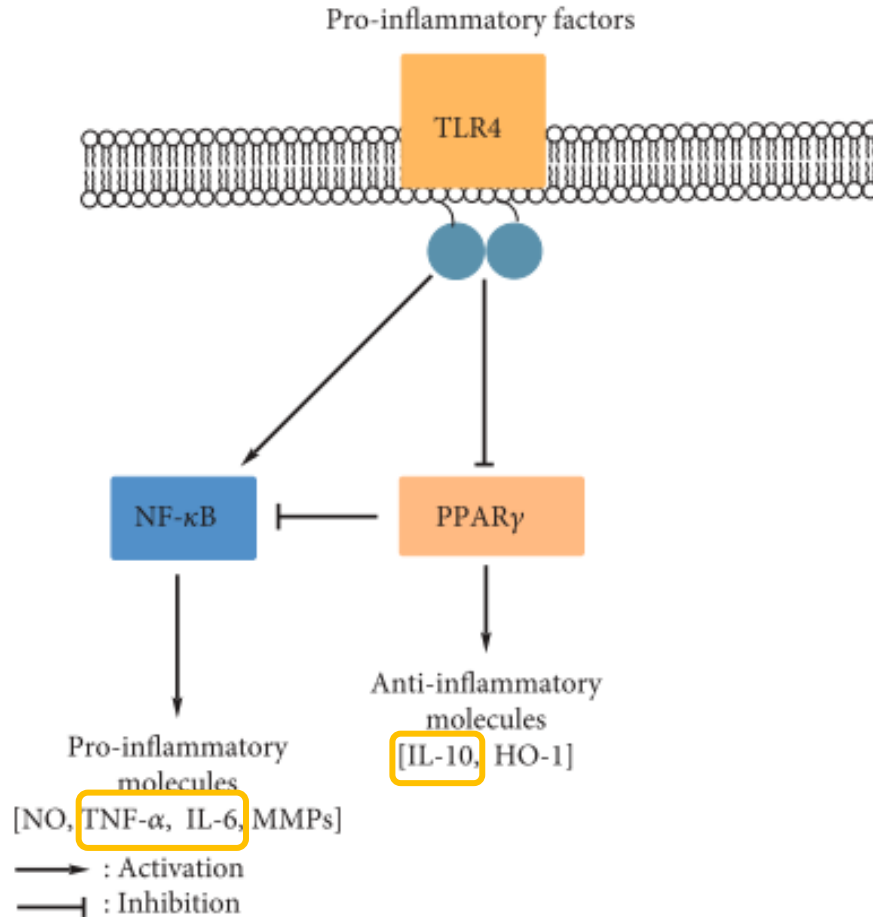
Figure 6. Cross-talk between PPARs and TLRs and NFkβ. Adapted from (105)

C. Anti-inflammatory properties of CB$_2$

The first record of medical application of the strong anti-inflammatory effect of cannabinoids comes from the world's oldest pharmacopoeia, which was found in China (82). Endocannabinoids mediate inflammation by regulating cytokines at different steps throughout the inflammatory response (88). CB$_2$ receptors are expressed mostly in the immune system, including the thymus, spleen, lymphatic nodes, and circulating leukocytes, where they mediate cytokine release (82). Levels of CB$_2$ expression varies among different immune cell populations, with B lymphocytes expressing the highest levels followed by macrophages, monocytes, natural killer (NK) cells, and polymorphonuclear cells, in that order (91). An important development has

been the identification of low levels of CB_2 receptor expression in tissues previously thought to be devoid of these receptors. These include specific regions of the brain (

Figure **7**), spinal cord and dorsal root ganglia, neurons in the myenteric and submucosal plexus of the enteric nervous system, in myocardium or cardiomyocytes (*Figure 8*), human vascular smooth muscle and endothelium, activated hepatic stellate cells, Kupffer cells, in reproductive organs/cells, colonic epithelial cells, bone, mouse and human exocrine and endocrine pancreas, and in various human tumors (107). An interesting biologic property of CB_2 receptors is their high inducibility, with CB_2 mRNA levels often increasing as much as 100-fold following nerve injury or during inflammation (108).
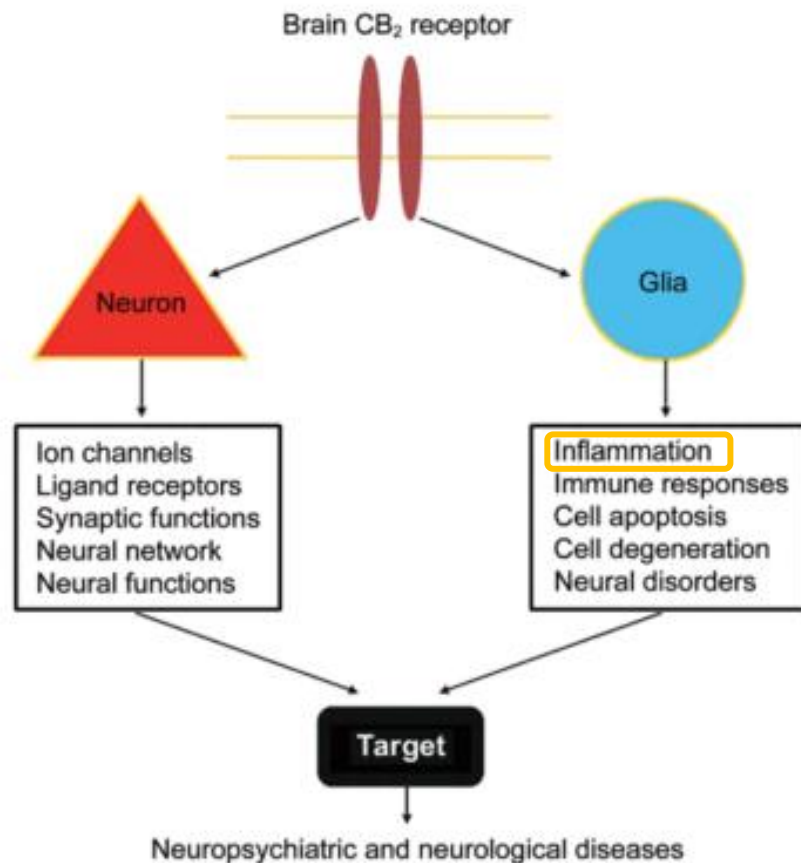
Figure 7. Brain CB_2 expression and function and association with neuropsychiatric and neurological diseases. Adapted from (109).

39
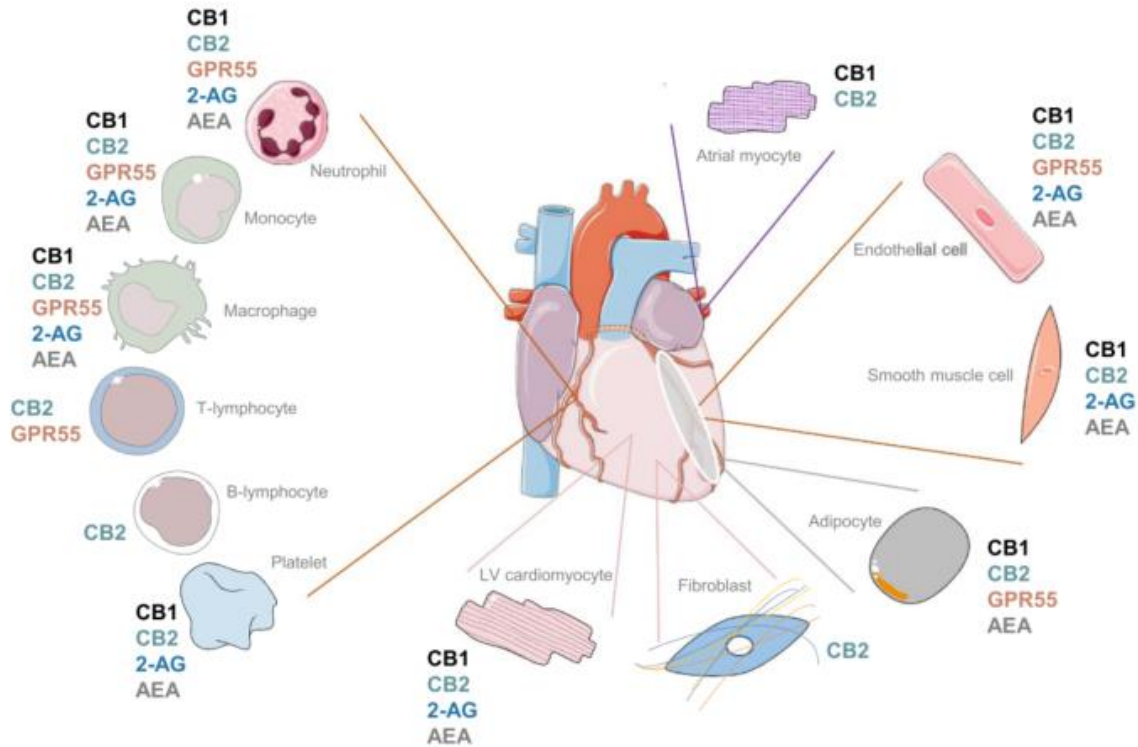
Figure 8. Mapping of cannabinoid-sensitive receptors and eCBs in the heart (97).

A large body of preclinical research demonstrates the effectiveness of cannabinoids in rodent models of acute and chronic inflammatory pain, as well as neuropathic pain (88). The inflammatory response to insult must be tightly regulated in order to minimize damage to healthy tissues. Thus, in addition to proinflammatory cytokines, active immune cells produce and release anti-inflammatory mediators, including IL10, which are regulated by the endocannabinoid system (88). Accumulating evidence supports the development of selective CB_2 receptor agonists for the management of acute tissue injury associated with inflammation (such as myocardial infarction, stroke, or organ transplantation) (83). Since CB_2 activation dampens inflammatory responses in the absence of psychotropic effects, it has the potential to serve as a molecular target for attenuating inflammation linked to pathogenic disorders (91). Consistent with the protective role of CB_2 receptor activation, CB2 $^{-/-}$ mice develop increased IR

40

induced tissue damage and proinflammatory phenotype (8). Selective activation of the CB_2 receptor a few minutes before reperfusion markedly improves myocardial infarction (110).

Mechanistic investigations reveal that the protective effect of CB_2 receptor may ascribe to reduction of cardiac leukocyte recruitment, reduction of superoxide generation, or increase of ERK1/2 and STAT-3 phosphorylation (37). CB_2 signaling in the heart and vasculature may activate cardioprotective mechanisms and limit inflammation (*Figure 9*) (107). Evidence from *in vitro* and *in vivo* models suggests that CB_2 activation might reduce atherosclerotic inflammation (110). CB_2 receptor stimulation limits hepatic injury by decreasing the expression of ICAM-1, CVAM-1, neutrophil infiltration, TNFα, chemokine (MIP-1α and MIP-2) levels, and lipid peroxidation. The decrease in lipid peroxidation can be secondary to the decrease of inflammatory cell infiltration and activation (8). However, the lack of highly selective CB_2 receptor antibodies limits interpretation of some studies. Thus, the use of stringent negative controls is crucial for the correct detection and quantification of protein targets (88).
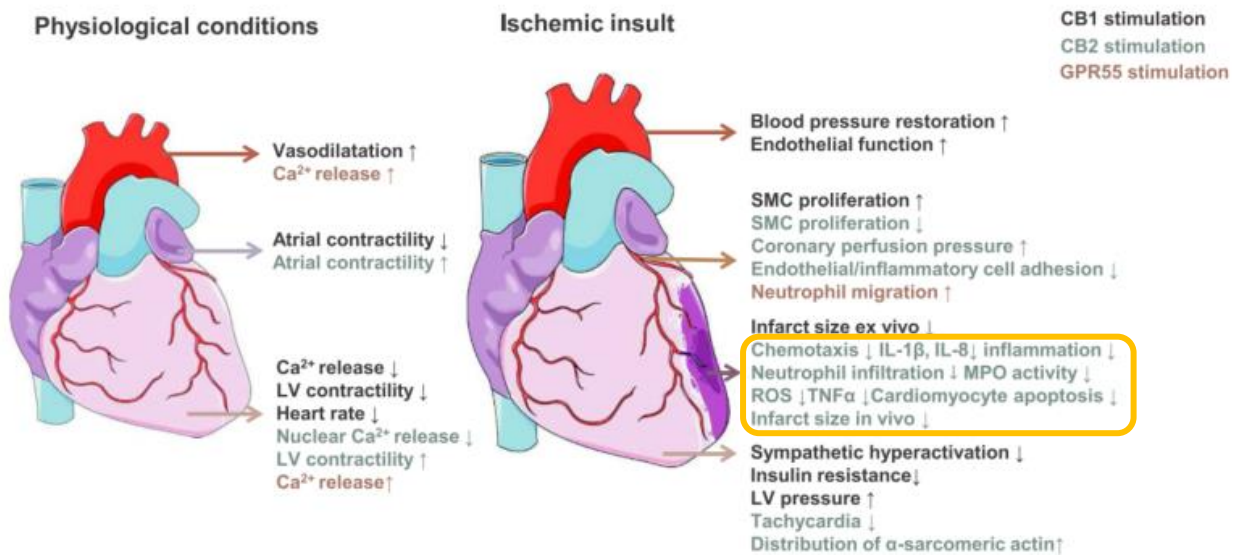
Figure 9. Cardiac impact of cannabinoid receptors. Adapted from (97).

Collectively, a number of studies suggest that exogenous cannabinoids elicit a shift in the cytokine expression profile from that which is Th_1 proinflammatory to one that is Th_2 anti-inflammatory and that the CB_2 receptor may be linked to this effect (111). It has been observed that the CB_2 agonist HU-308 attenuated hepatic ischemia/reperfusion injury by decreasing levels of $TNF\alpha$, MIP-1α and MIP-2 in serum and liver homogenates (112). Cannabinoid CB_2 receptor knockout ($CB_2^{-/-}$) mice are fertile, care for their offspring, and have a similar phenotype as their wild-type littermates (8), which shows CB_2 knockout is not lethal.

Possible mechanisms between systemic inflammation and hemodynamics have not been fully characterized but direct effects of inflammatory mediators on the contractility of the myocardium and vascular smooth muscle have been suggested (113). Though WIN55 has been demonstrated to have anti-inflammatory and anti-oxidative effects in inflammatory or ischemia diseases independent of its hypothermic effects, previous studies could not exclude other effects (114). Recent studies have indicated that activation of CB_2 leads to an anti-inflammatory response; therefore, the beneficial effects of WIN55 following resuscitation may be related to both CB_1 and CB_2 receptor activation.

IV.   Research Objectives

Cannabinoids produce hypothermia in normal rats through the activation of central CB_1 receptors. WIN55, the nonselective cannabinoid CB_1/CB_2 receptor agonist, produced hypothermia in a dose-dependent manner when injected intramuscularly. The body temperature reduced from 37 to 34°C, 60 to 180 mins post injection and hypothermia was maintained up to 5 hours. The effect was completely blocked by the selective CB_1 antagonist SR141716A (115, 116). CB_2 receptor ligands have potential therapeutic applications as immunomodulators for the treatment of inflammation (117). Hypothesized effects of WIN55 summarized in *Figure 10*.

42
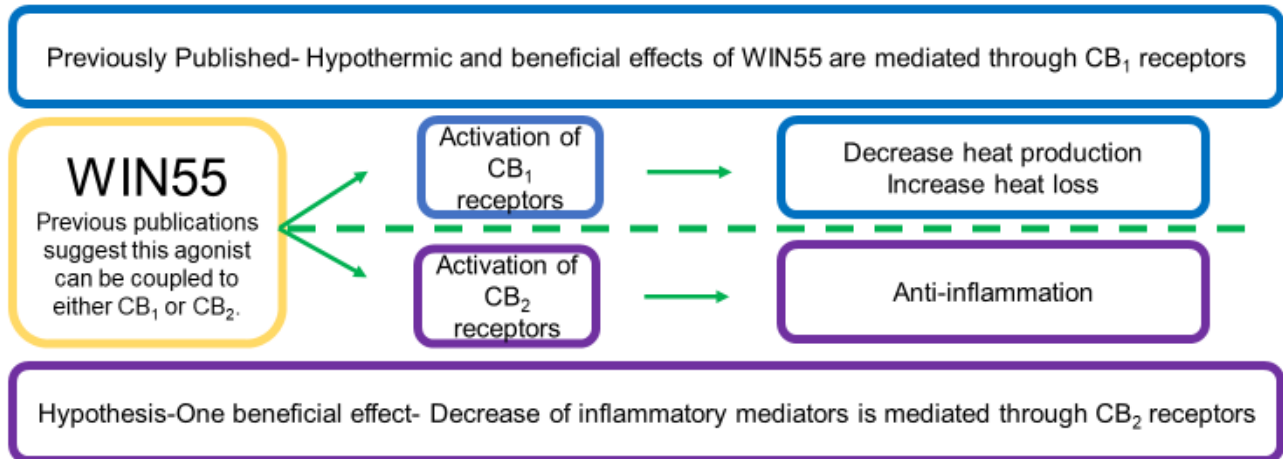
Figure 10. WIN55, 212-2 can be coupled to either CB$_1$ or CB$_2$ with different functional consequences.

The effects of WIN55 were investigated initially in our rat model of CA and CPR. WIN55 was selected based on the following reasons: 1) the described hypothermia effect of CB$_1$ agonist is convincing and well documented, 2) it is highly selective for cannabinoid receptors and interacts negligibly with other neurotransmitter and ion channels (118), 3) it is expressed in thermoregulatory areas of the central nervous system and therefore decreases body temperature via a central mechanism (119), 4) It has been shown to be neuroprotective (120) and 5) It has been demonstrated in both mice and rats that the CB$_2$ receptor activation effects of WIN55 have significant anti-inflammatory effects (121-123). CB$_2$ expression has been demonstrated in cardiac myocytes and endothelial and smooth muscle cells of coronary arteries (84).

Hypothesis: Cardiac arrest will cause mitochondrial dysfunction and increase plasma concentrations of TNFα, IL6 and IL10. IM Administration of SR141716A before VF+CPR followed by infusion of WIN55 5 min after ROSC will prohibit the release of inflammatory mediators caused by cardiac arrest via the CB$_2$ receptor.

CHAPTER 2: Materials and Methods

I.   Reagents

Lipopolysaccharide (LPS), sodium chloride (NaCl), (R)-(+)-WIN55,212-2 mesylate salt, polysorbate 80, dimethyl sulfoxide, DTT (Pro#1000748546), iodoacetamide (Pro#122270250), LC-MS/MS grade water, methanol, acetonitrile and common laboratory chemicals were purchased from Sigma Aldrich (St. Louis, MO). Pierce Trypsin Protease, MS grade (Pro# 90057), Pierce BCA Protein Assay Kit (Pro# 23250) and Formic Acid Optima LC/MS (A11-50) were purchased from Fisher Scientific (Waltham, MA). A TMT10plex Isobaric Label Reagent Set plus TMT11-131C Label Reagent (A34808) was purchased from Thermo Scientific (Rockford, IL). Dulbecco's Modified Eagle Medium (DMEM), 100x Penicilin/Streptomycin and 1M HEPES were obtained from Life Techonologies, Gibco (Waltham, MA). Heat inactivated Fetal Bovine Serum (FBS) was from Atlanta Biologicals (Flowery Branch, GA). CB_1 receptor antagonist SR141716A and (+)-WIN55,212-2 (mesylate) were purchased from Cayman Chemicals (Ann Arbor, MI).

II.   *In vivo*-Mitochondria

Guanghui Zheng performed surgical technique, Xianfei Ji performed mitochondrial isolation and measurement and helped draft manuscript, Jeremy Thompson trained Xianfei Ji and Jennifer Bradley on all mitochondrial techniques, Rabiya Shabnam ran ETC assay, Jennifer Bradley analyzed all data and drafted manuscript and Qun Chen, Edward Lesnefsky and Wanchun Tang reviewed data and manuscript drafts. This study was approved by the Institutional Animal Care and Use Committee of Virginia Commonwealth University. Animal care and handling were in

44

accordance with the Guide for the Care and Use of Laboratory Animals and the ARRIVE guidelines.

Animal Preparation

Male Sprague Dawley rats, weighing between 450g and 550g were anesthetized by intraperitoneal injection of pentobarbital (45 mg/kg). The trachea was orally intubated with a 14-gauge cannula (Abbocath- T; Abbott Hospital Products Division, North Chicago, IL). End-tidal CO_2 (ETCO$_2$) was continuously monitored with a side-stream infrared CO_2 analyzer (Capstar-100 Carbon Dioxide Analyzer; CWE, Ardmore, PA). A conventional lead II electrocardiogram (ECG) was monitored continuously. A PE-50 catheter (Becton Dickinson, Franklin Lakes, NJ, USA) inserted into the descending aorta measured arterial pressure. A thermocouple microprobe (9030-12-D-30, Columbus instruments, Columbus, OH, USA) inserted into the left femoral vein measured blood temperature. Another PE-50 catheter advanced into the right atrium measured right atrial pressure. A 3F catheter (Model C-PMS-301J; Cook Critical Care, Bloomington, IN) advanced into the right atrium was utilized to advance a pre-curved guidewire into the right ventricle to induce VF. Aortic blood temperature was maintained at 37°C ± 0.5°C by a heated surgical board. ECG, aortic and right atrial pressures, ETCO$_2$, and blood temperature were continuously recorded on a personal computer–based data acquisition system supported by WINDAQ software (DATAQ, Akron, OH).

Experimental Procedures

Animals were randomized into 4 groups (n=6 each group): 1) Sham (underwent surgery, no VF or CPR), 2) VF (VF only for 8 min), 3) VF+CPR (VF 8 min + CPR 8 min, no defibrillation) and 4) Return of Spontaneous Circulation (ROSC 1 hr) (VF 8 min, CPR8 min, defibrillation, and observe 1 hr after ROSC) (*Figure 11*). Mechanical ventilation was established at a tidal volume

45

of 0.60 mL/100g of body weight, a frequency of 100 breaths/min, and FiO2 of 1.0. VF was then

induced with a progressive increase in 60-Hz current to a maximum of 3.5 mA delivered to the

right ventricular endocardium. Current flow continued for 3 min to prevent spontaneous

defibrillation. After 8 min of untreated VF, precordial chest compressions, together with

mechanical ventilation, were initiated using a pneumatically driven mechanical chest

compressor. Precordial chest compressions were maintained at a rate of 200/min and

synchronized to provide a compression/ventilation ratio of 2:1 with equal compression-relaxation

for 8 min. Defibrillation was attempted with up to three 4-J counter shocks. ROSC was defined

as the return of supraventricular rhythm with a mean aortic pressure (MAP) above 50 mm Hg for

5 min.
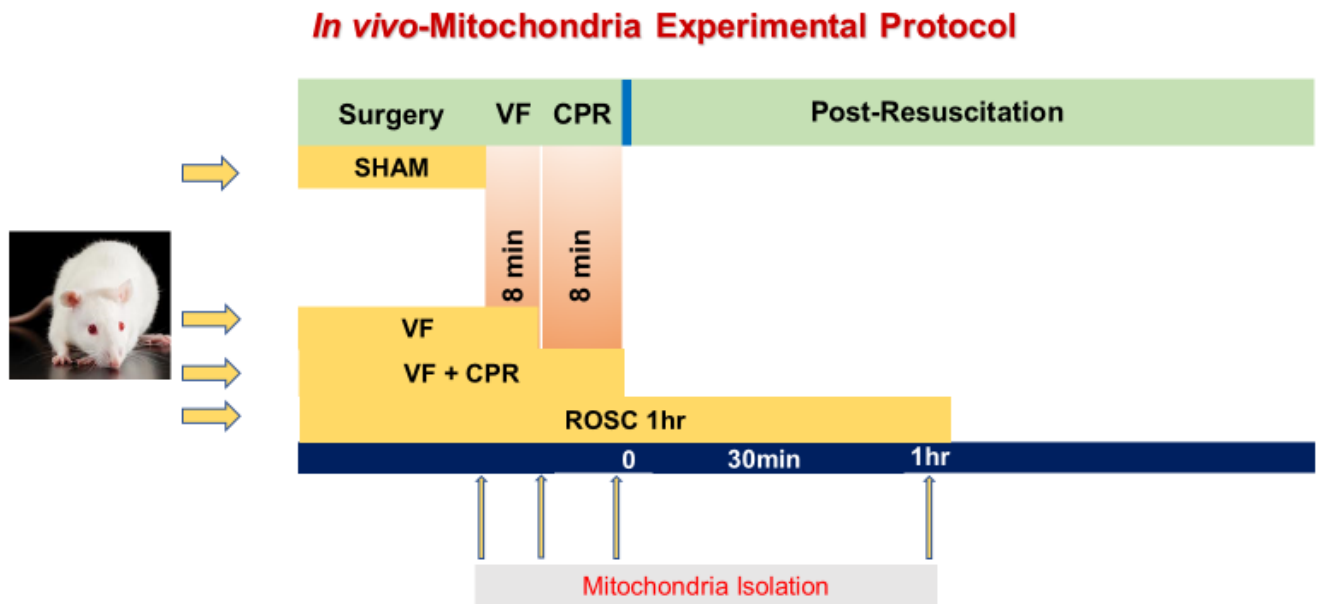
Figure 11. *In vivo*-Mitochondria Experimental Protocol-N=6 for each group. Sham is time zero control.

Cardiac mitochondria were isolated by a method previously described with slight

modifications (124, 125). Hearts were removed and placed into buffer A [100 mM KCl, 50 mM

3-(N-morpholino) propanesulfonic acid (MOPS), 1 mM EGTA, 5 mM MgSO4-7 H2O, and 1

mM ATP, pH 7.4] at 4°C. Cardiac tissue was finely minced and placed in buffer A containing 0.2% bovine serum albumin (BSA) and homogenized with a polytron tissue processor (Brinkman Instruments, Westbury, NY) for 2.5 s at a rheostat setting of 14. The polytron homogenate was centrifuged at 2,200 rpm for 10 min, supernatant was saved for isolation of subsarcolemmal mitochondria (SSM), and the pellet was washed. Combined supernatants were centrifuged at 5,000 rpm for 10 min to sediment SSM. Interfibrillar mitochondria (IFM) were isolated by incubation of skinned myofibers, obtained after polytron treatment (2.5 sec at a setting of 14), with 5 mg/g (wet weight) trypsin for 10 min at 4°C. SSM and IFM were washed twice and then suspended in 100 mM KCl, 50 mM MOPS, and 0.5 mM EGTA. Mitochondrial protein concentration was measured by the Lowry method using BSA as a standard (125).

Brain mitochondria were isolated by a method previously described with slight modifications (126). Brain (cerebrum) was rapidly removed and homogenized at 4ºC in 10ml of isolation buffer B (215mM mannitol, 75mM sucrose, 20 mM HEPES, 1mM EGTA, pH 7.4) containing 5mg of the bacterial protease type VIII (Subtilsin A). Brain homogenates were brought to 30 ml and then centrifuged at 12,000 rpm for 10 min. The pellet was resuspended in 10 ml of buffer C (buffer B+1mg/ml bovine serum albumin) and centrifuged at 2,420 rpm for 10 min. The mitochondrial pellet was resuspended in 10 ml of buffer C and centrifuged at 2,420 rpm for 10 min. Combined supernatants were centrifuged at 9,000 rpm for 10 min. The pellet was then resuspended in 3 ml buffer C, and centrifuged at 9,000 rpm for 10 min. The pellet was resuspended in 2 ml buffer B, and centrifuged at 9,000 rpm for 10 min. Finally, the mitochondrial pellet was resuspended in 100 μl buffer B.

Measurements

47

Oxygen consumption in mitochondria was measured using a Clark-type oxygen electrode at 30°C as previously described (127, 128) using glutamate (20 mM) (complex I substrate), succinate (20 mM) (complex II substrate), plus 7.5 mM rotenone and N,N,N',N' tetramethyl p-phenylenediamine (TMPD; 1 mM)-ascorbate (10 mM) (complex IV substrate) + rotenone (*Figure 12*). Maximal ADP-stimulated respiration (2 mM ADP) was determined. Mitochondria were used within 6 hrs after isolation.
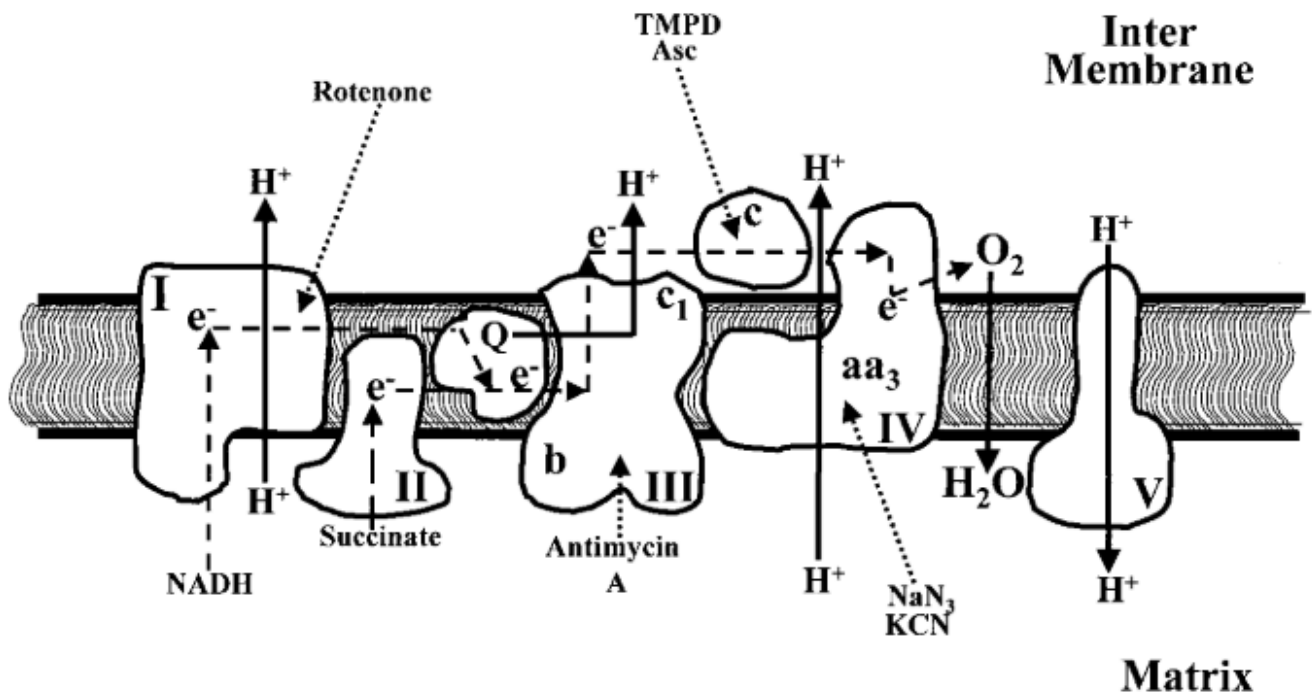
Figure 12. Mitochondria Electron Transport Chain Complex substrates and inhibitors.
Adapted from (22)

Enzyme activities were measured spectrophotometrically in detergent-solubilized frozen-thawed mitochondria using previously described methods (129): NADH-ubiquinone oxidoreductase, rotenone- sensitive (complex I=340nm), NADH-ferricyanide reductase (NFR=340nm); succinate-ubiquinone oxidoreductase, thenoyltrifluoroacetone sensitive (complex II=600nm); ubiquinol-cytochrome *c* oxidoreductase, antimycin A sensitive (complex III=550 and 600nm); and citrate synthase (=412nm). Frozen-thawed mitochondria were solubilized at a

48

final protein concentration of 1 μg/μl in 0.5% cholate in MSM/EDTA buffer, pH 7.4 (220 mM mannitol, 70 mM sucrose, 5 mM MOPS, 2 mM EDTA) (130).

Calcium retention capacity (CRC) was used to assess calcium-induced MPTP opening as previously described (131) in mitochondria (125 μg/ml) incubated in medium containing 150 mM sucrose, 50 mM KCl, 2 mM KH_2PO_4, 5 mM succinate, in 20 mM Tris·HCl, pH 7.4, by sequential pulses of 5 nmol calcium. Extramitochondrial Ca^{2+} concentration was recorded with 0.5 μM calcium Green-5N (Life Technologies City State), and fluorescence monitored with excitation and emission wavelengths at 500 and 530 nm, respectively (131). The calcium retention capacity CRC assay measures the susceptibility to opening of the permeability transition pore; and is performed in a non-acidic environment.

III.   *In vivo*-Proteomics

Fenglian He and Christine Moore performed surgical technique, Gea-Ny Tseng performed tissue lysate preparation and Poochon Scientific LLC performed proteomic analysis. Jennifer Bradley reviewed proteomic results focusing on S100A8/A9 expression (132) and found it increased within LV Apex Epicardium following CA and CPR. This study was approved by the Institutional Animal Care and Use Committee of Virginia Commonwealth University. Animal care and handling were in accordance with the Guide for the Care and Use of Laboratory Animals and the ARRIVE guidelines.

Animal Preparation

Male Sprague Dawley rats, weighing between 450g and 550g were anesthetized by intraperitoneal injection of pentobarbital (45 mg/kg). The trachea was orally intubated with a 14-gauge cannula (Abbocath- T; Abbott Hospital Products Division, North Chicago, IL). $ETCO_2$ was continuously monitored with a side-stream infrared CO_2 analyzer (Capstar-100 Carbon

49

Dioxide Analyzer; CWE, Ardmore, PA). A conventional lead II ECG was monitored continuously. A PE-50 catheter (Becton Dickinson, Franklin Lakes, NJ, USA) inserted into the descending aorta measured arterial pressure. A thermocouple microprobe (9030-12-D-30, Columbus instruments, Columbus, OH, USA) inserted into the left femoral vein measured blood temperature. Another PE-50 catheter advanced into the right atrium measured right atrial pressure. A 3F catheter (Model C-PMS-301J; Cook Critical Care, Bloomington, IN) advanced into the right atrium was utilized to advance a pre-curved guidewire into the right ventricle to induce VF. Aortic blood temperature was maintained at 37°C ± 0.5°C by a heated surgical board. ECG, aortic and right atrial pressures, ETCO$_2$, and blood temperature were continuously recorded on a personal computer–based data acquisition system supported by WINDAQ software (DATAQ, Akron, OH).

Experimental Procedures

Animals were randomized into 3 groups: 1) Sham (underwent surgery, no VF or CPR) (n=4), 2) CPR (VF 8 min + CPR 8 min, defibrillation and ROSC) (n=4), 3) Norm (nothing done to animal) (n=3) (*Figure 13*). Mechanical ventilation was established at a tidal volume of 0.60 mL/100g of body weight, a frequency of 100 breaths/min, and FiO2 of 1.0. VF was then induced with a progressive increase in 60-Hz current to a maximum of 3.5 mA delivered to the right ventricular endocardium. Current flow continued for 3 min to prevent spontaneous defibrillation. After 8 min of untreated VF, precordial chest compressions, together with mechanical ventilation, were initiated using a pneumatically driven mechanical chest compressor. Precordial chest compressions were maintained at a rate of 200/min and synchronized to provide a compression/ ventilation ratio of 2:1 with equal compression-relaxation for 8 min. Defibrillation

50

was attempted with up to three 4-J counter shocks. ROSC was defined as the return of

supraventricular rhythm with a MAP above 50 mm Hg for 5 min.

Figure 13. *In vivo*-**Proteomics Experimental Protocol**

Measurements

Once ROSC was reached Christine Moore or Dr. Tseng removed the heart for further

analysis. Samples sent to Poochon Scientific were labeled Left Ventricle Apex epicardial

(LV Apex EPI) (*Figure 14*).
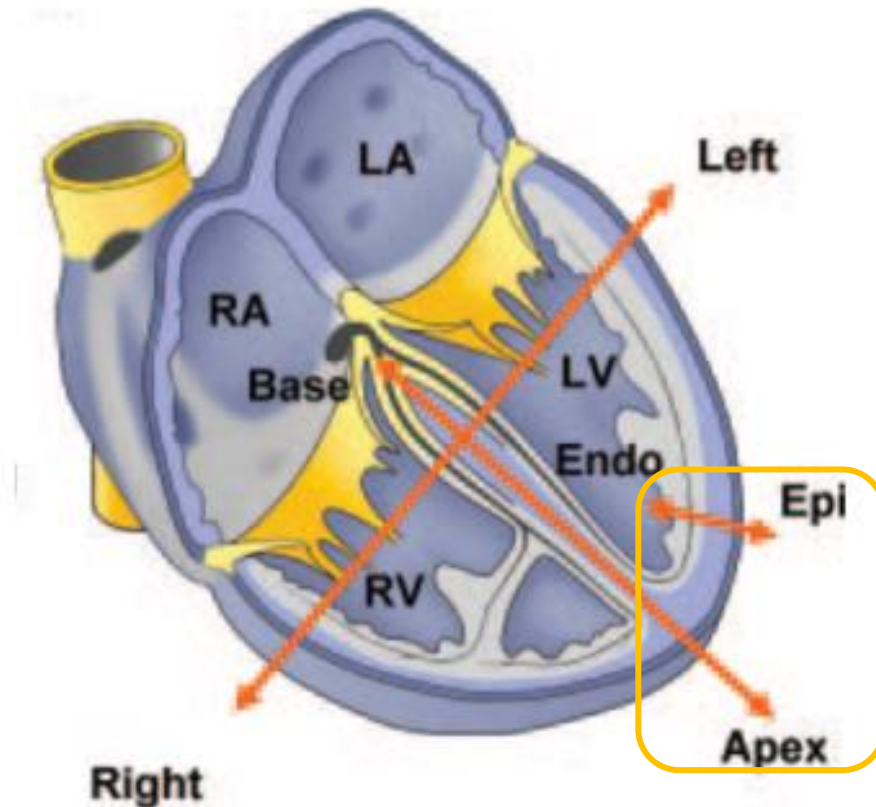
Figure 14. LV Apex Epi- Samples sent to Poochon Scientific for further analysis were labeled LV Apex Epi from Dr. Tseng's laboratory. Adapted from (133).

General Protocol of protein lysate preparation performed by Dr. Tseng's laboratory

RIPA buffer: 20mM Tris-HCL pH7.4, 150mM Na\Cl, 1mM EDTA, 1% Triton-X100, 1% sodium deoxycholate, 0.1% SDS with freshly added PMSF to 1mM and with freshly added aprotinin and leupeptin to 5ug/ml was prepared just before use. The left ventricular (LV) apex was removed and placed in RIPA on ice for 10 min before homogenizing. Tissue was kept on ice during homogenization until tissue was liquified. Then liquified tissue lysate was centrifuged at 13,000 rpm for 3min at 4°C. Clear supernatant was transferred to new clearly labelled tubes for shipment to Poochon Scientific (134).

BCA Assay performed by Poochon Scientific

52

Tissue lysate samples were thawed at room temperature and a precipitation (cloud) was observed. 20 µl of 10% SDS was added to the sample and heated at 95°C for 10 minutes. After treatment the lysate became clear. Protein concentration of supernatant was determined by a BCA™ Reducing Reagent compatible assay kit from Thermo Scientific (Rockford, IL). The BCA Protein Assay is a popular method for colorimetric detection and quantitation of total protein (135). The assay was read at an optical density (OD) of 562nm. One major advantage of the BCA assay is that it produces a linear response curve. This response curve allows accurate determination of unknown protein concentrations and provides a higher dynamic range than other standard assays (135).

TMT-11plex labeling performed by Poochon Scientific

100 µg of protein lysate was taken from each sample for in-solution trypsin digestion. Predigestion was ran along with digested samples on SDS-PAGE and stained to check digestion efficiency. Isobaric labeling was performed using a commercial TMT10plex Isobaric Label Reagent Set plus TMT11-131C Label Reagent kit according to the product manual and samples were labeled as described in Table 1. The 11 labeled peptide mixture was then dried in a vacuum concentrator and stored at -80 ℃ for the next step.

Table 1. Summary of 11 cell pellet sample labeling

Sample Label	Description	TMT-tag	TMT Quantification (ratio)
S1	Norm_1	126	126/131
S2	Norm_2	127C	127C/131
S3	Norm_3	127N	127N/131
S4	CPR_1	128C	128C/131
S5	CPR_2	128N	128N/131
S6	CPR_3	129C	129C/131
S7	CPR_4	129N	129N/131
S8	Sham_1	130C	130C/131
S9	Sham_2	130N	130N/131
S10	Sham_3	131	131/131
S11	Sham_4	131C	131/131-C

Fractionation of labeled peptides by basic reversed phase UHPLC

Dried labeled peptides were resuspended in 10 mM TEABC. Labeling efficiency was

determined before fractionation by analysis of a small sample aliquot (1%). A minimum labeling

efficiency of 95% was required. The fractionation of TMT-10plex labeled peptide mixture was

carried out using an Agilent AdvanceBio Column (2.7 µm, 2.1 x 250 mm) at Solvent A (10 mM

TEABC, pH 8.0) and an Agilent UHPLC 1290 system. Separation was performed by running a

gradient of Solvent B (10 mM TEABC, pH 8.0, 90% ACN) and Solvent A (10 mM TEABC, pH

8.0) at a flow rate 250 µL/min. Elute fractions were collected into a 96-well plate using a 1260

series auto-sample fraction collector. The 96 elute fractions were further combined into 24

fractions according to collection time (e.g. Ax/Cx/Ex/Gx, and Bx/Dx/Fx/Hx, A/B/C/D/E/F/G/H

represents column, x represents row 1 through row 12) for LC/MS/MS analysis.

Nanospray LC/MS/MS analysis and database search performed by Poochon Scientific

54

LC/MS/MS analysis was carried out using a Thermo Scientific Q-Exactive hybrid Quadrupole-Orbitrap Mass Spectrometer and a Thermo Dionex UltiMate 3000 RSLCnano System. Each peptide fraction from a set of 24 fractions was loaded onto a peptide trap cartridge at a flow rate of 5 µL/min. Trapped peptides were eluted onto a reversed-phase 20 cm C18 PicoFrit column (New Objective, Woburn, MA) using a linear gradient of acetonitrile (3-36%) in 0.1% formic acid. The elution duration was 110 min at a flow rate of 0.3 µL/min. Eluted peptides from the PicoFrit column were ionized and sprayed into the mass spectrometer, using a Nanospray Flex Ion Source ES071 (Thermo) under the following settings: spray voltage, 1.8 kV, Capillary temperature, 250°C. 24 fractions were analyzed sequentially. The Q Exactive instrument was operated in the data dependent mode to automatically switch between full scan MS and MS/MS acquisition. Survey full scan MS spectra (m/z 300−1800) was acquired in the Orbitrap with 70,000 resolutions (m/z 200) after accumulation of ions to a 1×10^6 target value based on predictive automatic gain control (AGC). Dynamic exclusion was set to 20 s. The 15 most intense multiply charged ions ($z \geq 2$) were sequentially isolated and fragmented in the octopole collision cell by higher-energy collisional dissociation (HCD) using normalized HCD collision energy 28% with an AGC target 1×10^5 and a maximal injection time of 100 ms at 17,500 resolutions. MS Raw data files (24 files from 24 fractions) were searched against the Rattus norvegicus (Rat) protein sequences database obtained from UniprotKB website using Proteome Discoverer 1.4 software (Thermo, San Jose, CA) based on the SEQUEST and percolator algorithms. False positive discovery rates (FDR) was set on 5%. A Proteome Discoverer Report was generated containing all assembled proteins with peptides sequences and peptide spectrum match counts (PSM#) and TMT-tag based quantification ratio.

TMT-tag based quantification was used to determine the relative abundance of proteins identified from each set of 11 samples using one TMT-10plex. The TMT-Tag-131 was used as the common denominator for calculation of the ratio (e.g. A1-TMT-tag-126 versus sample 11-Tag131). Relative abundance of proteins was normalized based on the sum of ratios (*Figure 15 and Figure 16*).
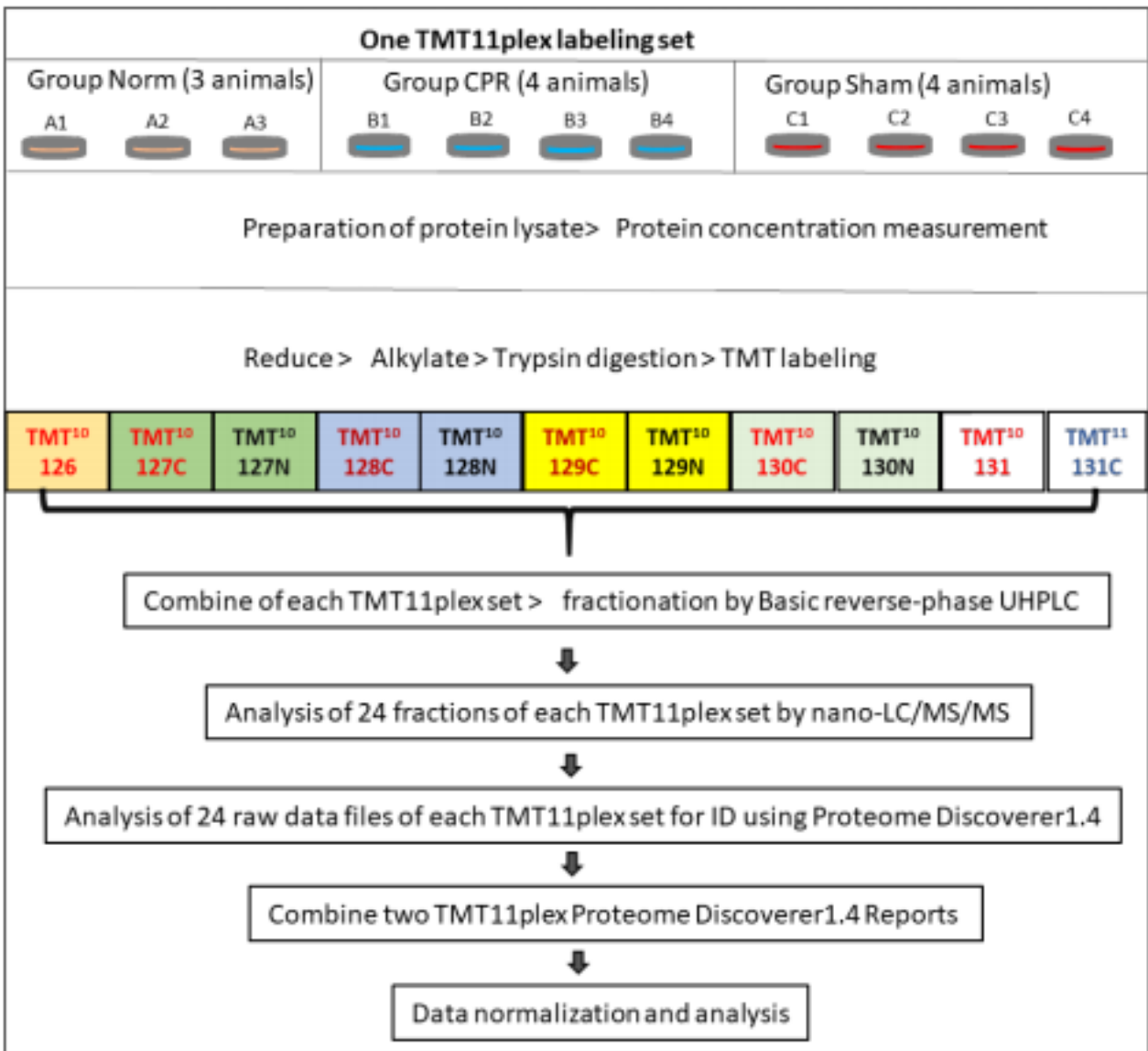
Figure 15. Poochon Scientific Schematic of Experimental Workflow. One TMT set labeled 11 samples. Procedures included preparation of lysates, trypsin digestion, TMT-ll plex of

labeling of tryptic peptides, fractionation of labeled peptides by basic reverse-phase UHPLC, nano-LC-MS/MS analysis on a Q-Exactive mass spectrometer, database search, normalization and data analysis.
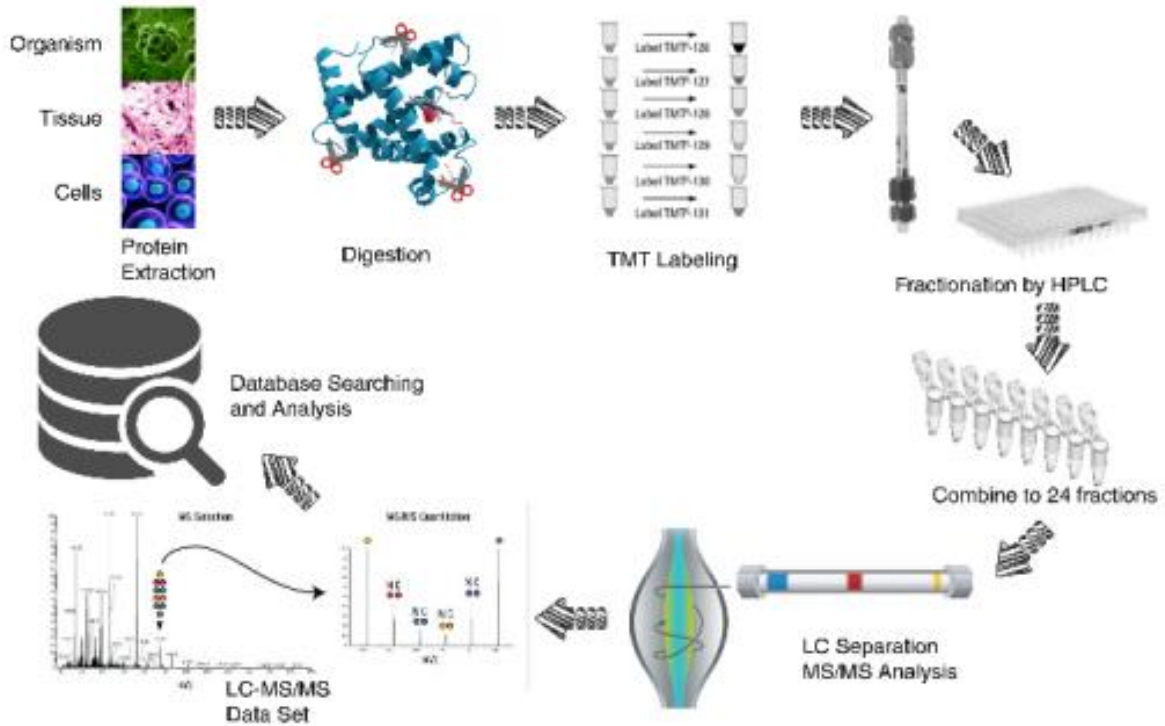
Figure 16. Poochon Scientific Schematic of Experimental Workflow. One TMT set labeled 11 samples. Procedures included preparation of lysates, trypsin digestion, TMT-ll plex of labeling of tryptic peptides, fractionation of labeled peptides by basic reverse-phase UHPLC, nano-LC-MS/MS analysis on a Q-Exactive mass spectrometer, database search, normalization and data analysis.

Analysis performed by Jennifer Bradley

Kyoto Encyclopedia of Genes and Genomes (KEGG), a collection of genomes and biological pathways, was used to map pathways from proteins identified. NCBI accession numbers (136) (4,997) were converted to Kegg (137) (3,195). One KEGG pathway was identified to have been significantly regulated by CA/CPR (138). NCBI terms were converted to Go terms by Biological DataBase network with p values obtained by Poochon Scientific for Revigo analysis. Revigo uses a clustering algorithm to sort GO terms by similarity into similar biological processes (139).

57

IV. *In vitro*-WIN55

Yanyan Wang trained Jennifer Bradley on *in vitro* techniques, Jennifer Bradley performed cell culture with reagents prepared by Yanyan Wang, ELISA, analyzed all data and drafted SCCM 2020 abstract. Huiping Zhou and Wanchun Tang reviewed data and abstract drafts. Mouse RAW 264.7 macrophage cells (ATCC, Rockville MD, USA) were plated into 60mm dishes with a density of $10*10^5$ cells/dish and incubated with DMEM containing 10%FBS, 1%PS overnight. Cell media was then changed to DMEM containing 1% FBS, 1%PS, and incubated for 4hrs (140, 141). They were then pretreated with WIN55 (5 µM) (142) for 2 hrs, then treated with LPS (12.5 ng/mL) for 6hrs and 24 hrs. At the end of treatment, culture media was collected and centrifuged at 14,000 x rpm for 1 min (143). Media protein levels of TNFα, IL6, and IL1β were quantified using commercial enzyme-linked immunosorbent assays (ELISAs) (R&D Systems, Minneapolis, MN, USA) (144). Concentrations were expressed as pg/mL.

V. *In vivo-WIN55*

Yan Xiao, Jadd Khoraki and Jennifer Bradley performed surgical technique. Jennifer Bradley performed ELISA and analyzed all dissertation data and Wanchun Tang reviewed. This study was approved by the Institutional Animal Care and Use Committee of Virginia Commonwealth University. Animal care and handling were in accordance with the Guide for the Care and Use of Laboratory Animals and the ARRIVE guidelines.

Animal Preparation

Male Sprague Dawley rats, weighing between 450g and 550g were anesthetized by intraperitoneal injection of pentobarbital (45 mg/kg). The trachea was orally intubated with a 14-gauge cannula (Abbocath- T; Abbott Hospital Products Division, North Chicago, IL). ETCO$_2$

58

was continuously monitored with a side-stream infrared CO_2 analyzer (Capstar-100 Carbon Dioxide Analyzer; CWE, Ardmore, PA). A conventional lead II ECG was monitored continuously. A PE-50 catheter (Becton Dickinson, Franklin Lakes, NJ, USA) inserted into the descending aorta measured arterial pressure and was utilized for blood withdrawal. A thermocouple microprobe (9030-12-D-30, Columbus instruments, Columbus, OH, USA) inserted into the left femoral vein measured blood temperature. Another PE-50 catheter advanced into the right atrium measured right atrial pressure. A 3F catheter (Model C-PMS-301J; Cook Critical Care, Bloomington, IN) advanced into the right atrium was utilized to advance a pre-curved guidewire into the right ventricle to induce VF. Another PE-50 catheter inserted into the right femoral vein was utilized for drug infusion (*Figure 17*). All catheters were flushed intermittently with saline containing 2.5 IU/mL of crystalline bovine heparin (145). Aortic blood temperature was maintained at $37°C \pm 0.5°C$ by a heated surgical board. ECG, aortic and right atrial pressures, $ETCO_2$, and blood temperature were continuously recorded on a personal computer–based data acquisition system supported by WINDAQ software (DATAQ, Akron, OH).

Figure 17. *In vivo*-Study Design
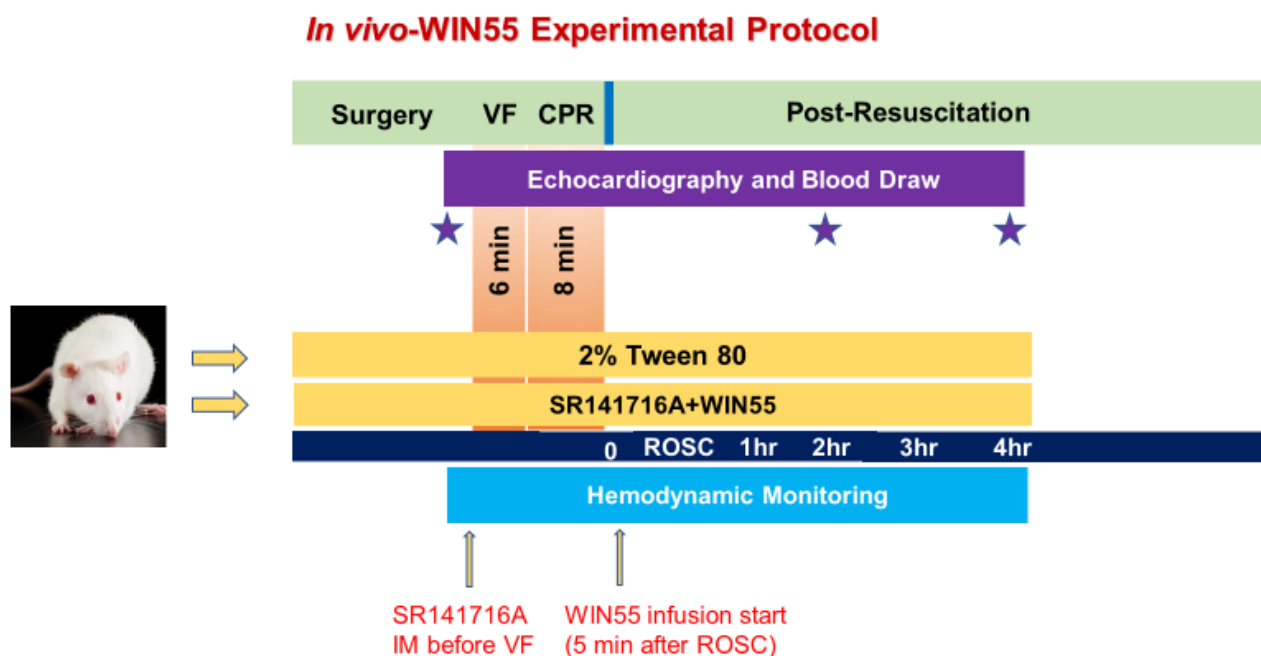
Figure 18. *In vivo*-WIN55 Experimental Protocol

Experimental Procedures

Animals were randomized into 2 groups (*Figure 18*) : 1) 2% Tween 80 (VF 6 min + CPR 8 min, defibrillation and ROSC followed by infusion) (n=3), 2) SR141716A+WIN55 (IM Administration of SR141716A (*Figure 19*) (5 mg/kg, dissolved in 0.1 mL dimethylsulfoxide) before VF 6 min + CPR 8 min, defibrillation and ROSC followed by infusion) (n=6). At 5 minutes after ROSC, either WIN55 (1 mg/kg/h) or vehicle (2% Tween-80 in 0.9% NaCl solution) was administered by continuous intravenous infusion with a syringe pump (Genie Touch; Kent Scientific Corporation) for 4 hours at a rate of 1.4 mL/kg/h (114). Mechanical ventilation was established at a tidal volume of 0.60 mL/100g of body weight, a frequency of 100 breaths/min, and FiO_2 of 1.0. VF was then induced with a progressive increase in 60-Hz current to a maximum of 3.5 mA delivered to the right ventricular endocardium. Current flow continued for 3 min to prevent spontaneous defibrillation. After 6 min of untreated VF,

61

precordial chest compressions, together with mechanical ventilation, were initiated using a pneumatically driven mechanical chest compressor. Precordial chest compressions were maintained at a rate of 200/min and synchronized to provide a compression/ ventilation ratio of 2:1 with equal compression-relaxation for 8 min. Defibrillation was attempted with up to three 4-J counter shocks. ROSC was defined as the return of supraventricular rhythm with a MAP above 50 mm Hg for 5 min.
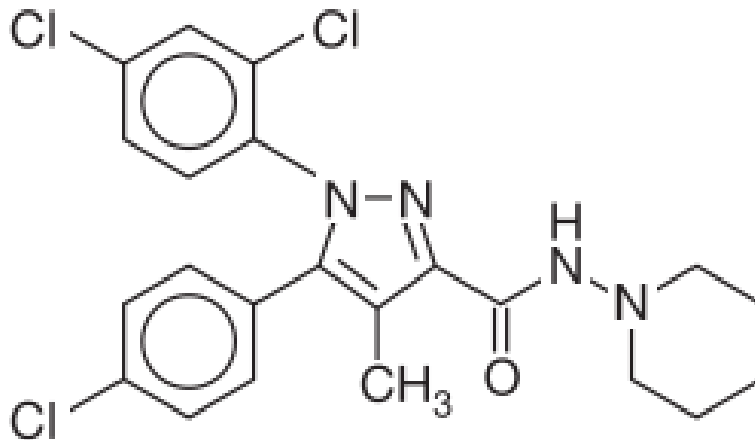
Figure 19. SR141716A is an antagonist for CB_1 (111)

Measurements

Hemodynamics and myocardial function

Electrocardiogram, aortic and right atrial pressures, blood temperature, and $ETCO_2$ values were continuously recorded on a personal computer-based data-acquisition system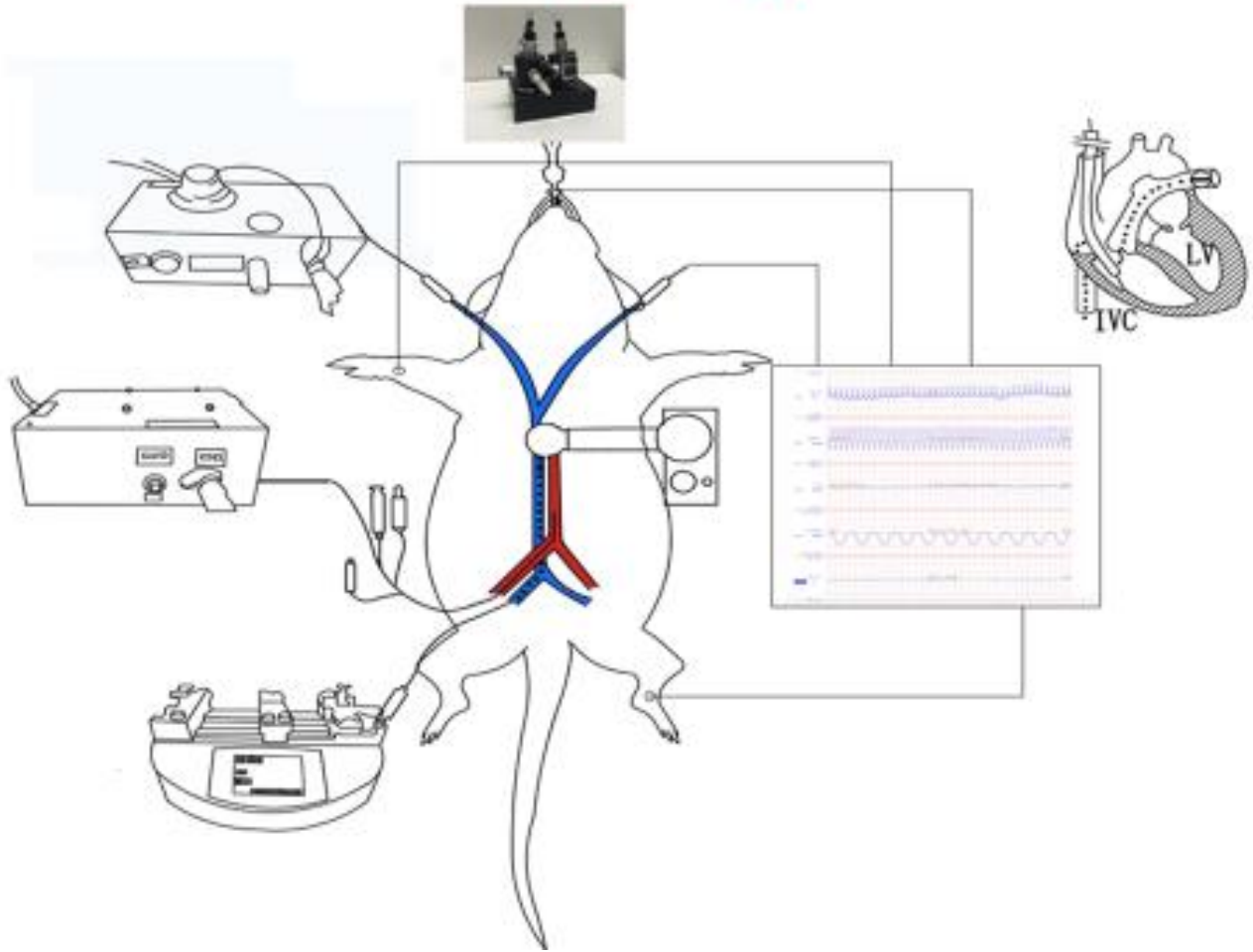 supported by WINDAQ software (DATAQ, Akron, OH). At baseline, 2 and 4 hours after ROSC, EF, CO, and myocardial performance index (MPI) were measured by echocardiography (HD11XE; Philips

Medical Systems, Eindhoven, Netherlands) with a 12.5 Hz transducer. EF and CO are adopted to estimate the myocardial contractility; MPI is adopted to estimate left ventricular diastolic function. The MPI, which combines time intervals related to systolic and diastolic functions reflecting the global cardiac function, is also calculated using the formula $(a - b)/b$, where a = mitral closure-to-opening interval (time interval from cessation to onset of mitral inflow) and b = ET (aortic flow ejection time, obtained at the left ventricle outflow tract) (145).

ELISA Analysis

One ml blood samples were collected at baseline, 2 and 4 hours after ROSC. After centrifugation ($2,100 \times g$, 10 min, 4°C) (146), plasma was removed and stored at −80°C for further ELISA analysis. Protein levels of TNFα, IL6, IL10 (R&D Systems, Minneapolis, MN, USA) S100A8 and cardiac troponin I (TNNI3) (LifeSpan BioSciences, Seattle, WA, USA) were quantified using commercial ELISA kits. ELISA measurement was performed following manufacturer's instructions.

VI.   Statistical Analysis

GraphPad PRISM version 9.0 for Windows (GraphPad Software Inc., San Diego, CA) was used to conduct analyses. Data are expressed as mean ± standard deviation (SD). Differences between greater than three groups were compared using a one-way analysis of variance (ANOVA) (Tukey or Bonferonni test for multiple comparisons). When only two groups were present, an unpaired student's t-test was conducted. A p-value of <0.05 was considered statistically significant.

CHAPTER 3: Cerebral and myocardial mitochondrial injury differ in a rat model of cardiac arrest and cardiopulmonary resuscitation

RATIONALE

Mitochondria are both targets and sources of damage during ischemia and reperfusion (22, 147). Following ischemia and reperfusion, mitochondrial dysfunction involves the increased production of reactive oxygen species (ROS), alteration of electron transfer activity, opening of the mitochondrial permeability transition pore (MPTP) and cytochrome *c* release (148-155). Ischemia damages the electron transport chain (ETC) (156) and decreases the rate of oxidative phosphorylation (OXPHOS) (157, 158). However, little is known regarding the effects of VF and CPR consistent with salvage by resuscitation on brain and heart mitochondrial function.

We hypothesize that mitochondrial damage differs between the brain and heart. Brain mitochondria are more vulnerable to ischemia and suffer reperfusion injury in addition to ischemic alterations, resulting in diminished overall mitochondrial respiration following resuscitation (159). The purpose of this study was to measure mitochondrial function following cardiac arrest (CA) with and without cardiopulmonary resuscitation (CPR) using OXPHOS, ETC enzyme activity and calcium retention capacity (CRC) as an index of susceptibility to MPTP opening.

RESULTS

Body weight, blood temperature, $ETCO_2$ and CPP during CPR were not different between VF+CPR and ROSC 1hr (Table 2). The maximal rate of OXPHOS was measured stimulated by 2 mM ADP with glutamate as a complex I substrate. Oxidative phosphorylation was decreased by CA in brain and remained depressed through CPR and ROSC (*Figure 20*). Cardiac mitochondria were less susceptible to injury, with preserved OXPHOS until the reperfusion of

64

ROSC in SSM (*Figure 21*) and preserved function throughout in IFM (*Figure 22*). As previously described, SSM were more susceptible to injury than IFM (127, 150, 160). Inhibition of complex I activity is one of the earliest alterations in mitochondrial function due to ischemia (161). Maximal rate of OXPHOS stimulated by 2 mM ADP with TMPD-ascorbate as a complex IV substrate was no different in brain compared to heart mitochondria (Table 3).

Table 2. Physiologic parameters

Variables	VF+CPR	ROSC 1hr	
Body Weight (g)	487.8±19.2	487.2±6.4	
Blood temperature (°C)	36.7±0.4	36.7±0.3	
ETCO$_2$ (mmHg)	25.5±3.1	25.9±4.9	
CPP (mmHg)	27±3	27.5±2.9	

Mean ± SD, Unpaired t test, p>0.05 vs VF+CPR N=6 in each group.

BM Glutamate 2mM ADP
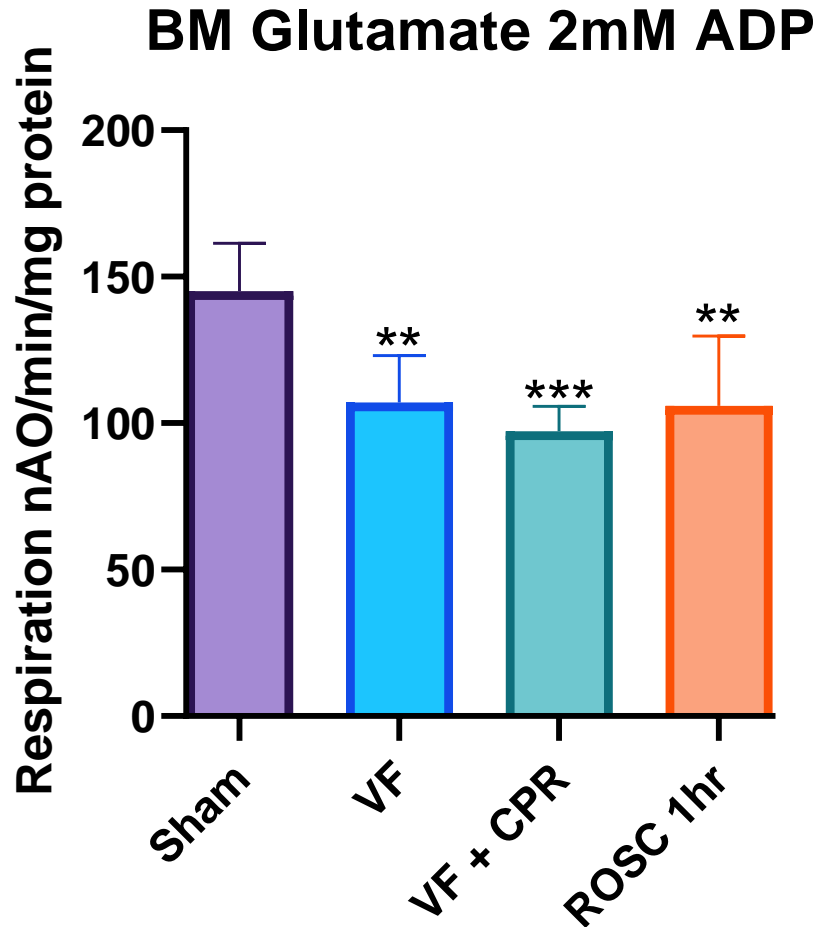
Figure 20. BM oxidative phosphorylation with glutamate as a complex I substrate- Oxygen consumption in mitochondria was measured using a Clark-type oxygen electrode at 30°C. Mitochondria were incubated in a solution containing 80 mM KCl, 50 mM MOPS, 1 mM EGTA, 5 mM KH2PO4, and 1 mg/ml bovine serum albumin, at pH 7.4. After depletion of endogenous substrates by addition of ADP, glutamate (complex I substrate) was added as an electron donor. Oxidative phosphorylation with glutamate as a complex I substrate was decreased by cardiac arrest in brain, and remained depressed through cardiopulmonary resuscitation. Mean ± SD, One-way ANOVA, Tukey Post-hoc *$p<0.05$ **$p<0.01$ ***$p<0.001$ vs Sham N=6 in each group. My contribution (a) design of the experiments (c) Analysis of the data.
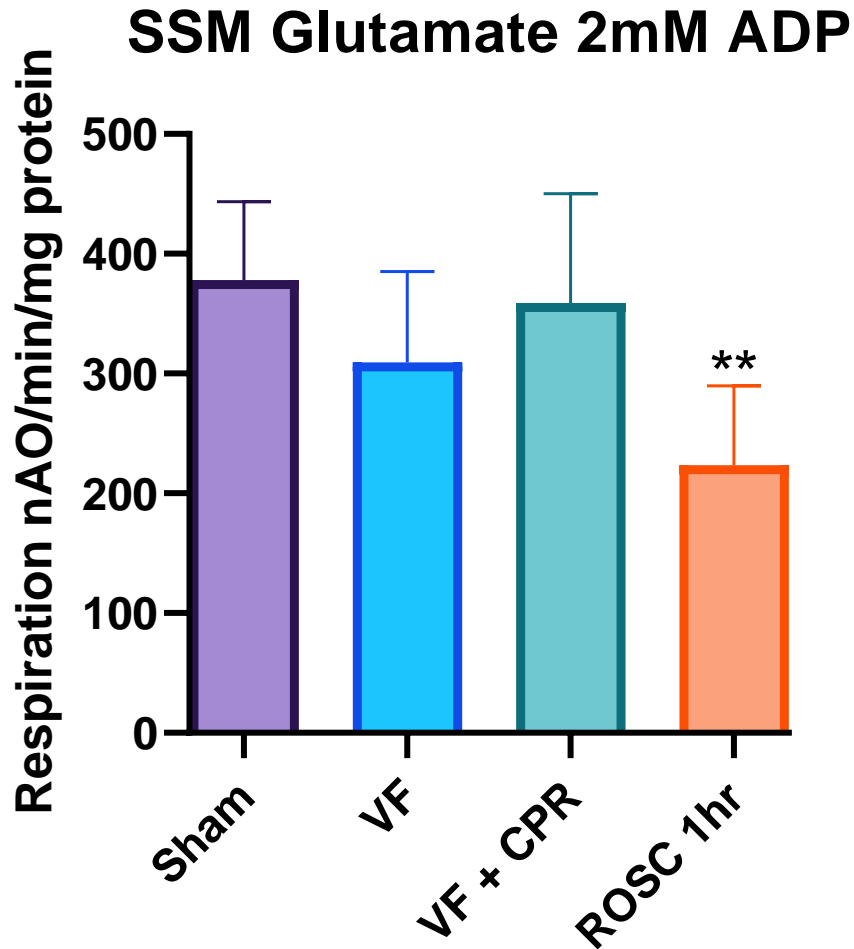
Figure 21. SSM oxidative phosphorylation with glutamate as a complex I substrate- Oxygen consumption in mitochondria was measured using a Clark-type oxygen electrode at 30°C. Mitochondria were incubated in a solution containing 80 mM KCl, 50 mM MOPS, 1 mM EGTA, 5 mM KH2PO4, and 1 mg/ml bovine serum albumin, at pH 7.4. After depletion of endogenous substrates by addition of ADP, glutamate (complex I substrate) was added as an electron donor. Oxidative phosphorylation with glutamate as a complex I substrate preserved OXPHOS until the reperfusion of ROSC in SSM. Mean ± SD, One-way ANOVA, Tukey Post-hoc *p<0.05 **p<0.01 ***p<0.001 vs Sham N=6 in each group. My contribution (a) design of the experiments (c) Analysis of the data.
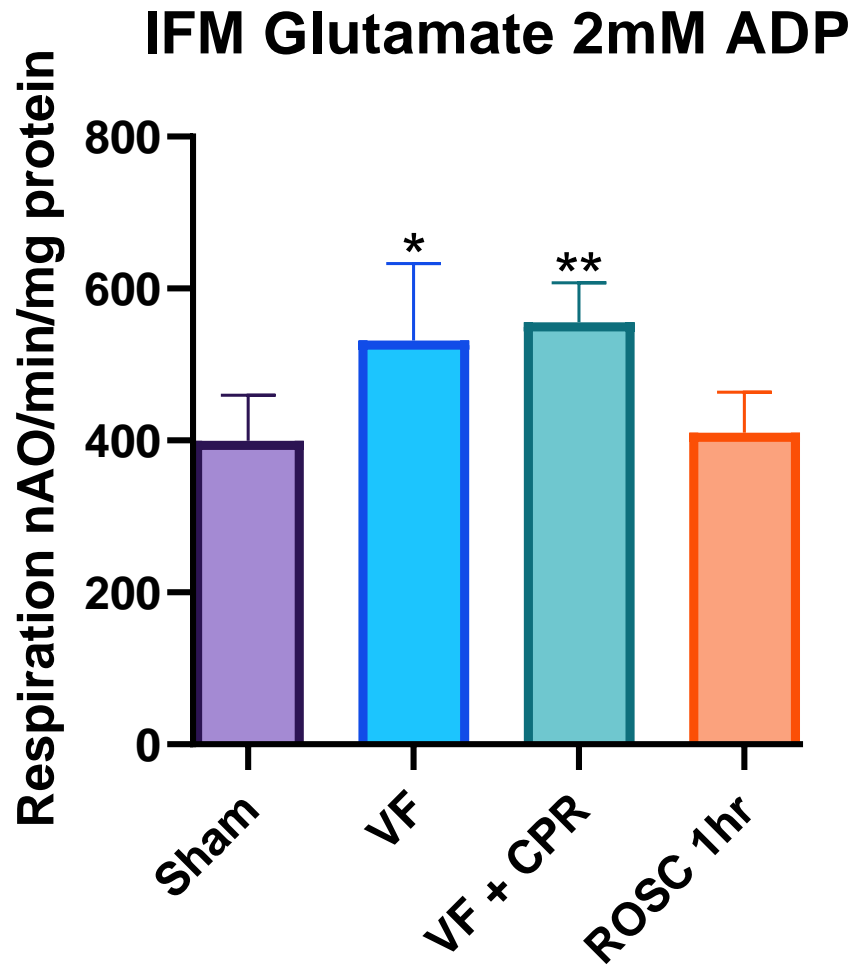
Figure 22. IFM oxidative phosphorylation with glutamate as a complex I substrate- Oxygen consumption in mitochondria was measured using a Clark-type oxygen electrode at 30°C. Mitochondria were incubated in a solution containing 80 mM KCl, 50 mM MOPS, 1 mM EGTA, 5 mM KH2PO4, and 1 mg/ml bovine serum albumin, at pH 7.4. After depletion of endogenous substrates by addition of ADP, glutamate (complex I substrate) was added as an electron donor. Oxidative phosphorylation with glutamate as a complex I substrate preserved OXPHOS throughout in IFM. Mean ± SD, One-way ANOVA, Tukey Post-hoc *$p<0.05$ **$p<0.01$ ***$p<0.001$ vs Sham N=6 in each group. My contribution (a) design of the experiments (c) Analysis of the data.

Table 3. Mean Percent Change of Rate of oxidative phosphorylation in brain and heart mitochondria using TMPD as complex IV substrate.

2mM ADP	BM	SSM	IFM
VF	Down 38±37.3	Down 28±14.3	Down 23±15.8
VF+CPR	Down 21±9.4	Down 17±10.2	Up 33±17.3
ROSC 1hr	Down 24±12	Down 33±29.7	Down 39±23.7

Mean ± SD, p>0.05 vs Sham rates: BM 2672±666.8; SSM 5844±1539.6; IFM 3968±1257.6 nAO/min/mg mitochondrial protein; N=6 in each group. Oxygen consumption in mitochondria was measured using a Clark-type oxygen electrode at 30°C. Mitochondria were incubated in a solution containing 80 mM KCl, 50 mM MOPS, 1 mM EGTA, 5 mM KH_2PO_4, and 1 mg/ml bovine serum albumin, at pH 7.4. After depletion of endogenous substrates by addition of ADP, TMPD-ascorbate (complex IV substrate) was added as an electron donor.

Enzyme activity of ETC complexes was measured to identify the primary sites most affected by ischemia within the ETC. CA resulted in sustained damage to complex I in brain mitochondria *(Figure 23)*. NADH:ferricyanide oxidoreductase activity decreased following ROSC, suggesting that reperfusion caused damage to the NADH oxidase portion of the complex (*Figure 24*). In contrast, complexes II and III remained unaltered (Table 4). In this rat model of CA and CPR, brain complex I is more vulnerable to damage during ischemia and reperfusion than complex II or complex III. Complex I in brain is also more susceptible to damage than complex I in heart.

BM Electron Transport Chain
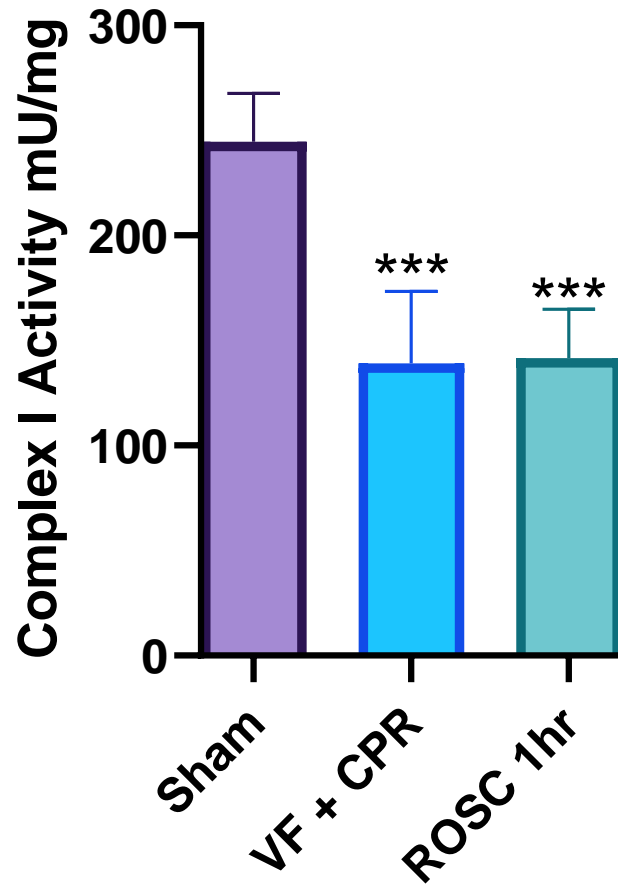
Figure 23. BM enzyme activity confirmation of Complex I damage. CA resulted in sustained damage to complex I in brain mitochondria. Mean ± SD, One-way ANOVA, Tukey Post-hoc *p<0.05 **p<0.01 ***p<0.001 vs Sham N=5 in each group. My contribution (a) design of the experiments (c) Analysis of the data.

BM Electron Transport Chain
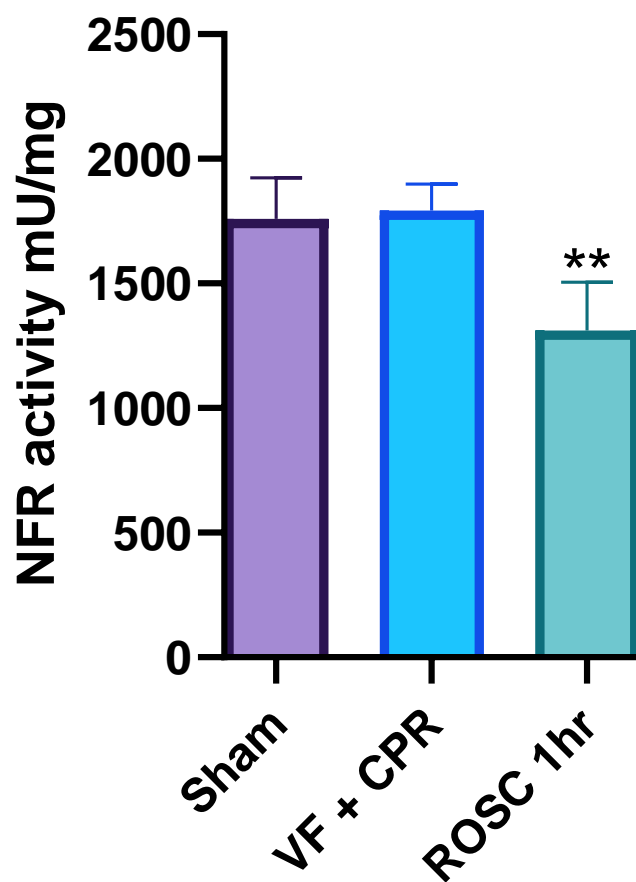
Figure 24. BM enzyme activity of NADH:ferricyanide oxidoreductase-decreased following return of spontaneous circulation. Mean ± SD, One-way ANOVA, Tukey Post-hoc *p<0.05 **p<0.01 ***p<0.001 vs Sham N=5 in each group. My contribution (a) design of the experiments (c) Analysis of the data.

Table 4. Brain and heart mitochondria Electron Transport Chain Results.

Complex II	BM	SSM	IFM
SHAM	274.8±69.3	101.4±47.9	119.6±28.2
VF	230.2±67.9	--	--
VF+CPR	223±39.6	70±10.4	150±26
ROSC 1hr	178±70.1	89.6±14	128.4±36.6

Complex III	BM	SSM	IFM
SHAM	3572±739.4	4128.2±1251.7	4974±554.3
VF	2896.4±672.5	--	--
VF+CPR	3039.8±365.8	1869.2±515*	4722±1065.7
ROSC 1hr	3043±698.3	2501.6±1543.9	4045.6±581.5

Mean ± SD, One-way ANOVA, Tukey Post-hoc $*p < 0.05$ $**p < 0.01$ $***p < 0.001$ vs Sham. Enzyme activity is mU/mg mitochondrial protein. N=5 in each group.

In the heart, VF+CPR decreased complex I activity in SSM and remained low during the first hour of ROSC (*Figure 25*). NADH:ferricyanide oxidoreductase activity was decreased concomitant with the decrease in complex I activity, suggesting that the site of damage is in the NADH oxidase portion of the complex (*Figure 26*). In contrast, IFM were relatively free of damage with a non-significant trend of decreased complex I activity (*Figure 27*). Complexes II and III did not sustain damage in IFM (*Table 4*).

SSM Electron Transport Chain
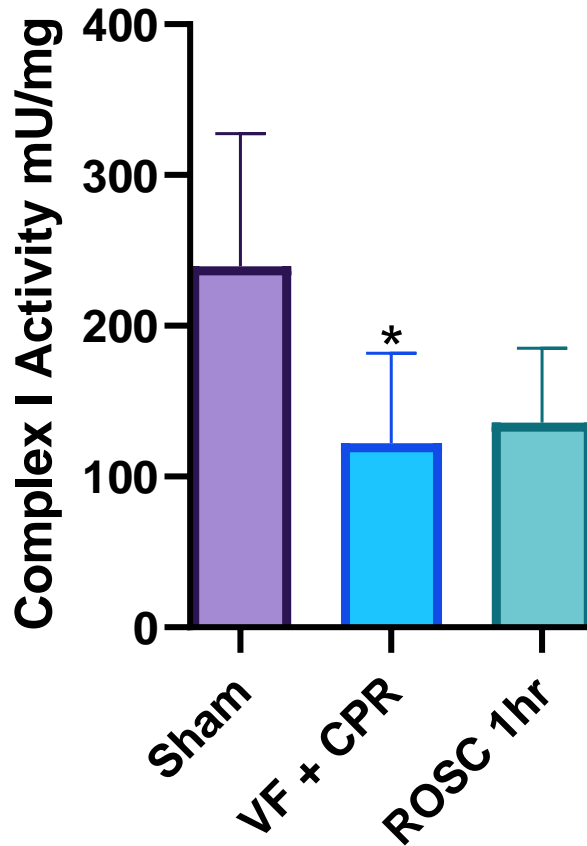
Figure 25. SSM enzyme activity confirmation of Complex I damage. VF+CPR decreased complex I activity. Mean ± SD, One-way ANOVA, Tukey Post-hoc *p<0.05 **p<0.01 ***p<0.001 vs Sham N=5 in each group. My contribution (a) design of the experiments (c) Analysis of the data.

SSM Electron Transport Chain
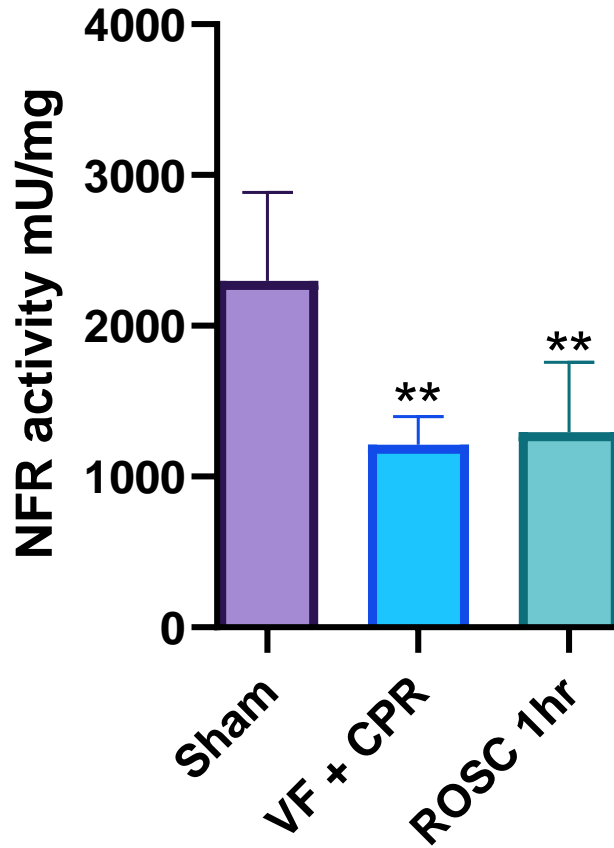
Figure 26. SSM enzyme activity of NADH:ferricyanide oxidoreductase-decreased NFR activity. Mean ± SD, One-way ANOVA, Tukey Post-hoc *p<0.05 **p<0.01 ***p<0.001 vs Sham N=5 in each group. My contribution (a) design of the experiments (c) Analysis of the data.
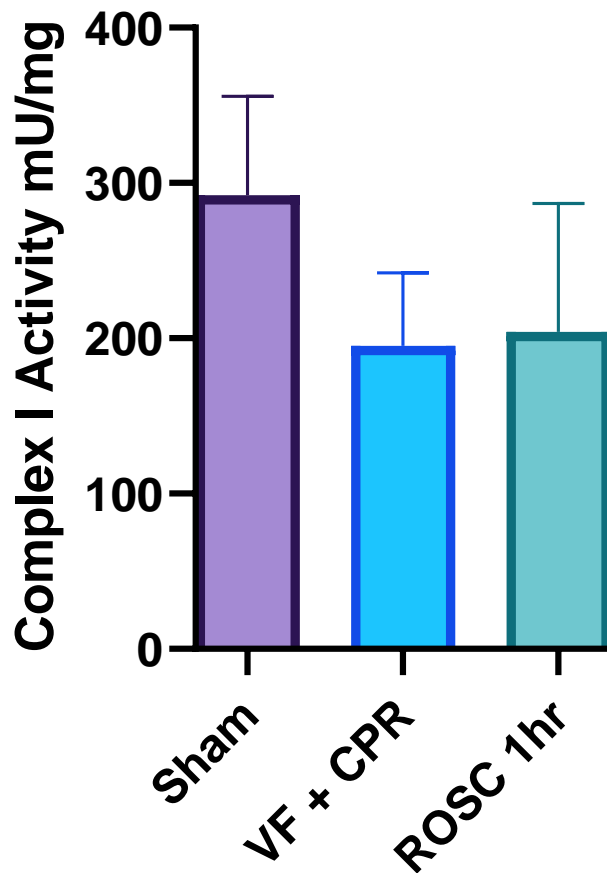
Figure 27. IFM enzyme activity of Complex I. Mean ± SD, One-way ANOVA, Tukey Post-hoc $p > 0.05$ vs Sham N=5 in each group. My contribution (a) design of the experiments (c) Analysis of the data.

Calcium retention capacity (CRC) in brain decreased rapidly and was abnormal throughout CA and CPR (*Figure 28*), in contrast to heart CRC that only decreased following ROSC in both SSM and IFM *(Figure 29 and Figure 30).* Thus, brain mitochondria are more susceptible to MPTP opening compared to heart mitochondria. Furthermore, an increased susceptibility to MPTP opening is already evident in brain mitochondria during the initial period of CA.

BM Calcum Retention Capacity
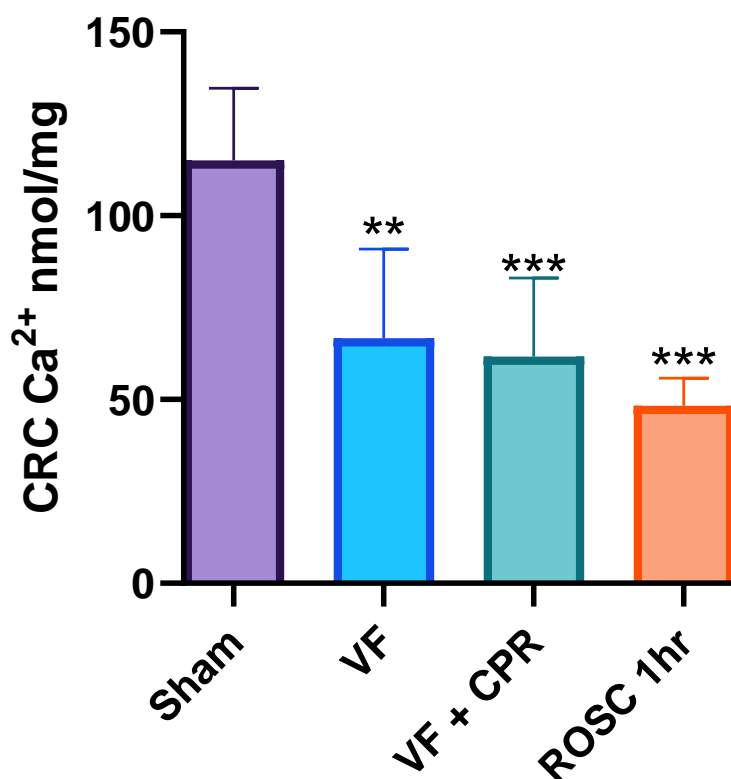
Figure 28. BM calcium retention capacity (CRC)-measured as an index of susceptibility to MPTP opening. CRC in brain rapidly decreased, and was abnormal throughout CA and CPR. Mean ± SD, One-way ANOVA, Tukey Post-hoc *p<0.05 **p<0.01 ***p<0.001 vs Sham N=6 in each group. My contribution (a) design of the experiments (c) Analysis of the data.

SSM Calcum Retention Capacity
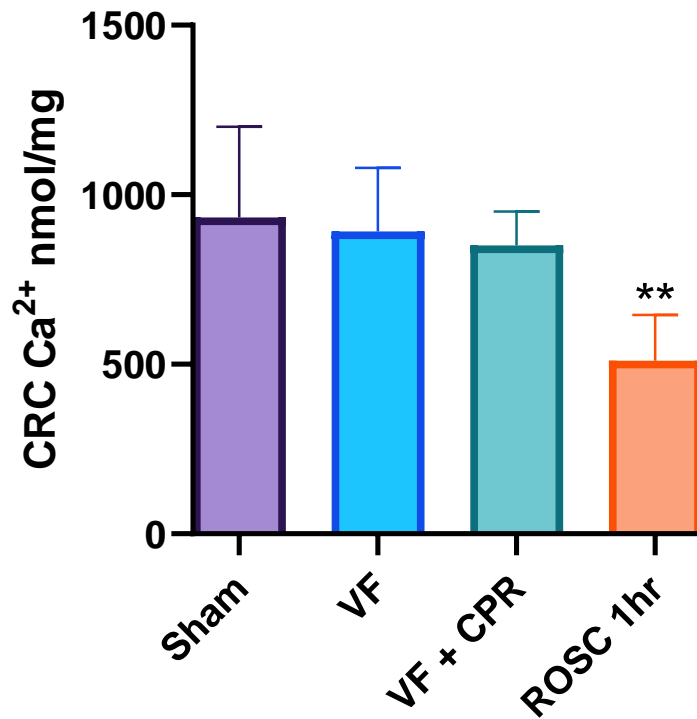
Figure 29. SSM calcium retention capacity (CRC)-measured as an index of susceptibility to MPTP opening. Heart mitochondria only decreased following ROSC. Mean ± SD, One-way ANOVA, Tukey Post-hoc *p<0.05 **p<0.01 ***p<0.001 vs Sham N=6 in each group. My contribution (a) design of the experiments (c) Analysis of the data.

IFM Calcum Retention Capacity
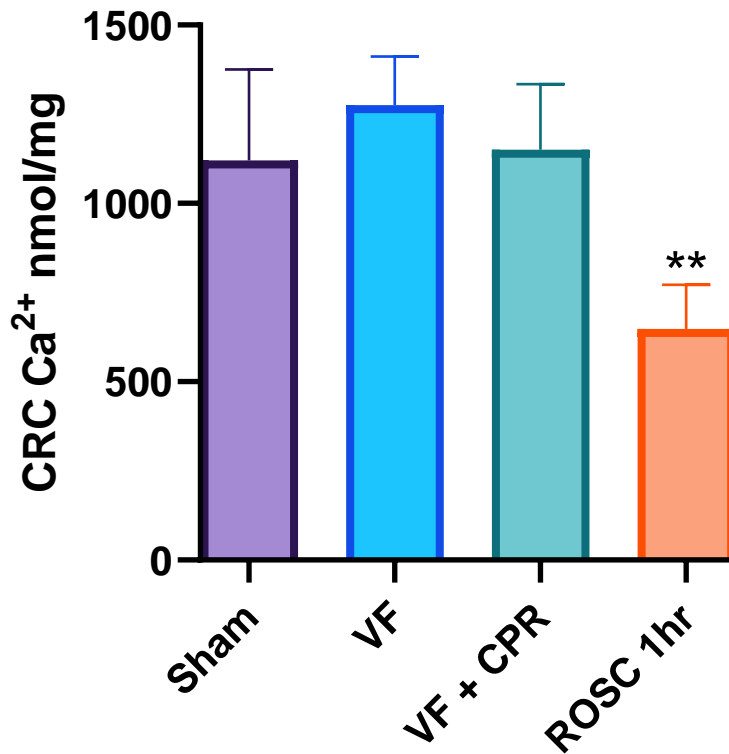
Figure 30. IFM calcium retention capacity (CRC)-measured as an index of susceptibility to MPTP opening. Heart mitochondria only decreased following ROSC. Mean ± SD, One-way ANOVA, Tukey Post-hoc *p<0.05 **p<0.01 ***p<0.001 vs Sham N=6 in each group. My contribution (a) design of the experiments (c) Analysis of the data.

DISCUSSION

Our experimental CA/CPR (145, 162, 163) model indicates that mitochondrial damage is different between rat brain and heart. Brain mitochondria are more sensitive to global ischemia. Heart SSM are minimally damaged whereas IFM remain intact. In contrast, mitochondrial OXPHOS and ETC indicate that complex I is markedly decreased in brain. This is in line with Borutaite et al. reporting a decrease in complex I activity after 20-25min of global no-flow ischemia (161). Alleviation of complex I injury may be an important therapeutic target to reduce brain injury during CA and CPR. Currently, no pharmacological treatment has been approved for

neuroprotection after CA (9). Donnino et al's characterization of mitochondrial injury after cardiac arrest (COMICA) clinical trial demonstrated mixed results with mitochondrial injury markers post-arrest. Pathways in humans remain incompletely characterized and need to be studied further (34).

OXPHOS, with glutamate is used to assess the response of intact mitochondria to ischemia (164). Ischemia leads to progressive injury to the ETC (22, 127) and ischemic mitochondrial damage occurs more rapidly in SSM, which are located beneath the plasma membrane, than in IFM, which are located between the myofibrils (127). SSM were more susceptible to injury than IFM, which is consistent with previous studies (127, 150, 160). SSM and IFM injury induced by 8 min of CA did not progress despite markedly reduced blood flow and oxygen supply during 8 min of CPR. Results are less severe than studies of more prolonged ischemia (15, 131, 150). Myocardial mitochondria show a markedly increased susceptibility to opening of the MPTP following a more robust reperfusion resulting from one hour of ROSC. There is a significant decrease in mitochondrial function following 25 min of stop-flow myocardial ischemia (129). CPR is sufficient to interrupt or slow the ongoing ischemic insult imposed on myocardial mitochondria, and possibly extends the period of mitochondrial viability during early stages of CA.

The rate of OXPHOS was markedly decreased in brain mitochondria oxidizing complex I substrate (*Figure 20*). A complex I defect occurs during cerebral ischemia or CA. This was confirmed by enzyme activity measurement (*Figure 23*). Furthermore, the activity of NADH:ferricyanide oxidoreductase (NFR) was decreased (127) (*Figure 24*). Ferricyanide is an artificial electron acceptor that is reduced by the flavin mononucleotide cofactor in the NADH dehydrogenase component of complex I (165). Complex I activity decreases during ischemia in

79

cardiac mitochondria due to a decrease in the NADH dehydrogenase component likely due to loss of the flavin mononucleotide coenzyme (156, 166-168). Damage to the NADH dehydrogenase component of complex I can increase electron leak and ROS production, contributing to brain damage after CA (168). Reperfusion of ischemic brain also leads to massive generation of ROS (169). Activated microglia convert into a pro-inflammatory (M1) phenotype that obtains macrophage-like properties (such as antigen presentation) and generates several pro-inflammatory mediators (such as IL1 β, TNFα, and ROS) that can disrupt the blood brain barrier (BBB) (9). Generation of ROS, including from complex I itself, can lead to complex I damage (125, 129, 169). Development of ischemic acidosis during CA might also facilitate flavoprotein dissociation, hindering electron transfer and impairing complex I activity (15). Consistent with the decrease in NFR, ischemia induced loss of FMN may contribute (170). Ischemia also damages complex I at sites more distal in the path of electron flow at iron sulfur centers, including immediately proximal to the quinol binding site (129, 171). Complex I also undergoes a conformational change from an active form to a "de-active" form (170). However, the de-active form of complex I should be reactivated under conditions of the ETC assay. Whether these potential contributing factors contribute to the beneficial effects of CPR remains to be explored. In general, brain mitochondrial dysfunction following ischemia is associated with impaired complex I activity.

Mitochondrial dysfunction after resuscitation from CA due to impaired electron transport through the respiratory complexes of the ETC leading to decreased rates of OXPHOS is poorly characterized in patients who achieve ROSC. ETC dysfunction reduces mitochondrial membrane potential. Impaired OXPHOS leads to decreased generation of high energy phosphates. Direct damage to mitochondria leads to diminished electron flow and increased ROS generation,

favoring oxidative tissue injury. Damage to the mitochondrial inner membrane leads to decreased membrane potential and favors cytochrome *c* release into the cytosol, which activates cell death (14). Mitochondrial defects are associated with reduced ATP generation, metabolic failure, altered signaling pathways, and induction of apoptosis.

Susceptibility of MPTP opening has been implicated as a key mechanism underlying both necrotic and apoptotic cell death during ischemia and reperfusion (172-174). Kristian et al. report mitochondria energized with either electron transport complex I or complex II substrates within an acidic environment promote permeability transition pore opening (175). MPTP opening increases the permeability of both inner and outer mitochondrial membranes. Because of MPTP opening, solutes with a molecular mass of up to 1,500 Da non-selectively diffuse across the mitochondrial inner membrane, leading to mitochondrial depolarization, uncoupling of OXPHOS, and large amplitude swelling, leading to ATP depletion and cell death (174). The effectiveness of mPTP inhibitors to protect the myocardium has not been observed in clinical trials of acute myocardial infarction (176). However, neuronal cyclophilin D represents a promising therapeutic target for Alzheimer's disease (177). The development of nopeptidic small molecule inhibitors of cyclophilin D could be a promising approach for cardiac arrest as our study demonstrates a markedly increased susceptibility to MPTP opening within brain mitochondria. This occurs during the initial period of ischemia due to CA and persists throughout the course of CPR, including resuscitation and ROSC. In contrast, the susceptibility of cardiac MPTP opening increases during ROSC. Therefore, brain MPTP susceptibility during ischemia is different than in heart (178). Briston et al. reports complex I-driven respiration is reduced after MPTP opening (179). Cardiac mitochondria are more resistant to damage during ischemia. However, increased susceptibility to MPTP opening occurred during ROSC, likely as a

81

result of calcium overload associated with reperfusion (180, 181). Therefore, reperfusion injury affects heart mitochondria even after short durations of ischemia.

A complex I targeted therapeutic could also potentially ameliorate brain mitochondrial dysfunction after cardiac arrest. Preservation of complex I activity could potentially provide better clinical outcomes of survival with good neurological function (currently only 8.2%) and survival to hospital discharge (currently 10.4%) (1). Further research is necessary regarding mechanism among cardiac arrest victims. In a middle cerebral artery occlusion (MCAO) rat model, decreased activity of Complex I, III, and IV after ischemia/reperfusion injury contributed to decreased mitochondrial function, which was restored with a low-dose of methylene blue (MB) (182). The neuroprotective role of MB in cerebral ischemia has been suggested to be caused by increased mitophagy and maintenance of mitochondrial membrane potential (182).

Therapeutic Hypothermia is a standard intervention to improve outcomes following cardiac arrest and cardiopulmonary resuscitation. Although therapeutic hypothermia can preserve energy stores, current work also suggests that reactive oxygen species production is also decreased (183, 184). This is plausible, since hypothermia decreases rates of electron transport. Transient, partial blockade of electron transport during early reperfusion protects the heart (125, 185, 186). Hypothermia slows electron transport and reactive oxygen species generation in the intact heart with a similar profile to that of blockade of electron transport (187). Thus, there is a premise for protection of the brain and heart following cardiac arrest by therapeutic hypothermia (WIN55 via CB_1).

Complex I preservation would mitigate lowered levels of ATP, dramatic shifts in calcium concentration and cell swelling. Our study demonstrates the brain is most reliant on mitochondrial bioenergetics (188). It takes less ischemia/reperfusion to cause dysfunction in the

82

brain compared to the heart. Reperfusion of ischemic brain will lead to massive generation of free radicals such as ROS and activation of several signaling pathways (9). Our findings suggest that CPR is able to preserve heart mitochondrial function and viability longer than that of brain during ongoing global ischemia despite low blood flow and oxygen delivery. A metabolic phase of cardiac arrest (188) occurs earlier than reported previously. Therefore, preservation of brain complex I activity during CA will likely continue to emerge as a critical therapeutic target. WIN55 could be a pharmacologic tool as it has been shown to decrease brain injury reducing both delayed cell death and glial damage (38).

CONCLUSIONS

Brain mitochondria are more sensitive to global ischemia compared to heart mitochondria. Additionally, complex I is the most sensitive ETC complex to ischemic injury and its activity determines rate of OXPHOS following CA and resuscitation. Preservation of brain mitochondrial activity and function during CA may enhance outcomes and recovery. Future work is needed to improve current clinical resuscitation success rates by addressing an early therapeutic target preserving complex I activity during CA.

LIMITATIONS

Our generalized use of brain and heart within this dissertation are the cerebrum and whole heart, which is a limitation within the current study. Future studies are needed to address the following: visualization of structural damage using electron microscopy, measurement of reactive oxygen species production, measurement of pro-inflammatory mediators and the use of interventions to enhance complex I activity to determine beneficial effects. Analysis of mitochondria with a treatment group of WIN55 would further enhance the mechanism of this pharmacologic tool.

83

CHAPTER 4: Quantitative mass spectrometric analysis of cardiac whole tissue lysate proteome changes from our rat cardiac arrest and cardiopulmonary resuscitation model

RATIONALE

For aerobic cells ischemia is a critical change in the oxygen demand to delivery ratio (189). CA is characterized by severe and generalized ischemia that persists during resuscitation efforts and reverses only after ROSC (2). Ischemia causes reperfusion injury. In general, reperfusion injury is proportional to the magnitude of the preceding period of ischemia. All tissues can withstand variably short periods of ischemia that do not produce detectable functional deficits or evidence of injury. However, once a critical duration of ischemia is exceeded, which varies by cell type and organ, cell injury and/or death ensues (190). Within the usual timeframe of CA and resuscitation, ischemic injury is most severe in organs with high metabolic demands, such as the brain and heart (2).

Studies have shown that S100A8/A9 levels positively correlate with risk of acute myocardial infarction (191, 192). Additionally, site-specific measurements of S100A8/A9 in patients with acute coronary syndrome demonstrate that S100A8/A9 is markedly more elevated at the site of coronary occlusion compared to systemic circulation (193). Further support of this finding, immunostaining, reveals S100A8/A9 is specifically expressed in neutrophils and macrophages infiltrating the myocardium post-infarction (192). Together, these studies demonstrate S100A8/A9 is a major player in local inflammation caused by acute cardiovascular events.

We hypothesize that S100A8/A9 expression increases within heart whole tissue lysate after CA and CPR. The purpose of this study was to measure proteome changes following CA using quantitative mass spectrometric analysis.

RESULTS

Quantification of total protein concentration of supernatant was determined by a BCA™ Protein Assay (*Figure 31*). 4,997 proteins (Sham 3) were quantitatively identified across 3 groups of 11 samples using one TMT10plex Isobaric Label Reagent Set plus TMT11-131C Label Reagent. 239 of the 4,997 proteins identified to be differentially expressed (fold change >=1.25, p<0.05, n=3 or 4) upon CPR compared to Sham+Norm (*Figure 32*). 104 proteins changed by at least 25% highlighted in purple (fold change >=1.25, p<0.05). Housekeeping proteins are not changed. Another volcano plot of the 171 proteins changed <0.75 and >1.25 was compared between CPR and Sham+Norm (*Figure 33*).

Four proteins that were most significant were Fibrinogen gamma chain precursor (functions in hemostasis as one primary component of blood clots and functions during the early stages of wound repair to guide cell migration during re-epithelialization) (194), Parvalbumin alpha (in muscle it is thought to be involved in relaxation after contraction) (195), G-protein coupled receptor (involved in cell recognition and communication processes) and Transketolase-like protein 2 isoform X1(protein has several cofactor biding sites including calcium binding) (196). These four proteins with the greatest change in expression are noted, however, we focused on S100A8 and S100A9 due to Li et al. connecting S100A8/A9 signaling with mitochondrial complex I dysfunction and cardiomyocyte death in response to myocardial ischemia reperfusion injury (132).

BCA Protein Assay
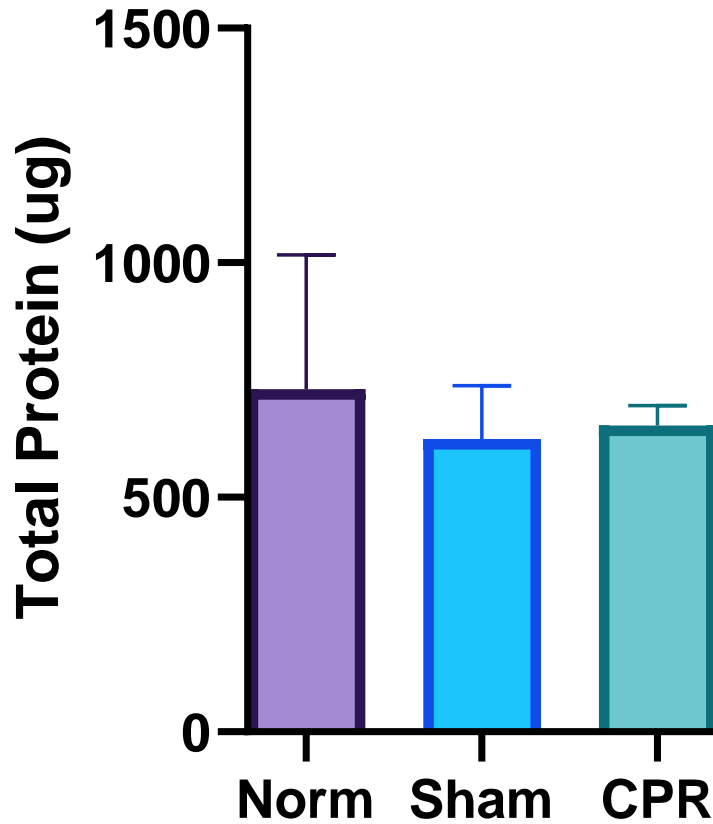
Figure 31. Supernatant BCA Assay. Mean ± SD, One-way ANOVA, Tukey Post-hoc p> 0.05 vs Norm N=3 (Norm) or 4 (Sham and CPR). Equal protein loading allows for comparison of TMT tags. My contribution (a) design of the experiments (c) Re-analysis of the data provided by Poochon Scientific.
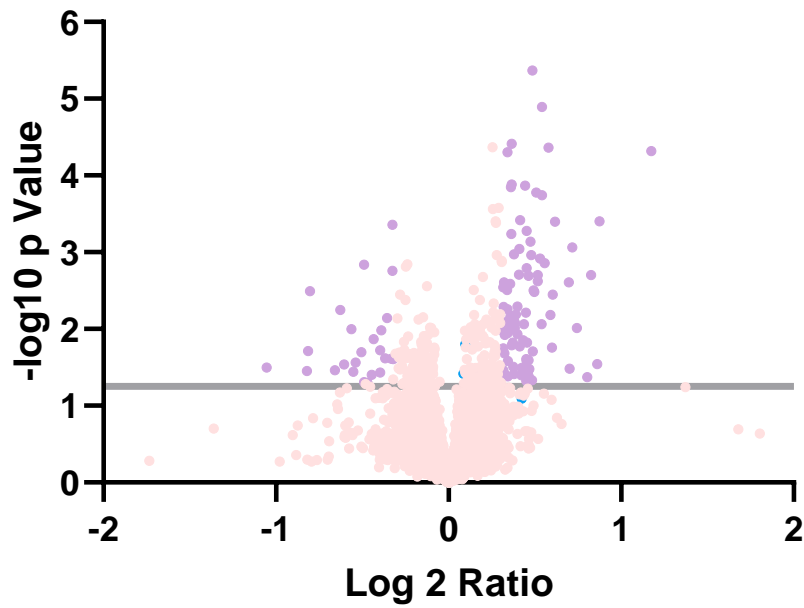
CPR/Sham+Norm

Figure 32. Volcano Plot 4,997 Proteins Identified by Poochon Scientific. My contribution (a) design of the experiments (c) Re-analysis of the data provided by Poochon Scientific.

CPR/Sham+Norm
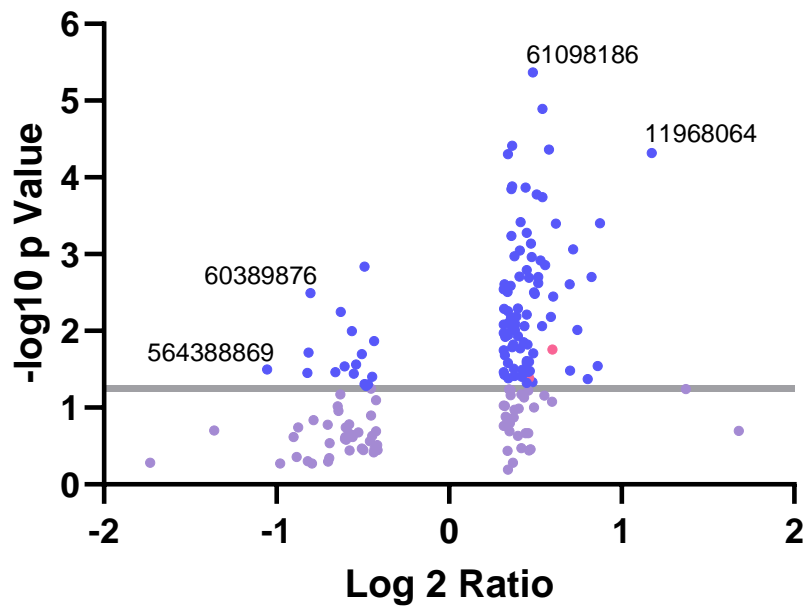
Figure 33. Volcano Plot CPR/Norm+Sham Ratio <0.75 and >1.25-171 Proteins Identified. Accession Numbers 61098186-Fibrinogen gamma chain precursor [Rattus norvegicus], 11968064-Parvalbumin alpha [Rattus norvegicus], 60389876- G-protein coupled receptor and 564388869- Transketolase-like protein 2 isoform X1 [Rattus norvegicus]. Pink are S100A8 and S100A9[Rattus norvegicus]. My contribution (a) design of the experiments (c) Re-analysis of the data provided by Poochon Scientific.

Kyoto Encyclopedia of Genes and Genomes (KEGG), a collection of genomes and biological pathways, was used to map pathways from the 4,997 proteins identified by Poochon Scientific (3,195 Kegg were able to be converted from the 4,997 NCBI). Biological pathways such as oxidative phosphorylation (*Figure 34*), complement and coagulation cascades (*Figure 35*), toll-like receptor signaling (*Figure 36*) and chemokine signaling were mapped (*Figure 37*). The complement and coagulation cascade was identified to have multiple proteins expressed after CA and CPR (64 Kegg were able to be converted from the 104 proteins >1.25) (*Figure 38*). Genes highlighted in red indicate presence.
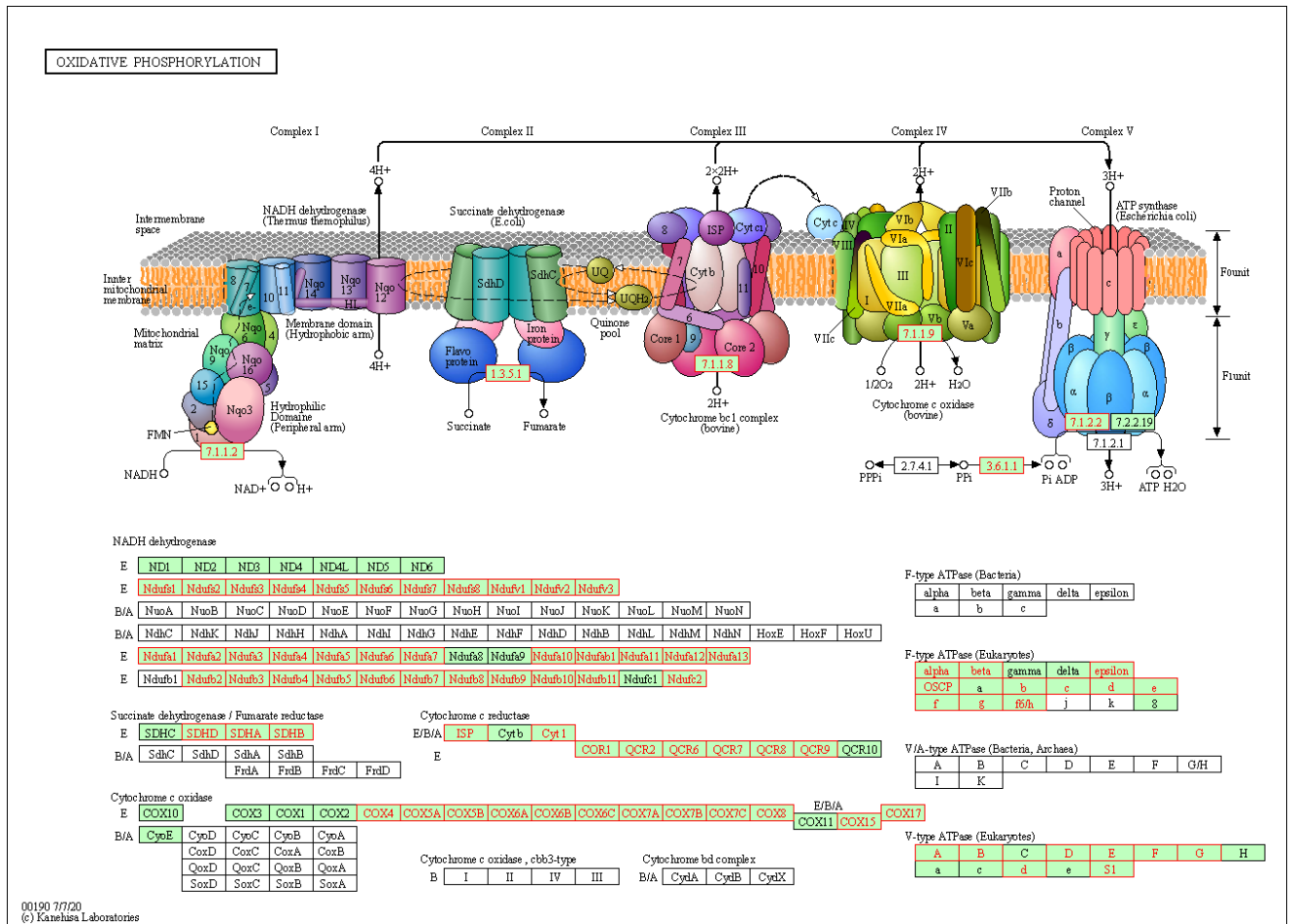
Figure 34. 3,195 converted Kegg proteins rno00190 Oxidative phosphorylation-Rattus norvegicus (rat) (81). Red indicates gene presence. My contribution (a) design of the experiments (c) Kegg pathway analysis of data provided by Poochon Scientific.

Figure 35. 3,195 converted Kegg proteins [rno04610](#) Complement and coagulation cascades-
Rattus norvegicus (rat) ([36](#)). Red indicates gene presence. (a) design of the experiments (c) Kegg
pathway analysis of data provided by Poochon Scientific.
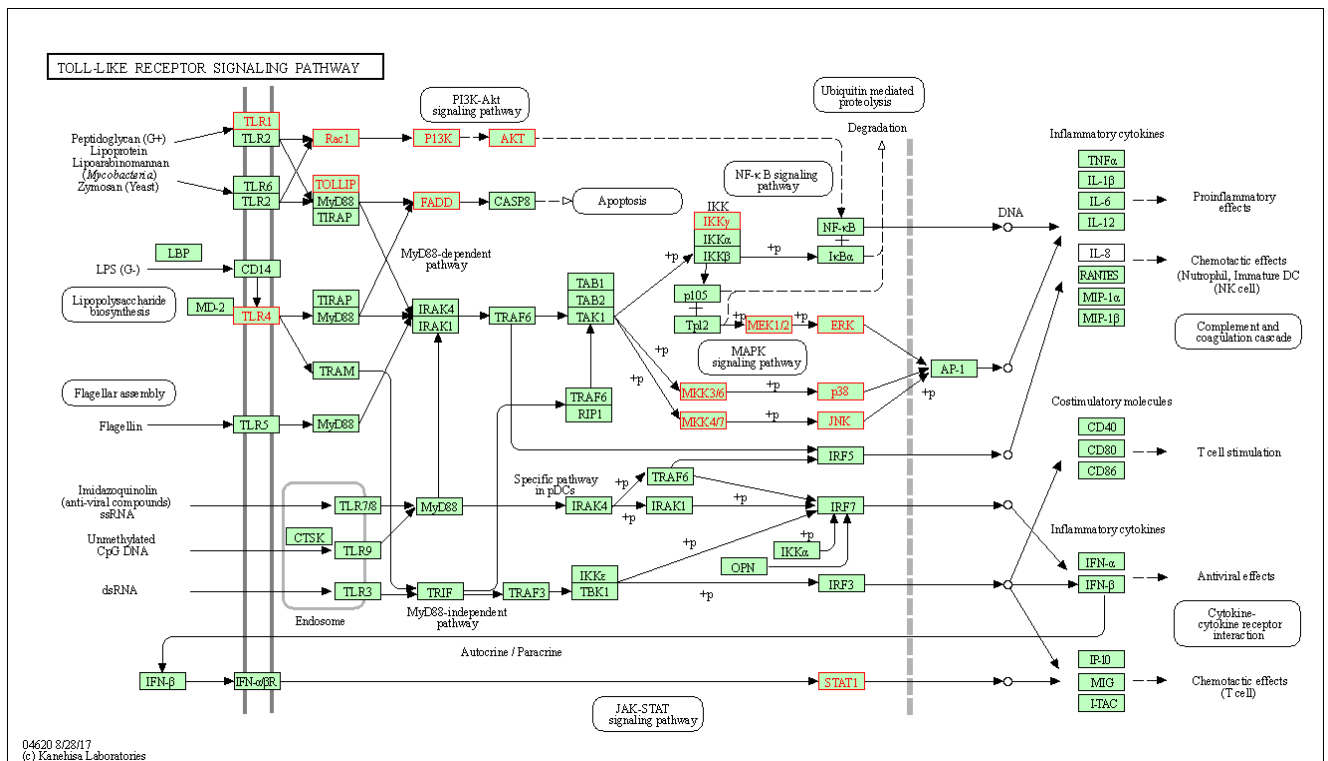
Figure 36. 3,195 converted Kegg proteins rno04620 Toll-like receptor signaling pathway-
Rattus norvegicus (rat) (16). Red indicates gene presence. (a) design of the experiments (c) Kegg
pathway analysis of data provided by Poochon Scientific.
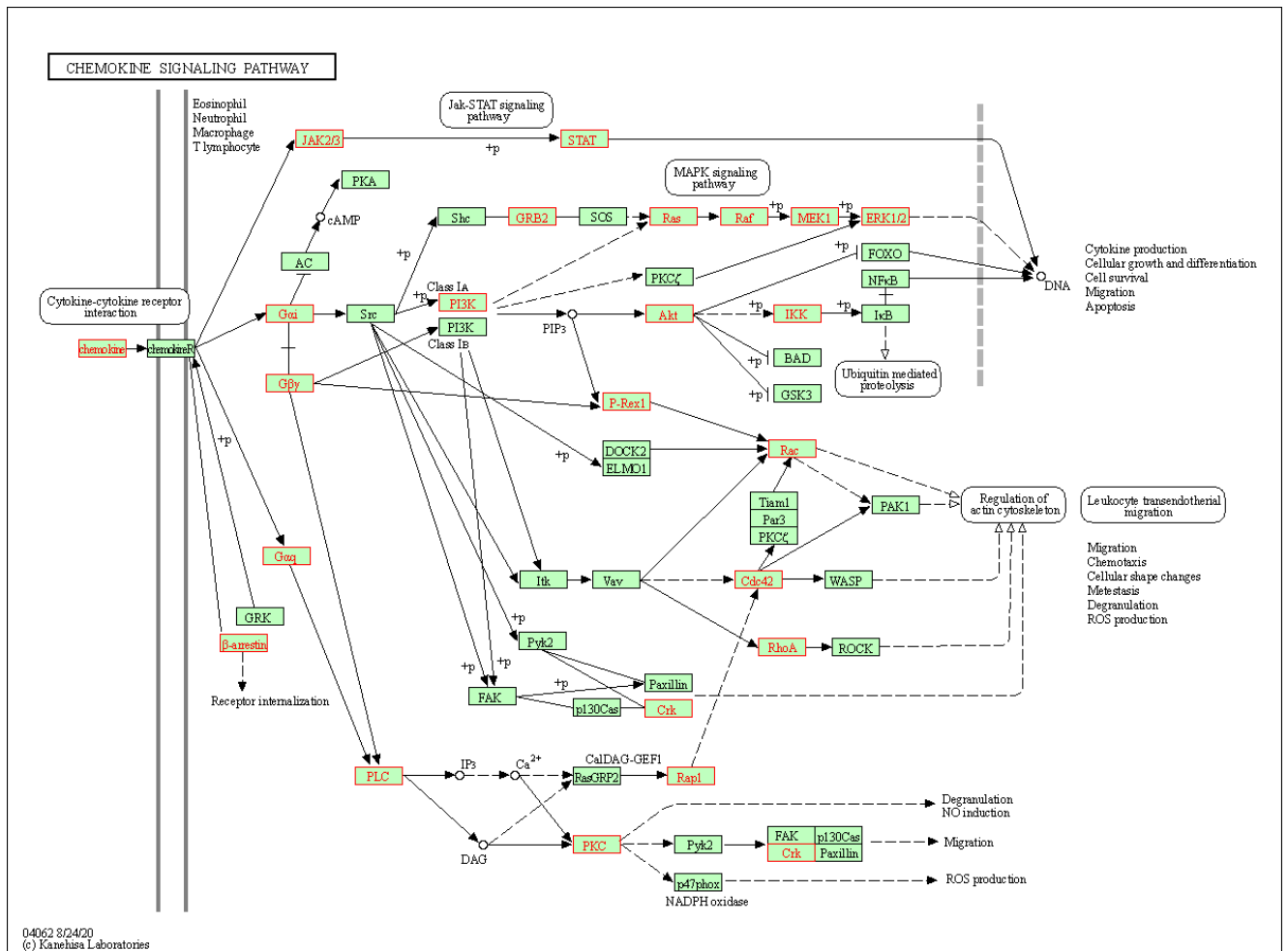
Figure 37. 3,195 converted Kegg proteins rno04062 Chemokine signaling pathway- Rattus norvegicus (rat) (37). Red indicates gene presence. (a) design of the experiments (c) Kegg pathway analysis of data provided by Poochon Scientific.
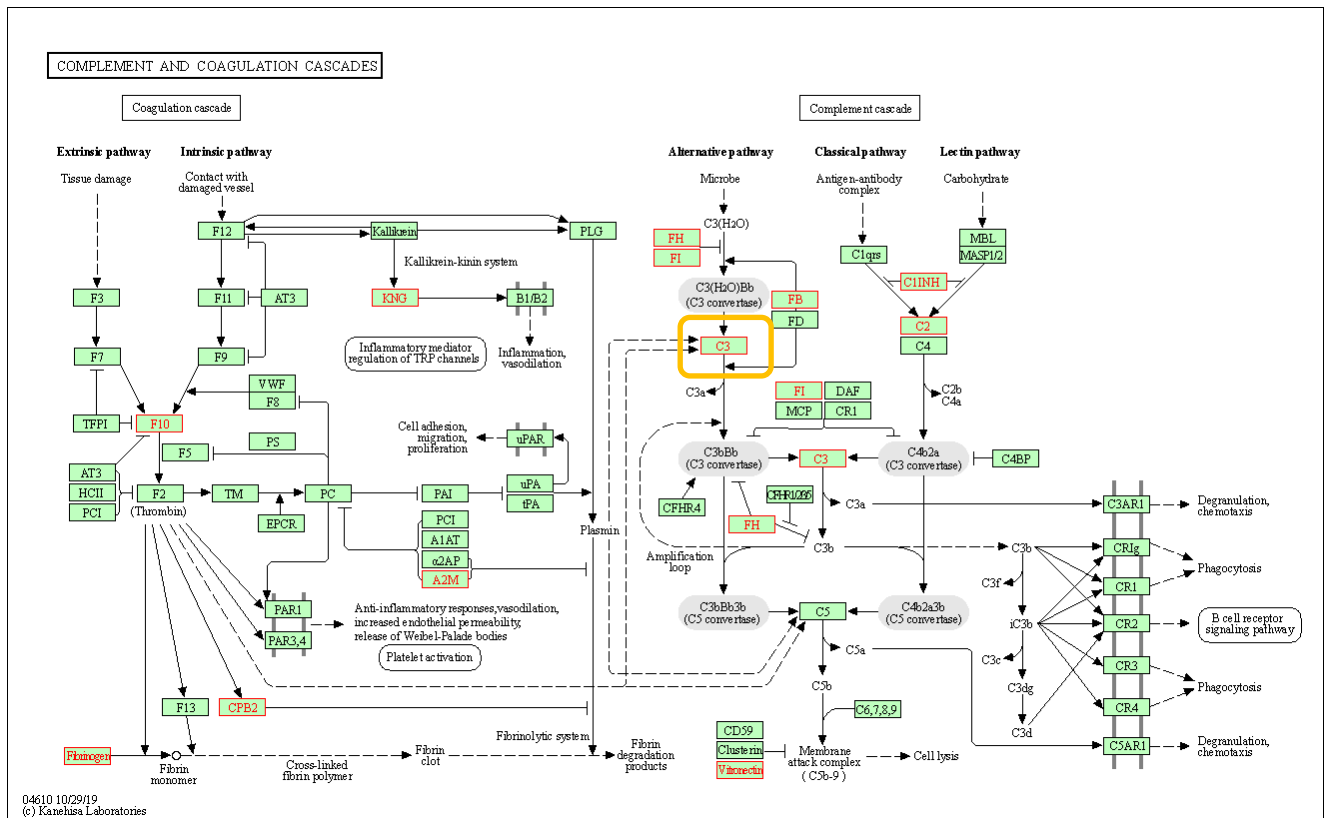
Figure 38. 64 converted Kegg proteins (CPR/Sham+Norm Ratio -log10 p>1.25) rno04610 Complement and coagulation cascades-Rattus norvegicus (rat) (13). Red indicates gene presence. (a) design of the experiments (c) Kegg pathway analysis of data provided by Poochon Scientific.

A scatter plot for the CA and CPR data that was used to create the KEGG pathway in

Figure 38 was generated through multidimensional scaling. Similar GO terms are grouped closer

together in the plot based on similar semantics (*Figure 39*). Color of biological processes clusters

corresponds to the p-value input provided by Poochon Scientific. Biological processes that are

most enriched and clustered together are pathways involved with ischemia reperfusion injury.
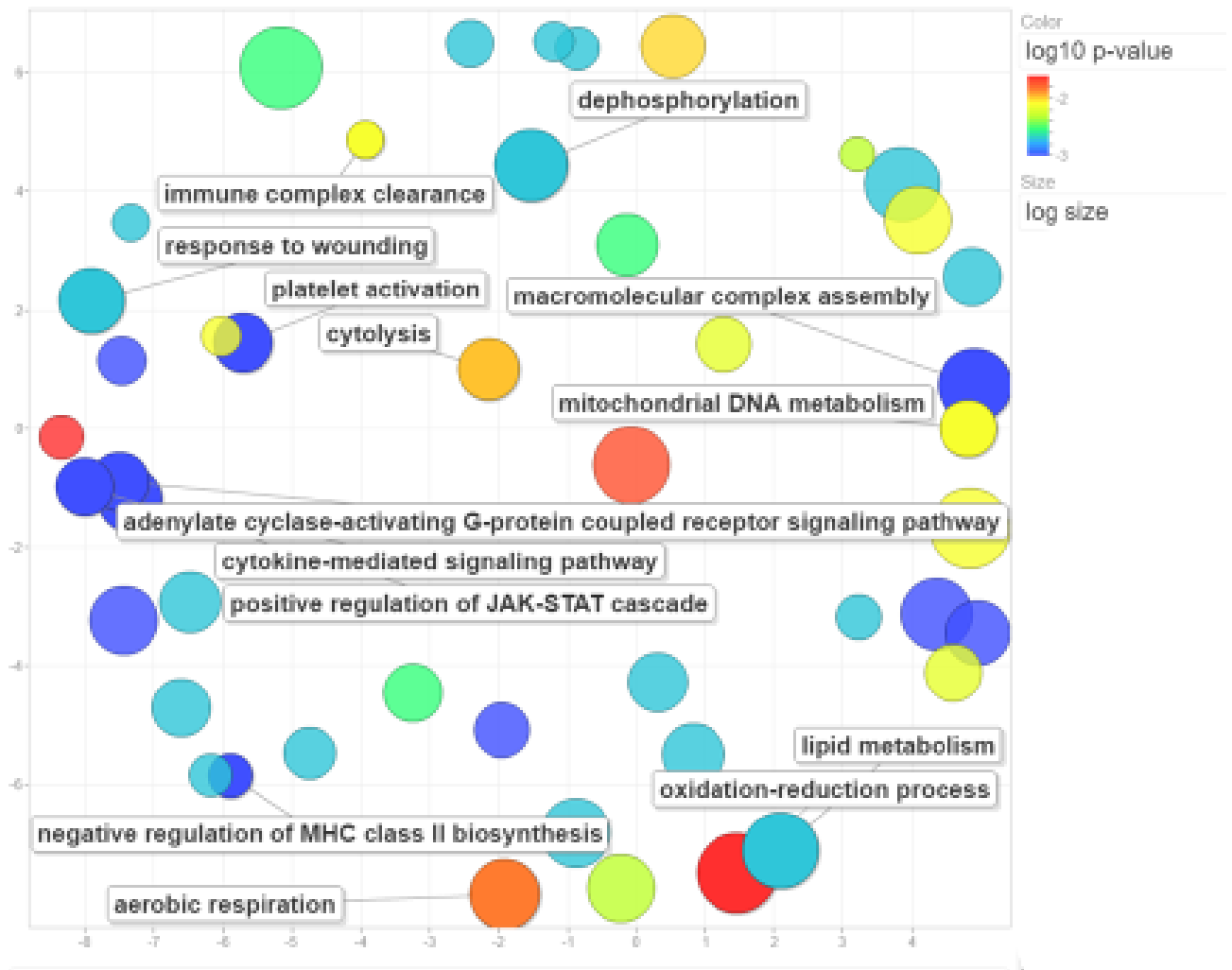
Figure 39. REVIGO gene ontology clustering of biological processes based on semantic similarity. (a) design of the experiments (c) Kegg pathway analysis of data provided by Poochon Scientific.

DISCUSSION

CPR/Sham+Norm ratio DAVID 6.8 analysis showed S100A8/A9 expression increased (CPR avg higher than Sham+Norm avg). Intracellular S100A8/A9 is best known for the ability to regulate transendothelial migration of leukocytes (73, 197). Both are constitutively expressed in neutrophils, monocytes and dendritic cells. However, they can also be intensely upregulated upon the onset of trauma, infection, heat, stress and other inflammatory processes (69).

Extracellular S100A8/A9 is a damage associated molecular pattern after being released from damaged or activated cells, therefore increased expression seen in heart tissue lysates obtained at ROSC is due to ischemia/reperfusion injury from CA.

Relative cardiac S100A8 and S100A9 mRNA expression in mice subjected to myocardial IR procedures had peak S100A8/A9 mRNA expression at 6hrs in the heart. Proteomic analysis from Poochon Scientific was performed on heart tissue lysate collected at ROSC (no more than 30 minutes from VF). S100A8/A9 is critical for IR induced myocardial death, the sequelae of adverse cardiac remodeling, and heart failure (132). The release of S100A8 and S100A9 can induce C3/CFB complement activation and secretion of multiple cytokines in inflammatory cells to sustain and exacerbate inflammation (69). Therefore, they control early stages of inflammation for cardiac IR injury after CA. Inhibition of S100A8/A9 activity during CA could be a potential therapeutic target.

CONCLUSIONS

S100A8 and S100A9 have promising potential as new biomarkers for cardiovascular inflammation. Inhibition of S100A8/A9 activity during CA may enhance outcomes and recovery.

LIMITATIONS

Confirmation of proteomic analysis still needs to be done at the tissue level. If we have tissue available after lipidomic analysis from a collaborator-a future study could include immunoblot of the brain and heart for S100A8 and S100A9. Du et al. discovered global ischemia did not alter immunoblot protein levels of S100A8 and S100A9 at 0, 30 and 60 min. *In vivo* ischemia for 2hrs resulted in strong S100A8 and S100A9 overexpression (198). Li et al reported serum S100A8/A9 levels were significantly increased 1 day after percutaneous coronary intervention in patients with acute myocardial infarction(132). Therefore, future studies could

look at expression of S100A8 and S100A9 peptides in brain and heart and protein levels in plasma at ROSC 4hrs or with a survival model at 24, 48 and 72hrs. Analysis of S100A8/A9 protein expression with a treatment group of WIN55 would further enhance the mechanism of this pharmacologic tool.

CHAPTER 5: Anti-Inflammatory activity of WIN55, 212-2, a non-selective cannabinoid CB$_1$/CB$_2$ receptor agonist in cultured RAW264.7 macrophage cells

RATIONALE

Macrophages are innate immune cells that form the first line of defense against invading pathogens (62). Under different pathophysiologic conditions, activated macrophages are capable of differentiating into phenotypically different states, including the classically activated (M1) and the alternatively activated (M2) (61). M1 macrophages are characterized by the production of pro-inflammatory cytokines, such as IL1, IL6, IL12, TNFα and chemokines, involved in various inflammatory processes (61). They are major producers of TNFα and are also highly responsive to TNFα (62). TNFα is rapidly released after trauma, infection, or exposure to bacterial-derived LPS and has been shown to be one of the most abundant early mediators in inflamed tissue (62).

TLR signals have an important role in regulating macrophage polarization. In particular, the TLR4 ligand LPS promotes macrophage differentiation toward M1 phenotype (61). TNFα has been shown to play a pivotal role in orchestrating the cytokine cascade in many inflammatory diseases and because of this role as a "master-regulator" of inflammatory cytokine production, it has been proposed as a therapeutic target for a number of diseases (62). IL6 is also another pro-inflammatory cytokine secreted by monocytes and macrophages after engagement of Toll-like receptors (TLRs) that promotes inflammatory events (66, 199).

Hao et al. reported oxLDL-induced TNFα expression and ROS generation in RAW 264.7 mouse macrophages is considerably reduced by the synthetic cannabinoid WIN55. Reduced TNFα expression and ROS production is mainly via the CB$_2$ receptor, and partially linked with the CB$_1$ receptor. MAPK and NF-kappa β are inhibited by WIN55 activated CB$_1$/CB$_2$ receptor signaling, suggesting their involvement in the attenuation of TNFα expression and ROS generation (200). Therefore, we hypothesize that pre-treatment with WIN55 will have anti-

inflammatory effects against LPS induced pro-inflammatory mediators TNFα, IL6 and IL1β. The purpose of this study was to measure LPS induced TNFα, IL6 and IL1β protein expression with and without pre-treatment of WIN55 in mouse RAW 264.7 macrophages.

RESULTS

TNFα, IL6 and IL1β were all increased following LPS stimulation. Pre-treatment with WIN55 decreased TNF-α (9,206±847 (SD) pg/mL) compared to 6hrs LPS (15,694±2,285 p<0.05) (*Figure 40*). Pre-treatment with WIN55 also decreased IL6 (7,136±1,238) and IL-1β (89±21) compared to 24hrs LPS (10,318±2,092 and 207±26 p<0.05) *(Figure 41 and Figure 42).*

TNFα 6hrs
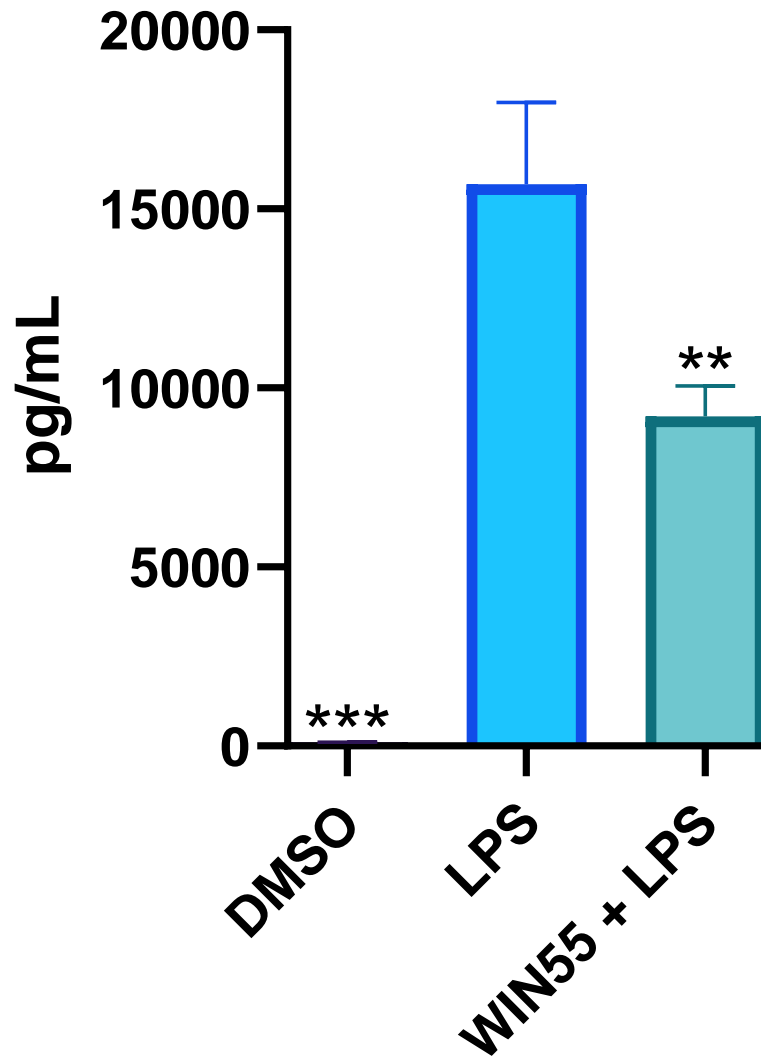
Figure 40. Pre-treatment with WIN55 decreased TNFα compared to 6hrs LPS Mean ± SD, One-way ANOVA, Tukey Post-hoc *p<0.05 **p<0.01 ***p<0.001 vs LPS N=3 in each group. My contribution (a) design of the experiments (b) execution of experimental procedure (c) Analysis of the data.

IL6 24hrs
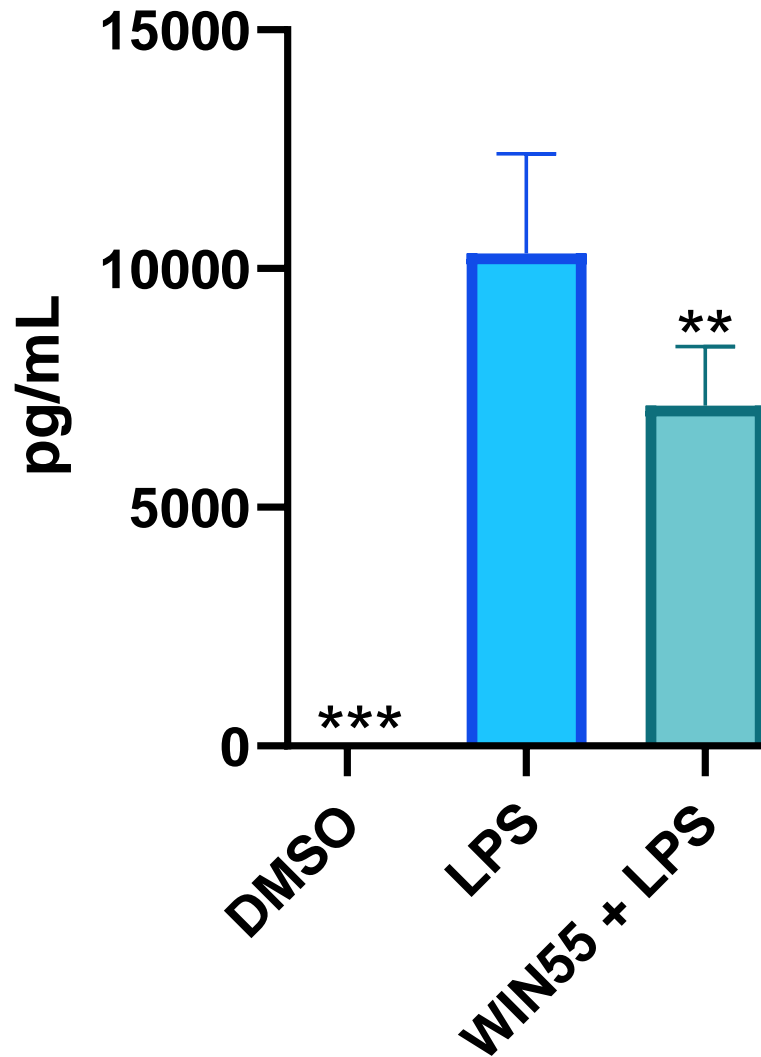
Figure 41. Pre-treatment with WIN55 decreased IL6 compared to 24hrs LPS Mean ± SD, One-way ANOVA, Tukey Post-hoc *p<0.05 **p<0.01 ***p<0.001 vs LPS N=6 in each group. My contribution (a) design of the experiments (b) execution of experimental procedure (c) Analysis of the data.

IL1β 24hrs
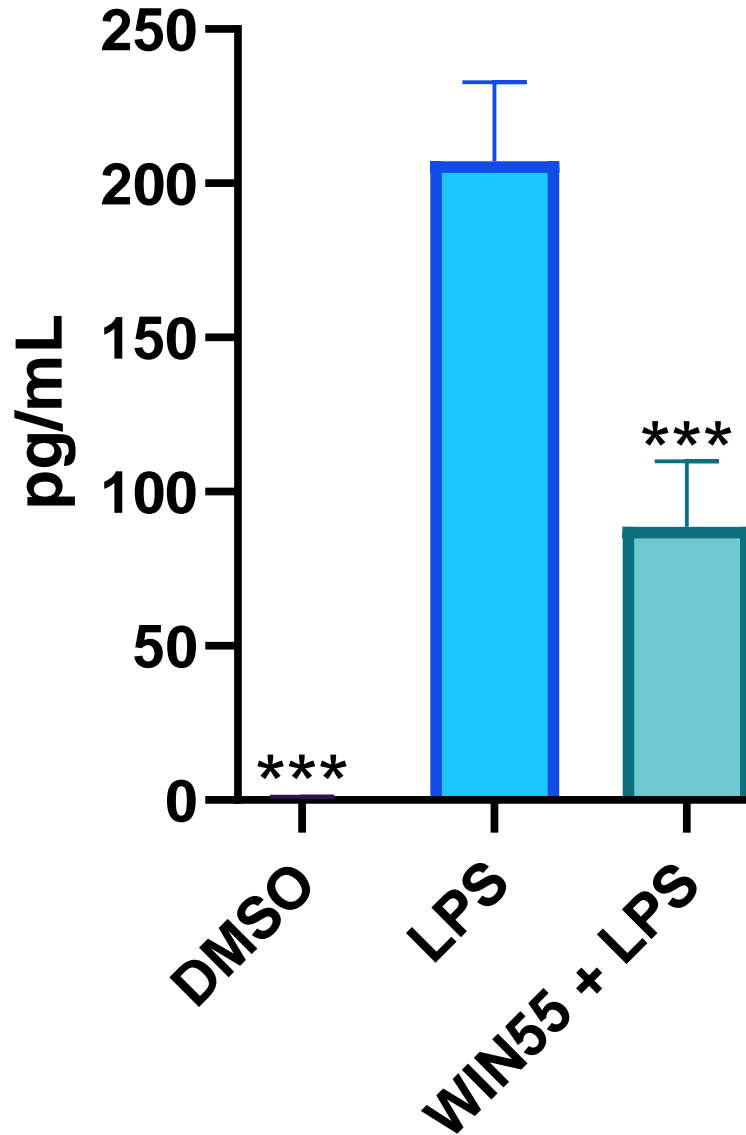
Figure 42. Pre-treatment with WIN55 decreased IL1β compared to 24hrs LPS Mean ± SD, One-way ANOVA, Tukey Post-hoc *p<0.05 **p<0.01 ***p<0.001 vs LPS N=6 in each group. My contribution (a) design of the experiments (b) execution of experimental procedure (c) Analysis of the data.

DISCUSSION

LPS is a ligand for TLR 4. It is an endotoxin from the walls of Gram-negative bacteria and is a potent stimulator of inflammatory cytokines in macrophages (201). The initial acute innate immune response to LPS primes the adaptive immune system against further infection (202). Macrophages are the major players in both innate and adaptive inflammatory responses. For this reason, WIN55 was examined for its effect on the expression of TNFα, IL6 and IL1β protein in mouse RAW 264.7 macrophage cells stimulated with LPS. Our macrophage cell culture model indicates that WIN55 inhibited LPS stimulated proinflammatory mediators.

CONCLUSION

WIN55 inhibited LPS induced expression of pro-inflammatory cytokines.

LIMITATIONS

Confirmation of the CB$_2$ receptor as anti-inflammatory still needs to be validated *in vitro*. There are two different antagonists of CB$_2$ (SR144528 (114) and AM630 (200)) that can be tested to determine if administration blocks the effect of WIN55. Antagonists of CB$_1$ such as SR141716A and AM251 also need to be tested to determine if administration blocks the effect of WIN55. Further studies are also needed using more specific CB$_2$ receptor agonists such as HU308 or JWH-133 (200). Treatment with recombinant S100A8 proteins should also be determined. RAW264.7 macrophage cells should be treated with WIN55 (5 μM) (142) for 2 h, then treated with S100A8 for 6hrs and 24 hrs. S100A8 acts not only as a chemoattractant to macrophages but also as a proinflammatory factor (203). Inhibitors of S100A8 and/or S100A9 should also be tested *in vitro*. PPARγ expression should also be determined as WIN55 induced PPARγ expression was partially attenuated by AM630 in BEL-7402 cells (204). The effects of WIN55 should also be tested to determine if they are attenuated by PPARγ antaonist GW9662

102

(204). PPAR-γ agonists significantly reduced adipose S100A8 mRNA level and plasma S100A8/A9 complex concentrations in obese diabetic mice and human subjects (203). After these effects are determined in RAW264.7 macrophage cells confirmation studies can be conducted in human THP-1 cell lines.

CHAPTER 6: One mechanism of anti-inflammatory activity of cannabinoid agonist WIN55, 212-2 on outcomes of CPR is binding cannabinoid receptor 2 (CB$_2$)

RATIONALE

In non-traumatic CA, common causes are ventricular fibrillation cardiac arrest (VFCA) and asphyxial cardiac arrest (ACA) (205). Recent data from several large population cohorts, covering over 40,000 patients, demonstrate proportions of initial ventricular tachycardia/ventricular fibrillation in the range of 20-25% (13). The 2016 weighted national estimate of emergency department visits with a principal diagnosis of either CA or ventricular fibrillation/flutter was 183,629 patients among the National Emergency Department Sample (1). For this reason, our physiologically relevant VF model developed in 1988 has been used in approximately 70 peer-reviewed publications examining resuscitation aspects including: its physiology and pathophysiology, determinants of resuscitability, pharmacologic interventions, and effects of cell therapies (206). Once we confirmed *in vitro* WIN55 inhibited LPS induced expression of pro-inflammatory cytokines within mouse RAW 264.7 macrophage cells we then explored our experimental *in vivo* CA/CPR (145, 162, 163) rat model.

The Weil Institute has published that infusion of WIN55 decreases body temperature from 37 to 34°C within 4 hours after infusion (114, 207). All animals that received WIN55 survive for more than 72 hours with minimal neurological deficits. Post-resuscitation myocardial function is significantly better than control. We therefore demonstrate the feasibility that therapeutic hypothermia could be induced pharmacologically in settings of CPR without compromising outcomes (207). We further demonstrate that hypothermia effects of WIN55 are completely abolished by selective CB$_1$ receptor antagonist SR141716A (114, 208).

104

The role of endocannabinoids (eCBs) in the cardiovascular system is paradoxical because both positive and negative effects are observed, particularly in conditions of cardiovascular dysfunction (209). We hypothesize that CA will increase plasma concentrations of TNFα, IL6 and IL10. Therefore, plasma cytokine levels will be elevated after resuscitation. Intramuscular (IM) administration of SR141716A before VF+CPR followed by infusion of WIN55 5 min after ROSC will prohibit the release of inflammatory mediators caused by CA via the CB_2 receptor. The purpose of this study was to measure hemodynamics (electrocardiogram, aortic and right atrial pressures, blood temperature, and $ETCO_2$ values), myocardial function (EF, CO, and MPI) and plasma protein concentrations following CA with and without administration of SR141716A before VF+CPR followed by infusion of WIN55 5 min after ROSC.

RESULTS

Our most recent WIN55 publication and our current studies administered WIN55 5 minutes after ROSC. Blood temperature in WIN55 + Hypothermia decreased progressively from $36.8°C \pm 0.2°C$ to $35.1°C \pm 0.5°C$ during the first hour of infusion and reached $33.3°C \pm 0.3°C$ at 4 hours after infusion (145). Duration of reduced blood temperatures did not have a significant difference between WIN55 + Hypothermia and Hypothermia, which had a similar rate for temperature drop. Due to the use of a heated surgical board, there was no significant reduction in blood temperature in animals with WIN55 + Normothermia which was similar to Normothermia. There was no significant reduction in blood temperature in animals pretreated with SR141716A (*Figure 43*) (114).
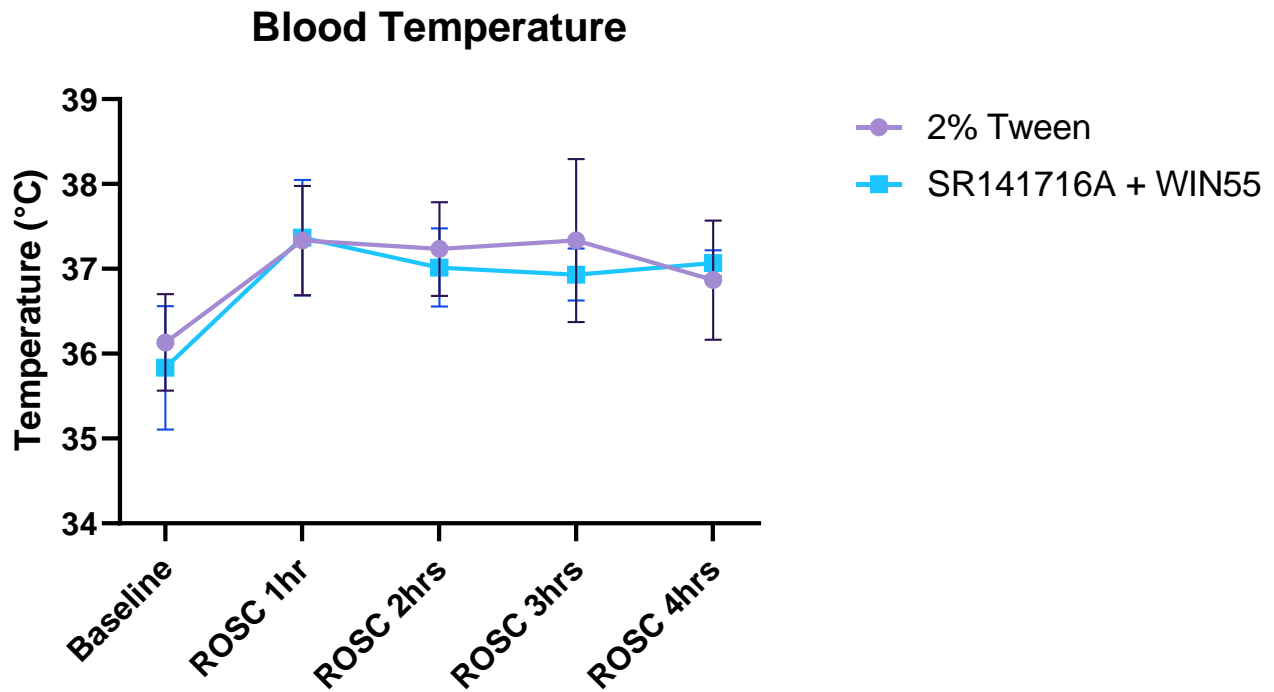
Blood Temperature

Figure 43. Blood temperature was not different between groups. Mean ± SD, Unpaired t test, p>0.05 vs 2% Tween N=3, SR141716A+WIN55 N=6. My contribution (a) design of the experiments (b) execution of experimental procedure (c) Analysis of the data.

MAP and HR in WIN55 + Hypothermia and WIN55 + Normothermia decreased significantly compared with Normothermia at ROSC 1hr, 2hrs, 3hrs, and 4hrs *(Figure 44 and Figure 45),* while ETCO$_2$ in WIN55 + Hypothermia increased significantly compared with Normothermia (*Figure 46*) (145). HR in SR141716A+WIN55 decreased significantly compared to 2% Tween 80 at ROSC 2hrs and 3hrs (*Figure 47*) while ETCO$_2$ increased significantly compared with 2% Tween 80 at ROSC 1hr and 4hrs (*Figure 48*). Administration of SR141716A+WIN55 followed similar hemodynamic changes from previously published results (145).
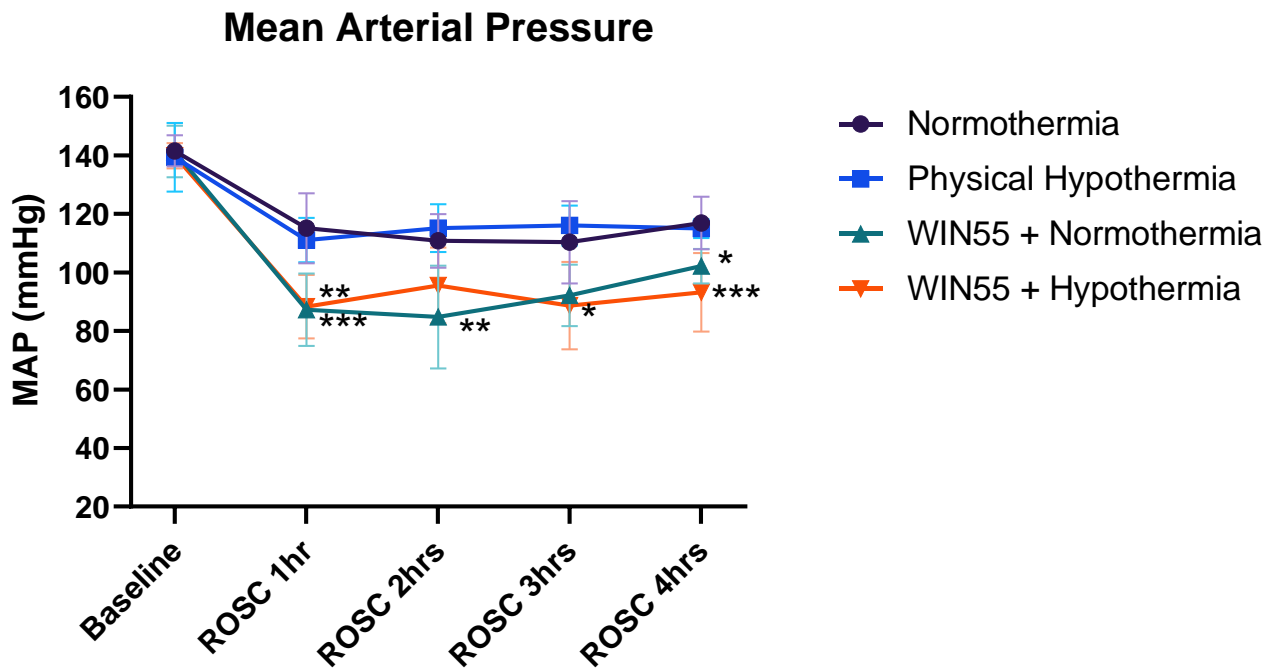
Figure 44. MAP in WIN55 + Hypothermia and WIN55 + Normothermia decreased significantly compared with Normothermia. Mean ± SD, One-way ANOVA, Bonferroni Post-hoc *p<0.05 **p<0.01 ***p<0.001 vs normothermia N=6 in each group. My contribution (a) design of the experiments (c) Re-analysis of the data.
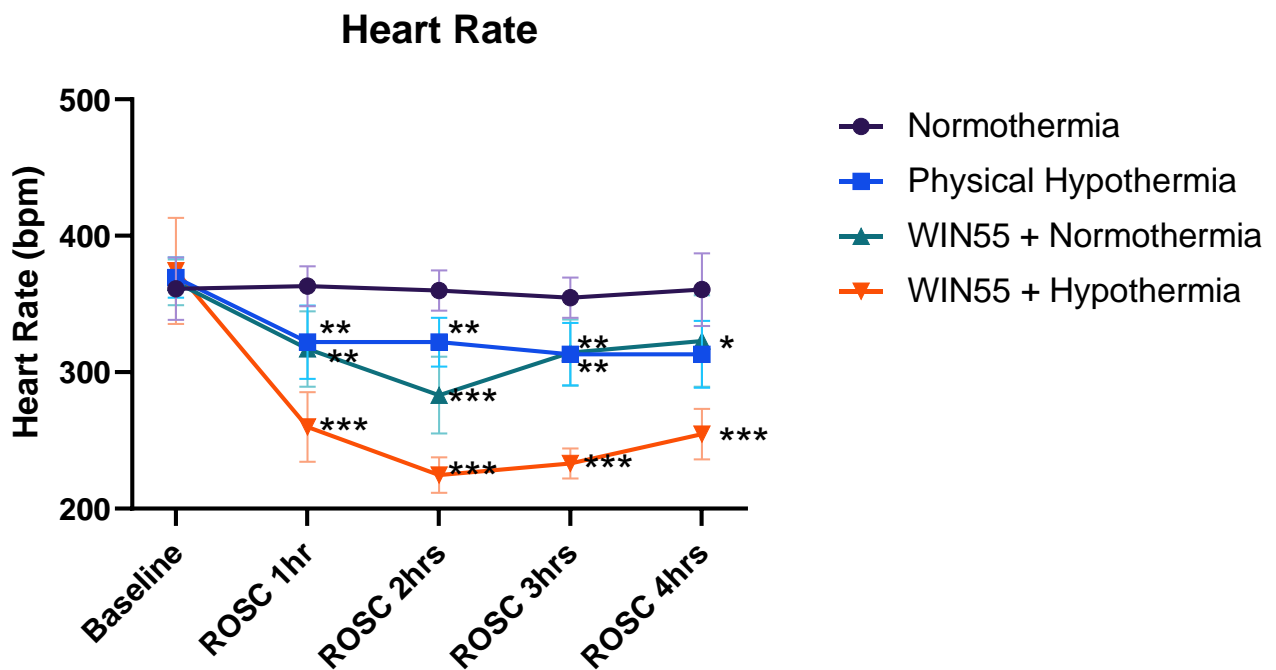
Figure 45. HR in WIN55 + Hypothermia and WIN55 + Normothermia decreased significantly compared with Normothermia. Mean ± SD, One-way ANOVA, Bonferroni Post-hoc *p<0.05 **p<0.01 ***p<0.001 vs normothermia N=6 in each group. My contribution (a) design of the experiments (c) Re-analysis of the data.

End Tidal Carbon Dioxide
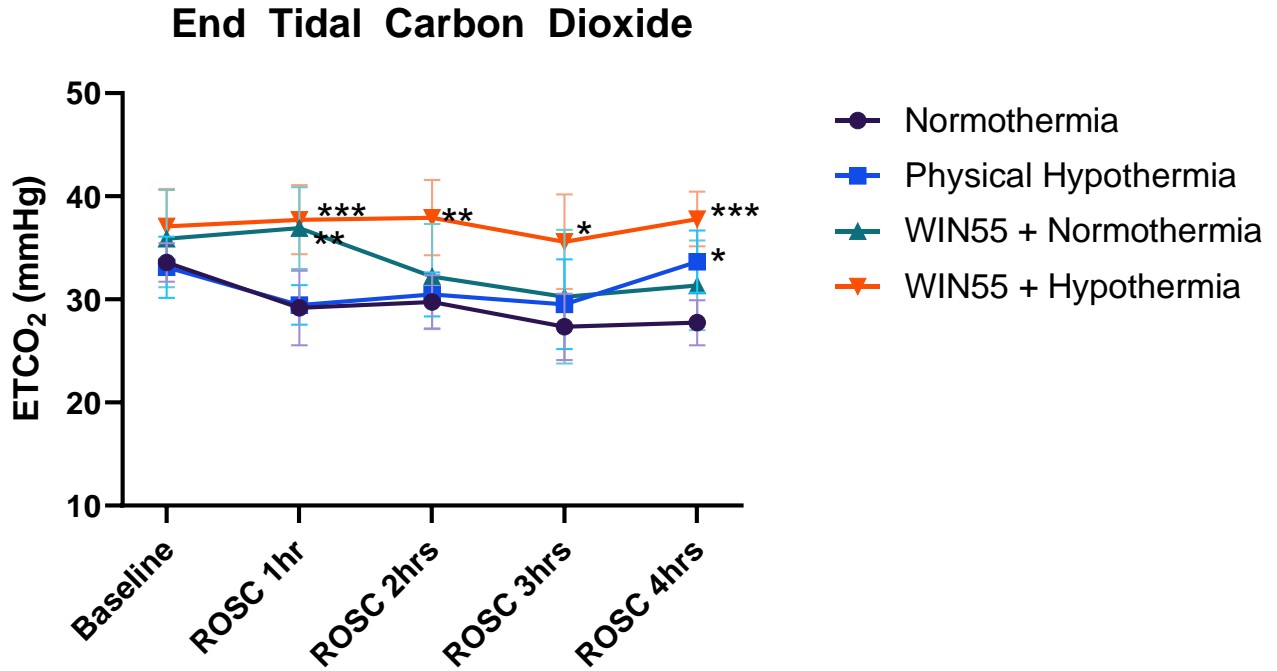
Figure 46. ETCO₂ in WIN55 + Hypothermia increased significantly compared with Normothermia. Mean ± SD, One-way ANOVA, Bonferroni Post-hoc *p<0.05 **p<0.01 ***p<0.001 vs normothermia N=6 in each group. My contribution (a) design of the experiments (c) Re-analysis of the data.
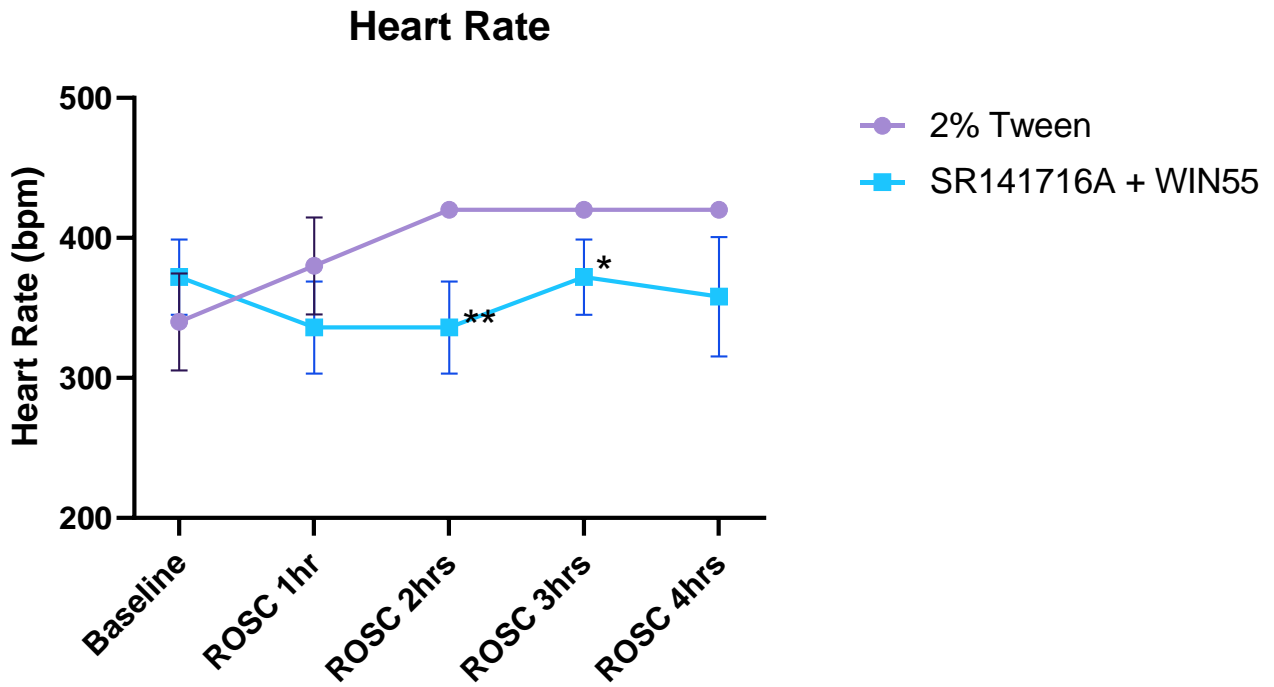
Figure 47. HR in SR141716A+WIN55 decreased significantly compared to 2% Tween 80 at ROSC 2hrs and 3hrs. Mean ± SD, Unpaired t test, *p<0.05 **p<0.01 ***p<0.001 vs 2% Tween N=3, SR141716A+WIN55 N=6. My contribution (a) design of the experiments (b) execution of experimental procedure (c) Analysis of the data.

End Tidal Carbon Dioxide
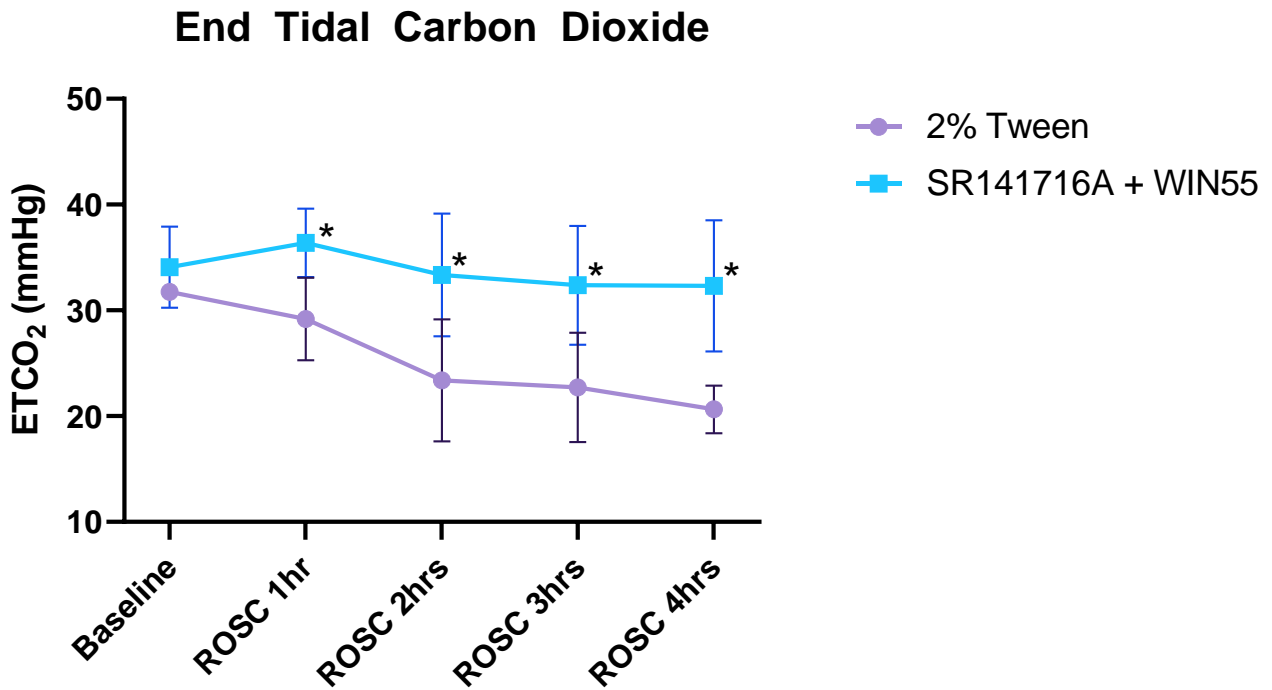
Figure 48. ETCO$_2$ increased significantly compared with 2% Tween 80 at ROSC 1hr and 4hrs. Mean ± SD, Unpaired t test, *p<0.05 **p<0.01 ***p<0.001 vs 2% Tween N=3, SR141716A+WIN55 N=6. My contribution (a) design of the experiments (b) execution of experimental procedure (c) Analysis of the data.

There was a significant improvement in myocardial function as measured by CO, EF, and

MPI, in animals treated with WIN55 + Hypothermia beginning at 1 hour after start of infusion.

WIN55 + Hypothermia significantly improved at ROSC 4hrs compared with Physical

Hypothermia (*Figure 49, Figure 50 and Figure 51*) (145). MPI in SR141716A+WIN55

increased significantly compared with 2% Tween 80 at ROSC 4hrs (*Figure 52*).

110

Cardiac Output
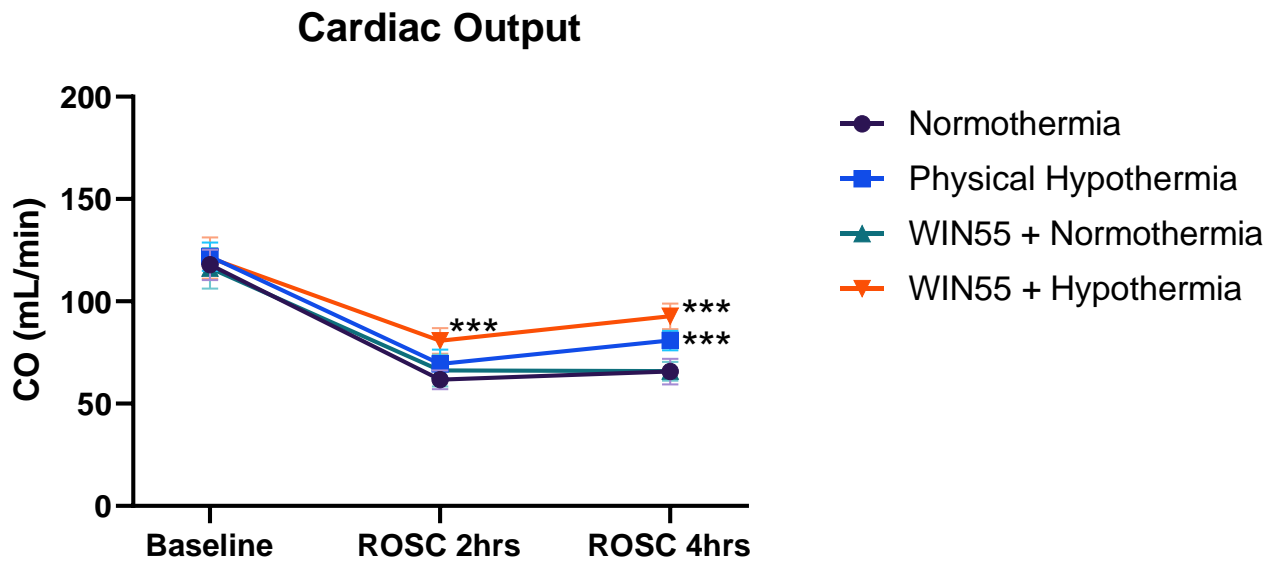
Figure 49. Significant improvement in myocardial function as measured by CO. Mean ± SD, One-way ANOVA, Bonferroni Post-hoc *p<0.05 **p<0.01 ***p<0.001 vs normothermia N=6 in each group. My contribution (a) design of the experiments (c) Re-analysis of the data.

Ejection Fraction
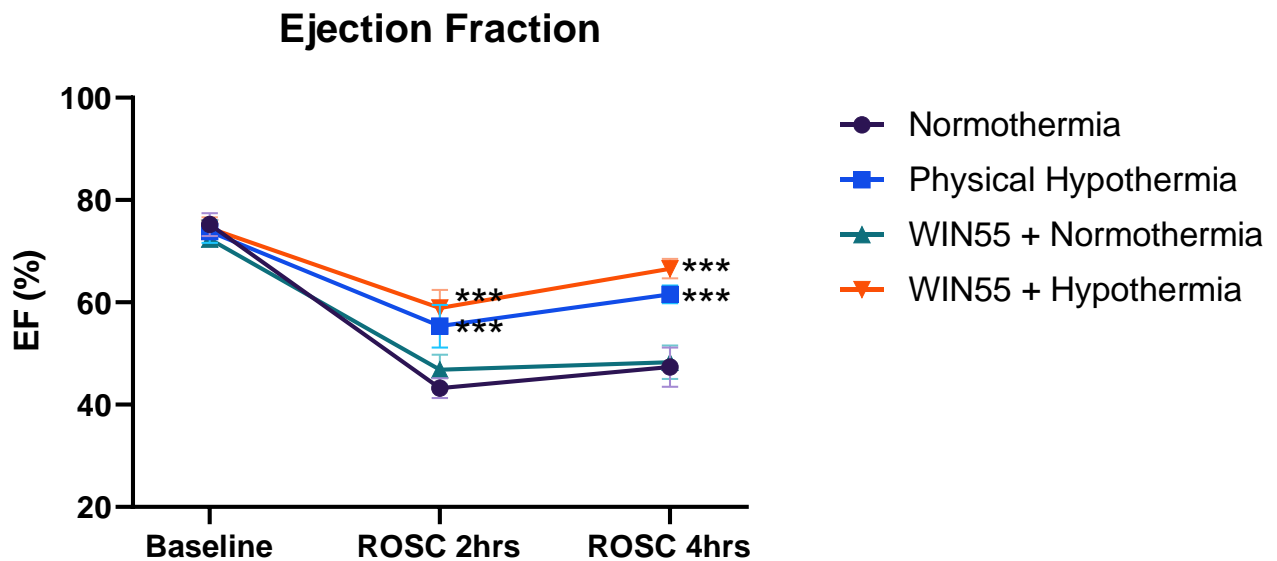
Figure 50. Significant improvement in myocardial function as measured by EF. Mean ± SD, One-way ANOVA, Bonferroni Post-hoc *p<0.05 **p<0.01 ***p<0.001 vs normothermia N=6 in each group. My contribution (a) design of the experiments (c) Re-analysis of the data.

111

Myocardial Performance Index
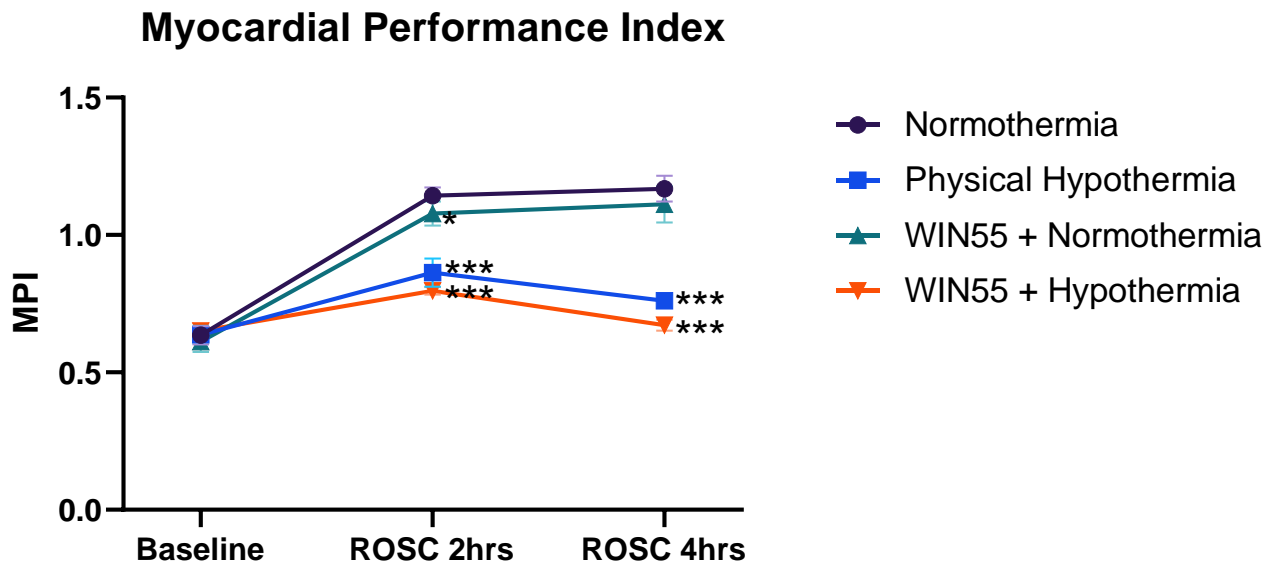
Figure 51. Significant improvement in myocardial function as measured by MPI. Mean ± SD, One-way ANOVA, Bonferroni Post-hoc *p<0.05 **p<0.01 ***p<0.001 vs normothermia N=6 in each group. My contribution (a) design of the experiments (c) Re-analysis of the data.

Myocardial Performance Index
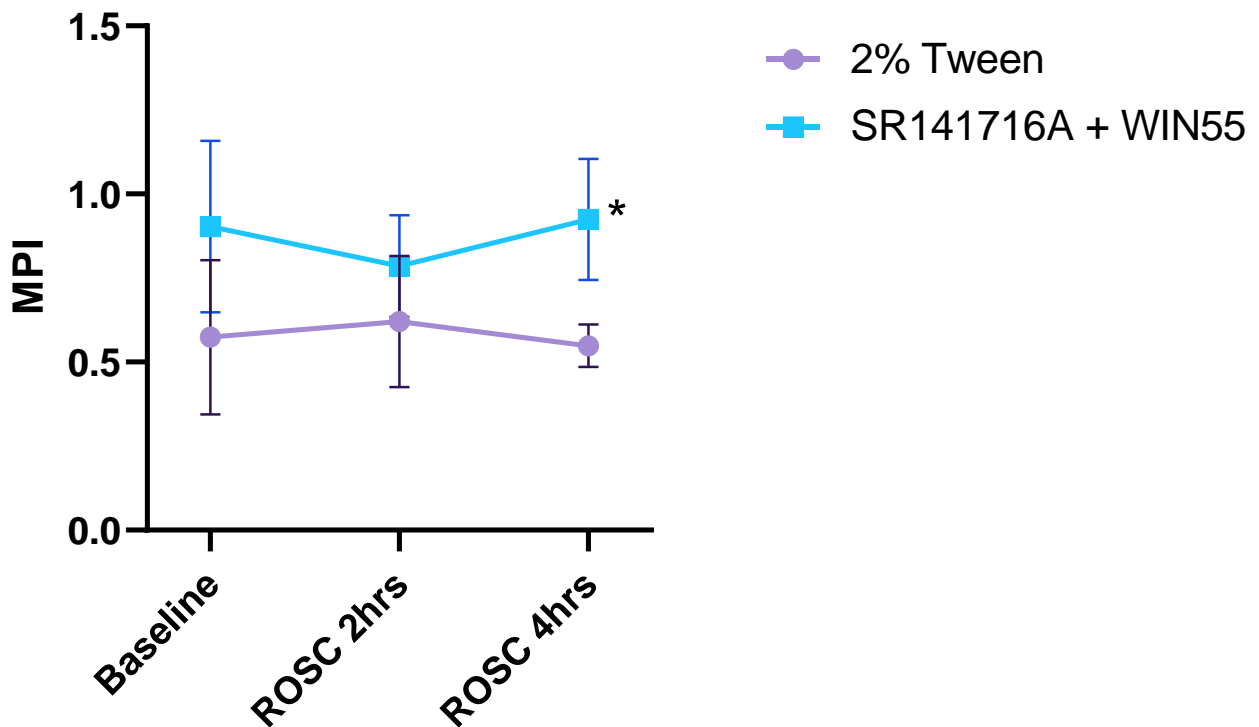
Figure 52. MPI in SR141716A+WIN55 increased significantly compared with 2% Tween 80 at ROSC 4hrs. Mean ± SD, Unpaired t test, *p<0.05 **p<0.01 ***p<0.001 vs 2% Tween N=3, SR141716A+WIN55 N=6. My contribution (a) design of the experiments (b) execution of experimental procedure (c) Analysis of the data.

TNFα, IL6, cardiac troponin I and IL10 expression in plasma were all increased following CA/CPR (*Figure 53, Figure 54, Figure 55 and Figure 56*). IM Administration of SR141716A (*Figure 19*) (5 mg/kg, dissolved in 0.1 mL dimethylsulfoxide) before VF 6 min + CPR 8 min, defibrillation and ROSC followed by infusion) of WIN55 (1 mg/kg/h) administered by continuous intravenous infusion with a syringe pump (Genie Touch; Kent Scientific Corporation) for 4 hours at a rate of 1.4 mL/kg/h (114) decreased expression in plasma TNFα, IL6, and IL10 at ROSC 4hrs (*Figure 53, Figure 54 and Figure 56*). Cardiac troponin I and S100A8 protein expression was not different between groups (*Figure 55 and Figure 57*).

TNFα
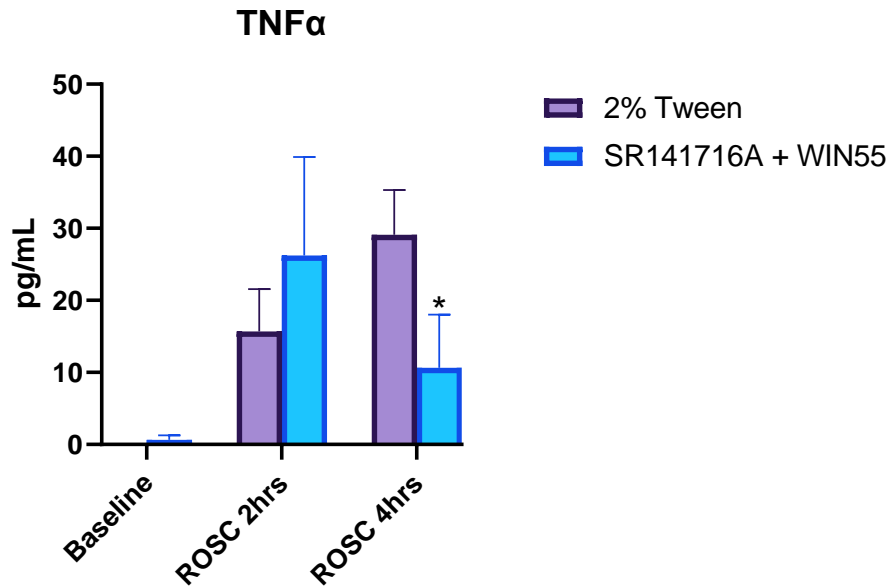
Figure 53. Plasma TNFα. IM Administration of SR141716A before VF+CPR followed by infusion of WIN55 5 min after ROSC significantly decreased TNFα plasma protein expression at ROSC 4hrs. Mean ± SD, Unpaired t test, *p<0.05 **p<0.01 ***p<0.001 vs 2% Tween N=3, SR141716A+WIN55 N=5. My contribution (a) design of the experiments (b) execution of experimental procedure (c) Analysis of the data.

IL6
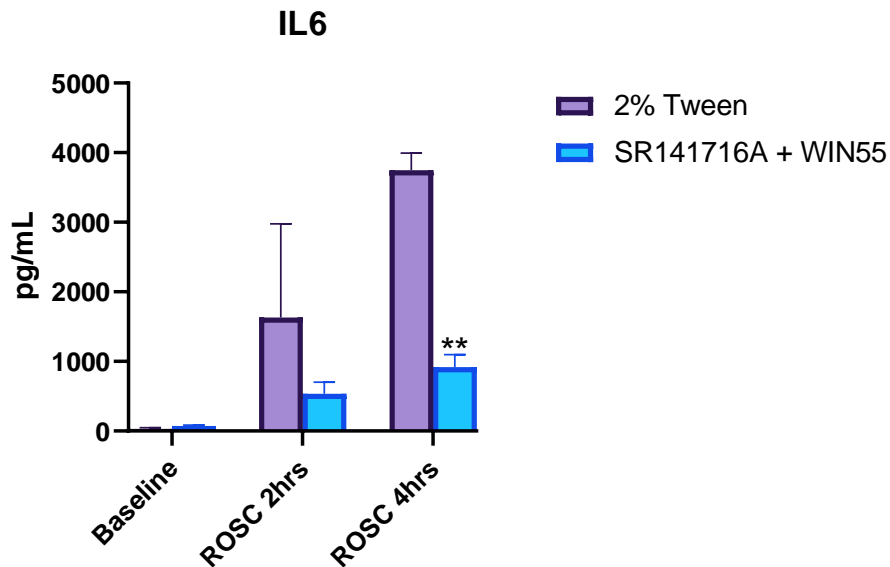
Figure 54. Plasma IL6. IM Administration of SR141716A before VF+CPR followed by infusion of WIN55 5 min after ROSC significantly decreased IL6 plasma protein expression at ROSC 4hrs. Mean ± SD, Unpaired t test, *p<0.05 **p<0.01 ***p<0.001 vs 2% Tween N=3, SR141716A+WIN55 N=3. My contribution (a) design of the experiments (b) execution of experimental procedure (c) Analysis of the data.

114

TNNI3
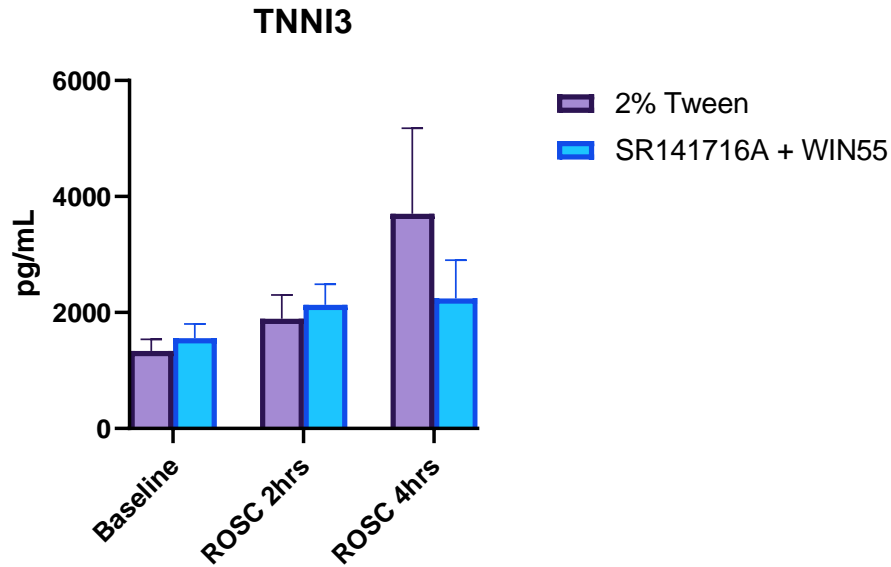
Figure 55. Plasma Troponin I. IM Administration of SR141716A before VF+CPR followed by infusion of WIN55 5 min after ROSC had no effect on cardiac troponin I plasma protein expression at ROSC 4hrs. Mean ± SD, Unpaired t test, $p > 0.05$ vs %Tween N=3, SR141716A+WIN55 N=5. My contribution (a) design of the experiments (b) execution of experimental procedure (c) Analysis of the data.
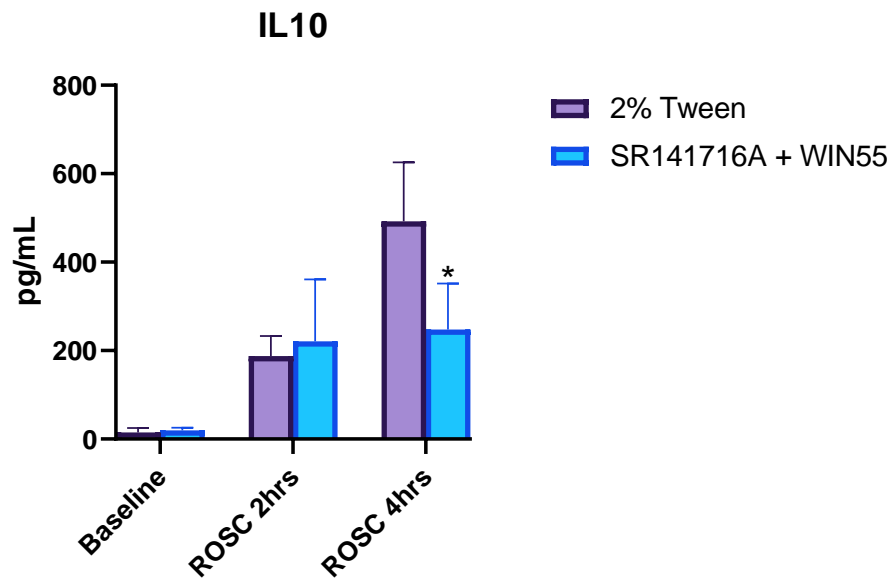
IL10

Figure 56. Plasma IL10. IM Administration of SR141716A before VF+CPR followed by infusion of WIN55 5 min after ROSC decreased IL10 plasma protein expression at ROSC 4hrs. Mean ± SD, Unpaired t test, $*p < 0.05$ $**p < 0.01$ $***p < 0.001$ vs %Tween N=3, SR141716A+WIN55 N=5. My contribution (a) design of the experiments (b) execution of experimental procedure (c) Analysis of the data.

115
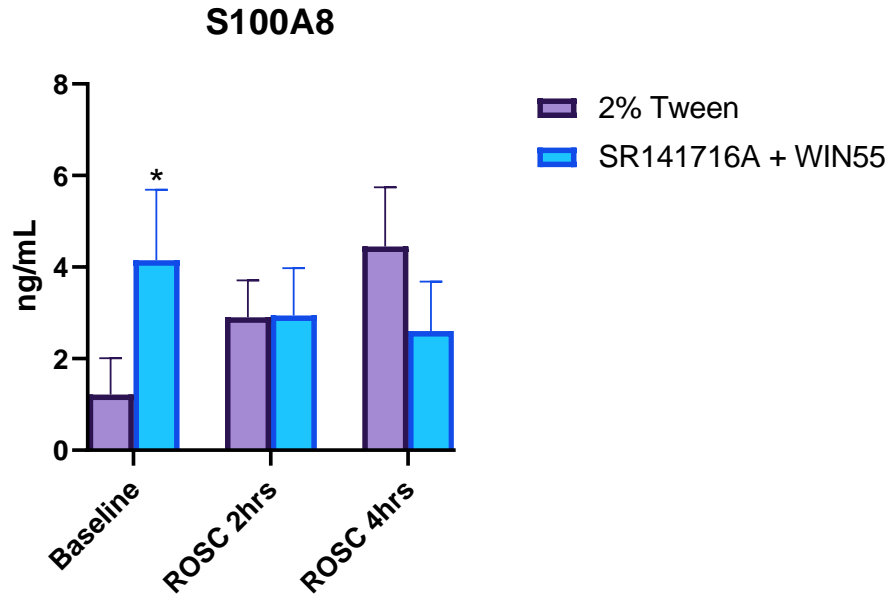
S100A8

Figure 57. Plasma S100A8. IM Administration of SR141716A before VF+CPR followed by infusion of WIN55 5 min after ROSC had no effect on S100A8 plasma protein expression at ROSC 4hrs. Mean $\pm$ SD, Unpaired t test, *$p<0.05$ **$p<0.01$ ***$p<0.001$ vs %Tween N=3, SR141716A+WIN55 N=5. My contribution (a) design of the experiments (b) execution of experimental procedure (c) Analysis of the data.

DISCUSSION

In the cardiovascular system, CB_2 is present in various cell types (97). Therefore, IM Administration of SR141716A (CB_1 antagonist) before VF+CPR followed by infusion of WIN55 (CB_1 and CB_2 agonist) 5 min after ROSC was used as a treatment group to determine CB_2 agonist response to CA/CPR. HR decreased significantly at ROSC 2hrs and 3hrs while $ETCO_2$ increased significantly at ROSC 1hr through 4hrs with treatment. MPI also increased significantly at ROSC 4hrs. Our experimental CA/CPR (145, 162, 163) model indicates that TNFα, IL6, and IL10 plasma protein expression is decreased at ROSC 4hrs with SR141716A+WIN55 treatment. Cardiac troponin I and S100A8 protein expression did not change between groups. This could be due to the timing of plasma collection (ROSC 4hrs).

116

Relative cardiac S100A8 and S100A9 mRNA expression in mice subjected to myocardial IR procedures had peak S100A8/A9 mRNA expression at 6hrs in the heart (132).

CONCLUSION

TNFα, IL6, and IL10 plasma protein expression decreased at ROSC 4hrs with SR141716A+WIN55 treatment. Cardiac troponin I and S100A8 protein expression does not change.

LIMITATIONS

Confirmation of the CB_2 receptor as anti-inflammatory still needs to be validated *in vivo*. There are two different antagonists of CB_2 (SR144528(114) and AM630(200)) that can be tested to determine if administration blocks the anti-inflammatory effect of WIN55. Antagonists of CB_1 such as AM251 also need to be tested to determine if administration blocks the anti-inflammatory effect of WIN55. Further studies are also needed using more specific CB_2 receptor agonists such as HU308 or JWH-133(200).

If we have tissue available after lipidomic analysis from a collaborator-a future study could include immunoblot of the brain and heart for S100A8 and S100A9. Therefore, future studies could look at expression of S100A8 and S100A9 peptides in brain and heart and protein levels in plasma at ROSC 4hrs or with a survival model at 24, 48 and 72hrs. Analysis of S100A8/A9 protein expression with a treatment group of WIN55 would further enhance the mechanism of this pharmacologic tool. Inhibitors of S100A8 and/or S100A9 should also be tested *in vivo*. The effects of WIN55 should also be tested to determine if they are attenuated by PPARγ antagonist GW9662 (204).

CHAPTER 7: Summary and Future Direction

Accumulating evidence indicates that synthetic or endogenous cannabinoids protect against central nervous system injury by factors including ischemia and reperfusion (200). Brain CB_2 receptors are highly inducible; thus, under some pathological conditions (inflammation), CB_2 expression is quickly enhanced (109). Di Filippo et al. demonstrate that treatment with the synthetic nonselective CB_1/CB_2 receptor agonist WIN55 significantly reduces the extent of myocardial infarct in mice suffering from myocardial IR injury; cardio protection is accompanied by lower myeloperoxidase activity and IL-1β and CXC chemokine ligand levels in injured tissue. This cardioprotective effect is almost abolished by the selective CB_2 antagonist AM630, but it is not affected by the selective CB_1 antagonist AM251 (200) (Fig 42). Although several rodent models have shown promising actions of cannabinoids on the cardiovascular system, we are a long way from seeing these compounds on the market (84). Selective CB_1 receptor antagonists were withdrawn from the market because of increased risk of depression (200).

The effects of WIN55 were investigated initially in our rat model of CA and CPR. WIN55 was selected based on the following reasons: 1) the described hypothermia effect of CB_1 agonist is convincing and well documented, 2) it is highly selective for cannabinoid receptors and interacts negligibly with other neurotransmitter and ion channels (118), 3) it is expressed in thermoregulatory areas of the central nervous system and therefore decreases body temperature via a central mechanism (119), 4) It has been shown to be neuroprotective (120) and 5) It has

118

been demonstrated in both mice and rats that the CB_2 receptor activation effects of WIN55 have significant anti-inflammatory effects (121-123). Our experimental CA/CPR (145, 162, 163) model indicates that local S100A8/A9 protein expression is increased within heart whole tissue lysates after CA and CPR. We then confirmed WIN55 inhibited LPS induced expression of pro-inflammatory cytokines in mouse RAW 264.7 macrophage cells. *In vivo* TNFα, IL6, and IL10 plasma protein expression decreased at ROSC 4hrs with SR141716A+WIN55 treatment. Li et al recently report S100A8/A9 causes mitochondrial dysfunction via suppression of TLR4/ERK subsequent to mitochondrial complex I inhibition. S100A8/A9 is significantly upregulated during the early reperfusion stage (132). Mitochondria have emerged as central organelles that integrate metabolism and inflammatory responses (79). Therefore, future studies are necessary to determine if WIN55 could be a potential therapeutic to mitigate brain and heart damage after CA and CPR by blocking S100A8/A9 expression. We have determined brain mitochondria are more sensitive to global ischemia compared to heart mitochondria. Additionally, complex I is the most sensitive ETC complex to ischemic injury and its activity determines rate of OXPHOS following CA and RES. Preservation of brain mitochondrial activity and function during CA by inhibition of S100A8/A9 may enhance outcomes and recovery. For this reason, WIN55 could be a pharmacologic tool that preserves complex I activity during CA.

The exact mechanism by which CB_2 activation leads to anti-inflammatory effects and possible S100A8/A9 inhibition needs further investigation with macrophage *in vitro* studies and our experimental CA/CPR (145, 162, 163) model survival studies (Fig 43). Li et al report serum S100A8/A9 levels 1 day post-percutaneous coronary intervention was significantly greater than

119

other points (132). We could then look at brain and heart mitochondria, local S100A8 histology and protein expression within the brain and heart along with systemic TNFα, IL6, IL10, cardiac troponin, and S100A8 plasma protein expression 24hrs and 48hrs after ROSC.
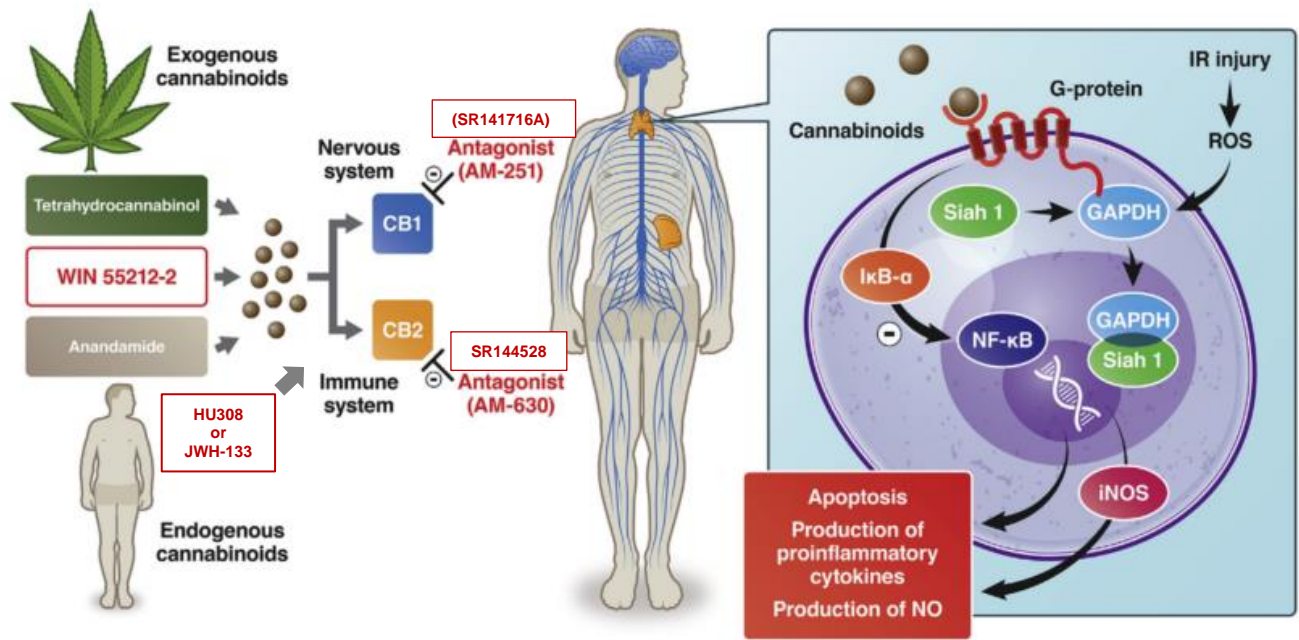
Figure 58. Pathways of cannabinoid receptor-mediated protection against Ischemia reperfusion injury. Adapted from (82)
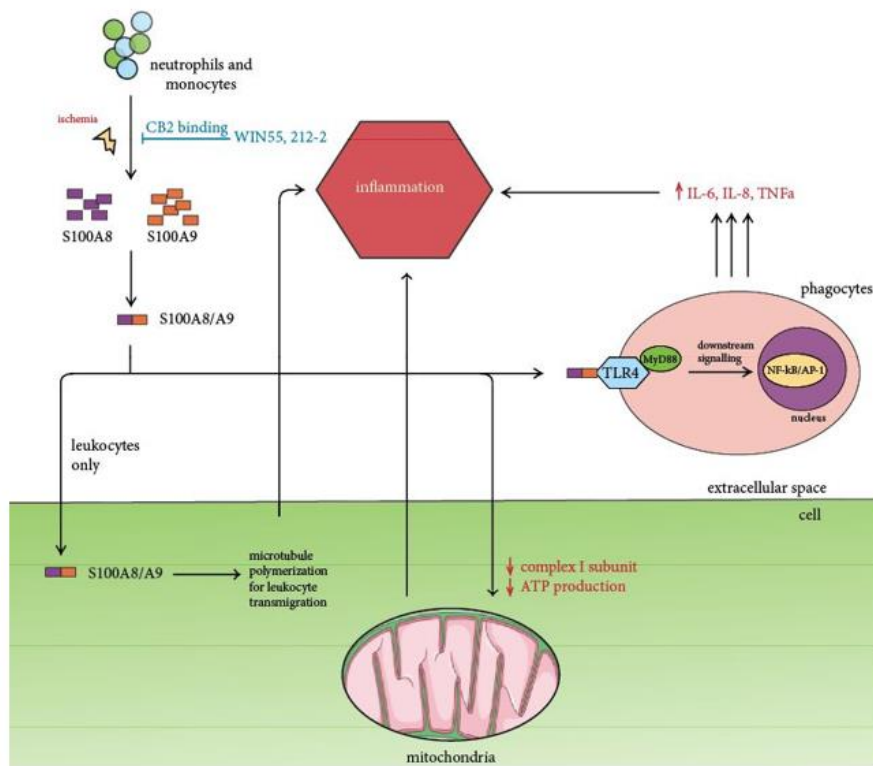
Figure 59. Potential WIN55 inhibition of S100A8 and S100A9. Upon forming a heterodimer, S100A8/A9 is able to exert both intracellular and extracellular effects. Intracellularly, S100A8/A9 serves as a regulator of leukocyte transendothelial migration by promoting microtubule polymerization. It also promotes the downregulation of mitochondrial electron transport chain complex I and ATP production. Extracellularly, S100A8/A9 acts as a damage-associated molecular pattern (DAMP) by binding to TLR4 receptors on phagocytes and triggering the production of inflammatory cytokines.

REFERENCES

1.   Virani SS, Alonso A, Benjamin EJ, Bittencourt MS, Callaway CW, Carson AP, et al. Heart Disease and Stroke Statistics-2020 Update: A Report From the American Heart Association. Circulation. 2020;141(9):e139-e596.

2.   Tang MHWaW. CPR Resuscitation of the Arrested Heart1999.

3.   Meybohm P, Gruenewald M, Albrecht M, Zacharowski KD, Lucius R, Zitta K, et al. Hypothermia and postconditioning after cardiopulmonary resuscitation reduce cardiac dysfunction by modulating inflammation, apoptosis and remodeling. PLoS One. 2009;4(10):e7588.

4.   Yang J, Miao C, Xiao Y, Huang W, Hu Z, Guo Q, et al. Abstract 16699: Effects of Polyethylene Glycol-20K on Post-Resuscitation Survival and Neurological Function in a Rat Model of Cardiopulmonary Resuscitation. Circulation. 2017;136(Suppl 1):A16699.

5.   Li X, Liu M, Sun R, Zeng Y, Chen S, Zhang P. Protective approaches against myocardial ischemia reperfusion injury. Exp Ther Med. 2016;12(6):3823-9.

6.   Hayman EG, Patel AP, Kimberly WT, Sheth KN, Simard JM. Cerebral Edema After Cardiopulmonary Resuscitation: A Therapeutic Target Following Cardiac Arrest? Neurocrit Care. 2018;28(3):276-87.

7.   Jentzer JC, Chonde MD, Dezfulian C. Myocardial Dysfunction and Shock after Cardiac Arrest. BioMed research international. 2015;2015:314796.

8.   Batkai S, Osei-Hyiaman D, Pan H, El-Assal O, Rajesh M, Mukhopadhyay P, et al. Cannabinoid-2 receptor mediates protection against hepatic ischemia/reperfusion injury. FASEB journal : official publication of the Federation of American Societies for Experimental Biology. 2007;21(8):1788-800.

9.   Tahsili-Fahadan P, Farrokh S, Geocadin RG. Hypothermia and brain inflammation after cardiac arrest. Brain circulation. 2018;4(1):1-13.

10.   Neumar RW, Nolan JP, Adrie C, Aibiki M, Berg RA, Bottiger BW, et al. Post-cardiac arrest syndrome: epidemiology, pathophysiology, treatment, and prognostication. A consensus statement from the International Liaison Committee on Resuscitation (American Heart Association, Australian and New Zealand Council on Resuscitation, European Resuscitation Council, Heart and Stroke Foundation of Canada, InterAmerican Heart Foundation, Resuscitation Council of Asia, and the Resuscitation Council of Southern Africa); the American Heart Association Emergency Cardiovascular Care Committee; the Council on Cardiovascular

Surgery and Anesthesia; the Council on Cardiopulmonary, Perioperative, and Critical Care; the Council on Clinical Cardiology; and the Stroke Council. Circulation. 2008;118(23):2452-83.

11.   Baker E, Lee G. The science of reperfusion injury post cardiac arrest--Implications for emergency nurses. International emergency nursing. 2016;24:66-70.

12.   Ayoub IM, Radhakrishnan J, Gazmuri RJ. Targeting mitochondria for resuscitation from cardiac arrest. Crit Care Med. 2008;36(11 Suppl):S440-6.

13.   Patil KD, Halperin HR, Becker LB. Cardiac arrest: resuscitation and reperfusion. Circ Res. 2015;116(12):2041-9.

14.   Han F, Da T, Riobo NA, Becker LB. Early mitochondrial dysfunction in electron transfer activity and reactive oxygen species generation after cardiac arrest. Crit Care Med. 2008;36(11 Suppl):S447-53.

15.   Yeh ST, Lee HL, Aune SE, Chen CL, Chen YR, Angelos MG. Preservation of mitochondrial function with cardiopulmonary resuscitation in prolonged cardiac arrest in rats. J Mol Cell Cardiol. 2009;47(6):789-97.

16.   Kim J, Villarroel JPP, Zhang W, Yin T, Shinozaki K, Hong A, et al. The Responses of Tissues from the Brain, Heart, Kidney, and Liver to Resuscitation following Prolonged Cardiac Arrest by Examining Mitochondrial Respiration in Rats. Oxidative medicine and cellular longevity. 2016;2016:7463407-.

17.   Gazmuri RJ, Radhakrishnan J. Protecting mitochondrial bioenergetic function during resuscitation from cardiac arrest. Critical care clinics. 2012;28(2):245-70.

18.   Mongardon N, Dumas F, Ricome S, Grimaldi D, Hissem T, Pène F, et al. Postcardiac arrest syndrome: from immediate resuscitation to long-term outcome. Ann Intensive Care. 2011;1(1):45-.

19.   Kuznetsov AV, Javadov S, Margreiter R, Grimm M, Hagenbuchner J, Ausserlechner MJ. The Role of Mitochondria in the Mechanisms of Cardiac Ischemia-Reperfusion Injury. Antioxidants (Basel). 2019;8(10):454.

20.   Vosler PS, Graham SH, Wechsler LR, Chen J. Mitochondrial targets for stroke: focusing basic science research toward development of clinically translatable therapeutics. Stroke. 2009;40(9):3149-55.

21.   Walters AM, Porter GA, Jr., Brookes PS. Mitochondria as a drug target in ischemic heart disease and cardiomyopathy. Circulation research. 2012;111(9):1222-36.

123

22.   Lesnefsky EJ, Moghaddas S, Tandler B, Kerner J, Hoppel CL. Mitochondrial dysfunction in cardiac disease: ischemia--reperfusion, aging, and heart failure. J Mol Cell Cardiol. 2001;33(6):1065-89.

23.   Archer SL. Mitochondrial dynamics--mitochondrial fission and fusion in human diseases. N Engl J Med. 2013;369(23):2236-51.

24.   Westermann B. Mitochondrial fusion and fission in cell life and death. Nat Rev Mol Cell Biol. 2010;11(12):872-84.

25.   Grazioli S, Pugin J. Mitochondrial Damage-Associated Molecular Patterns: From Inflammatory Signaling to Human Diseases. Frontiers in immunology. 2018;9:832.

26.   Yang M, Linn BS, Zhang Y, Ren J. Mitophagy and mitochondrial integrity in cardiac ischemia-reperfusion injury. Biochim Biophys Acta Mol Basis Dis. 2019;1865(9):2293-302.

27.   Zhang Q, Raoof M, Chen Y, Sumi Y, Sursal T, Junger W, et al. Circulating mitochondrial DAMPs cause inflammatory responses to injury. Nature. 2010;464(7285):104-7.

28.   Oka T, Hikoso S, Yamaguchi O, Taneike M, Takeda T, Tamai T, et al. Mitochondrial DNA that escapes from autophagy causes inflammation and heart failure. Nature. 2012;485(7397):251-5.

29.   Majdi F, Taheri F, Salehi P, Motaghinejad M, Safari S. Cannabinoids Δ(9)-tetrahydrocannabinol and cannabidiol may be effective against methamphetamine induced mitochondrial dysfunction and inflammation by modulation of Toll-like type-4(Toll-like 4) receptors and NF-κB signaling. Med Hypotheses. 2019;133:109371.

30.   Shekhova E. Mitochondrial reactive oxygen species as major effectors of antimicrobial immunity. PLOS Pathogens. 2020;16(5):e1008470.

31.   Schroder K, Tschopp J. The inflammasomes. Cell. 2010;140(6):821-32.

32.   Lee FY, Shao PL, Wallace CG, Chua S, Sung PH, Ko SF, et al. Combined Therapy with SS31 and Mitochondria Mitigates Myocardial Ischemia-Reperfusion Injury in Rats. International journal of molecular sciences. 2018;19(9).

33.   Arnalich F, Codoceo R, López-Collazo E, Montiel C. Circulating cell-free mitochondrial DNA: a better early prognostic marker in patients with out-of-hospital cardiac arrest. Resuscitation. 2012;83(7):e162-3.

124

34.   Donnino MW, Liu X, Andersen LW, Rittenberger JC, Abella BS, Gaieski DF, et al. Characterization of mitochondrial injury after cardiac arrest (COMICA). Resuscitation. 2017;113:56-62.

35.   Tian F, Liu R, Fan C, Sun Y, Huang X, Nie Z, et al. Effects of Thymoquinone on Small-Molecule Metabolites in a Rat Model of Cerebral Ischemia Reperfusion Injury Assessed using MALDI-MSI. Metabolites. 2020;10(1) 1-22.

36.   Huang JL, Manaenko A, Ye ZH, Sun XJ, Hu Q. Hypoxia therapy--a new hope for the treatment of mitochondrial dysfunctions. Med Gas Res. 2016;6(3):174-6.

37.   Li Q, Wang F, Zhang YM, Zhou JJ, Zhang Y. Activation of cannabinoid type 2 receptor by JWH133 protects heart against ischemia/reperfusion-induced apoptosis. Cellular physiology and biochemistry : international journal of experimental cellular physiology, biochemistry, and pharmacology. 2013;31(4-5):693-702.

38.   Alonso-Alconada D, Alvarez A, Alvarez FJ, Martinez-Orgado JA, Hilario E. The cannabinoid WIN 55212-2 mitigates apoptosis and mitochondrial dysfunction after hypoxia ischemia. Neurochemical research. 2012;37(1):161-70.

39.   Wada T. Coagulofibrinolytic Changes in Patients with Post-cardiac Arrest Syndrome. Front Med (Lausanne). 2017;4:156.

40.   Huet O, Dupic L, Batteux F, Matar C, Conti M, Chereau C, et al. Postresuscitation syndrome: potential role of hydroxyl radical-induced endothelial cell damage. Crit Care Med. 2011;39(7):1712-20.

41.   Nolan JP, Neumar RW, Adrie C, Aibiki M, Berg RA, Bottiger BW, et al. Post-cardiac arrest syndrome: epidemiology, pathophysiology, treatment, and prognostication. A Scientific Statement from the International Liaison Committee on Resuscitation; the American Heart Association Emergency Cardiovascular Care Committee; the Council on Cardiovascular Surgery and Anesthesia; the Council on Cardiopulmonary, Perioperative, and Critical Care; the Council on Clinical Cardiology; the Council on Stroke. Resuscitation. 2008;79(3):350-79.

42.   Kang Y. Management of post-cardiac arrest syndrome. Acute Crit Care. 2019;34(3):173-8.

43.   Binks A, Nolan J. Post-cardiac arrest syndrome2010. 362-8 p.

44.   Walker AC, Johnson NJ. Critical Care of the Post-Cardiac Arrest Patient. Cardiology clinics. 2018;36(3):419-28.

45.   Nolan JP, Soar J, Cariou A, Cronberg T, Moulaert VR, Deakin CD, et al. European Resuscitation Council and European Society of Intensive Care Medicine Guidelines for Post-resuscitation Care 2015: Section 5 of the European Resuscitation Council Guidelines for Resuscitation 2015. Resuscitation. 2015;95:202-22.

46.   Girotra S, Chan PS, Bradley SM. Post-resuscitation care following out-of-hospital and in-hospital cardiac arrest. Heart. 2015;101(24):1943-9.

47.   Laver S, Farrow C, Turner D, Nolan J. Mode of death after admission to an intensive care unit following cardiac arrest. Intensive Care Med. 2004;30(11):2126-8.

48.   Adrie C, Adib-Conquy M, Laurent I, Monchi M, Vinsonneau C, Fitting C, et al. Successful Cardiopulmonary Resuscitation After Cardiac Arrest as a "Sepsis-Like" Syndrome. Circulation. 2002;106(5):562.

49.   Teschendorf P, Albertsmeier M, Vogel P, Padosch SA, Spöhr F, Kirschfink M, et al. Neurological outcome and inflammation after cardiac arrest—Effects of protein C in rats. Resuscitation. 2008;79(2):316-24.

50.   Janata A, Magnet IAM, Uray T, Stezoski JP, Janesko-Feldman K, Tisherman SA, et al. Regional TNFα mapping in the brain reveals the striatum as a neuroinflammatory target after ventricular fibrillation cardiac arrest in rats. Resuscitation. 2014;85(5):694-701.

51.   Peberdy MA, Andersen LW, Abbate A, Thacker LR, Gaieski D, Abella BS, et al. Inflammatory markers following resuscitation from out-of-hospital cardiac arrest-A prospective multicenter observational study. Resuscitation. 2016;103:117-24.

52.   Rock KL, Latz E, Ontiveros F, Kono H. The sterile inflammatory response. Annu Rev Immunol. 2010;28:321-42.

53.   Madder RD, Reynolds JC. Multidisciplinary Management of the Post-Cardiac Arrest Patient. Cardiology clinics. 2018;36(1):85-101.

54.   Modi HR, Wang Q, Gd S, Sherman D, Greenwald E, Savonenko AV, et al. Intranasal post-cardiac arrest treatment with orexin-A facilitates arousal from coma and ameliorates neuroinflammation. PLoS One. 2017;12(9):e0182707.

55.   Adrie C, Adib-Conquy M, Laurent I, Monchi M, Vinsonneau C, Fitting C, et al. Successful cardiopulmonary resuscitation after cardiac arrest as a "sepsis-like" syndrome. Circulation. 2002;106(5):562-8.

56.   Teschendorf P, Albertsmeier M, Vogel P, Padosch SA, Spohr F, Kirschfink M, et al. Neurological outcome and inflammation after cardiac arrest--effects of protein C in rats. Resuscitation. 2008;79(2):316-24.

57.   Janata A, Magnet IA, Uray T, Stezoski JP, Janesko-Feldman K, Tisherman SA, et al. Regional TNFalpha mapping in the brain reveals the striatum as a neuroinflammatory target after ventricular fibrillation cardiac arrest in rats. Resuscitation. 2014;85(5):694-701.

58.   Xiang Y, Zhao H, Wang J, Zhang L, Liu A, Chen Y. Inflammatory mechanisms involved in brain injury following cardiac arrest and cardiopulmonary resuscitation. Biomedical reports. 2016;5(1):11-7.

59.   D'Oria R, Schipani R, Leonardini A, Natalicchio A, Perrini S, Cignarelli A, et al. The Role of Oxidative Stress in Cardiac Disease: From Physiological Response to Injury Factor. Oxidative medicine and cellular longevity. 2020;2020:5732956.

60.   Kalliolias GD, Ivashkiv LB. TNF biology, pathogenic mechanisms and emerging therapeutic strategies. Nat Rev Rheumatol. 2016;12(1):49-62.

61.   Liu T, Zhang L, Joo D, Sun S-C. NF-κB signaling in inflammation. Signal Transduction And Targeted Therapy. 2017;2:17023.

62.   Parameswaran N, Patial S. Tumor necrosis factor-α signaling in macrophages. Crit Rev Eukaryot Gene Expr. 2010;20(2):87-103.

63.   Bradley JR. TNF-mediated inflammatory disease. J Pathol. 2008;214(2):149-60.

64.   Niemann JT, Garner D, Lewis RJ. Tumor necrosis factor-alpha is associated with early postresuscitation myocardial dysfunction. Crit Care Med. 2004;32(8):1753-8.

65.   Hunter CA, Jones SA. IL-6 as a keystone cytokine in health and disease. Nat Immunol. 2015;16(5):448-57.

66.   Garbers C, Heink S, Korn T, Rose-John S. Interleukin-6: designing specific therapeutics for a complex cytokine. Nat Rev Drug Discov. 2018;17(6):395-412.

67.   Schiopu A, Cotoi OS. S100A8 and S100A9: DAMPs at the crossroads between innate immunity, traditional risk factors, and cardiovascular disease. Mediators Inflamm. 2013;2013:828354.

68.   Xu K, Geczy CL. IFN-gamma and TNF regulate macrophage expression of the chemotactic S100 protein S100A8. J Immunol. 2000;164(9):4916-23.

127

69.   Wang S, Song R, Wang Z, Jing Z, Wang S, Ma J. S100A8/A9 in Inflammation. Frontiers in immunology. 2018;9(1298).

70.   Xia C, Braunstein Z, Toomey AC, Zhong J, Rao X. S100 Proteins As an Important Regulator of Macrophage Inflammation. Frontiers in immunology. 2018;8(1908).

71.   Fritz G, Botelho HM, Morozova-Roche LA, Gomes CM. Natural and amyloid self-assembly of S100 proteins: structural basis of functional diversity. The FEBS journal. 2010;277(22):4578-90.

72.   Vogl T, Ludwig S, Goebeler M, Strey A, Thorey IS, Reichelt R, et al. MRP8 and MRP14 control microtubule reorganization during transendothelial migration of phagocytes. Blood. 2004;104(13):4260-8.

73.   Rammes A, Roth J, Goebeler M, Klempt M, Hartmann M, Sorg C. Myeloid-related protein (MRP) 8 and MRP14, calcium-binding proteins of the S100 family, are secreted by activated monocytes via a novel, tubulin-dependent pathway. J Biol Chem. 1997;272(14):9496-502.

74.   Eggers K, Sikora K, Lorenz M, Taubert T, Moobed M, Baumann G, et al. RAGE-dependent regulation of calcium-binding proteins S100A8 and S100A9 in human THP-1. Exp Clin Endocrinol Diabetes. 2011;119(6):353-7.

75.   Aleshin A, Ananthakrishnan R, Li Q, Rosario R, Lu Y, Qu W, et al. RAGE modulates myocardial injury consequent to LAD infarction via impact on JNK and STAT signaling in a murine model. Am J Physiol Heart Circ Physiol. 2008;294(4):H1823-32.

76.   Bucciarelli LG, Kaneko M, Ananthakrishnan R, Harja E, Lee LK, Hwang YC, et al. Receptor for advanced-glycation end products: key modulator of myocardial ischemic injury. Circulation. 2006;113(9):1226-34.

77.   Wang S, Song R, Wang Z, Jing Z, Wang S, Ma J. S100A8/A9 in Inflammation. Frontiers in immunology. 2018;9:1298.

78.   Zhang X, Li N, Shao H, Meng Y, Wang L, Wu Q, et al. Methane limit LPS-induced NF-kappaB/MAPKs signal in macrophages and suppress immune response in mice by enhancing PI3K/AKT/GSK-3beta-mediated IL-10 expression. Scientific reports. 2016;6:29359.

79.   Ip WKE, Hoshi N, Shouval DS, Snapper S, Medzhitov R. Anti-inflammatory effect of IL-10 mediated by metabolic reprogramming of macrophages. Science (New York, NY). 2017;356(6337):513-9.

128

80.   Saraiva M, O'Garra A. The regulation of IL-10 production by immune cells. Nat Rev Immunol. 2010;10(3):170-81.

81.   Kunos G, Jarai Z, Batkai S, Goparaju SK, Ishac EJ, Liu J, et al. Endocannabinoids as cardiovascular modulators. Chemistry and physics of lipids. 2000;108(1-2):159-68.

82.   Fricke TA, Konstantinov IE. A win in protection against ischemia-reperfusion injury? The Journal of Thoracic and Cardiovascular Surgery. 2019;157(2):504-5.

83.   Pacher P, Steffens S, Hasko G, Schindler TH, Kunos G. Cardiovascular effects of marijuana and synthetic cannabinoids: the good, the bad, and the ugly. Nature reviews Cardiology. 2018;15(3):151-66.

84.   Eid BG. Cannabinoids for Treating Cardiovascular Disorders: Putting Together a Complex Puzzle. Journal of microscopy and ultrastructure. 2018;6(4):171-6.

85.   Pacher P, Batkai S, Kunos G. Cardiovascular pharmacology of cannabinoids. Handb Exp Pharmacol. 2005(168):599-625.

86.   Cabral GA, Griffin-Thomas L. Emerging role of the cannabinoid receptor CB2 in immune regulation: therapeutic prospects for neuroinflammation. Expert reviews in molecular medicine. 2009;11:e3-e.

87.   Millipore Sigma. (R)-(+)-WIN 55,212-2 mesylate salt 2020 [Available from: https://www.sigmaaldrich.com/catalog/product/sigma/w102?lang=en&region=US#:~:text=Application%20%28R%29-%20%28%2B%29-WIN%2055%2C212-2%20mesylate%20salt%20has%20been,intraperitoneal%20injection%20into%20rats%20to%20induce%20behavioural%20sensitization.

88.   Donvito G, Nass SR, Wilkerson JL, Curry ZA, Schurman LD, Kinsey SG, et al. The Endogenous Cannabinoid System: A Budding Source of Targets for Treating Inflammatory and Neuropathic Pain. Neuropsychopharmacology : official publication of the American College of Neuropsychopharmacology. 2018;43(1):52-79.

89.   Sheng WS, Hu S, Min X, Cabral GA, Lokensgard JR, Peterson PK. Synthetic cannabinoid WIN55,212-2 inhibits generation of inflammatory mediators by IL-1beta-stimulated human astrocytes. Glia. 2005;49(2):211-9.

90.   Katchan V, David P, Shoenfeld Y. Cannabinoids and autoimmune diseases: A systematic review. Autoimmunity Reviews. 2016;15(6):513-28.

91.   Cabral GA, Rogers TJ, Lichtman AH. Turning Over a New Leaf: Cannabinoid and Endocannabinoid Modulation of Immune Function. Journal of neuroimmune pharmacology : the official journal of the Society on NeuroImmune Pharmacology. 2015;10(2):193-203.

92.   Li X, Hua T, Vemuri K, Ho JH, Wu Y, Wu L, et al. Crystal Structure of the Human Cannabinoid Receptor CB2. Cell. 2019;176(3):459-67.e13.

93.   Saroz Y, Kho DT, Glass M, Graham ES, Grimsey NL. Cannabinoid Receptor 2 (CB(2)) Signals via G-alpha-s and Induces IL-6 and IL-10 Cytokine Secretion in Human Primary Leukocytes. ACS Pharmacol Transl Sci. 2019;2(6):414-28.

94.   Shahbazi F, Grandi V, Banerjee A, Trant JF. Cannabinoids and Cannabinoid Receptors: The Story so Far. iScience. 2020;23(7):101301.

95.   Huo J, Ma R, Chai X, Liang HJ, Jiang P, Zhu XL, et al. Inhibiting a spinal cord signaling pathway protects against ischemia injury in rats. J Thorac Cardiovasc Surg. 2019;157(2):494-503.e1.

96.   Choi IY, Ju C, Anthony Jalin AM, Lee DI, Prather PL, Kim WK. Activation of cannabinoid CB2 receptor-mediated AMPK/CREB pathway reduces cerebral ischemic injury. The American journal of pathology. 2013;182(3):928-39.

97.   robePuhl SL. Cannabinoid-sensitive receptors in cardiac physiology and ischaemia. Biochim Biophys Acta Mol Cell Res. 2020;1867(3):118462.

98.   Sun H-J, Lu Y, Wang H-W, Zhang H, Wang S-R, Xu W-Y, et al. Activation of Endocannabinoid Receptor 2 as a Mechanism of Propofol Pretreatment-Induced Cardioprotection against Ischemia-Reperfusion Injury in Rats. Oxidative medicine and cellular longevity. 2017;2017:2186383-.

99.   Pacher P, Mechoulam R. Is lipid signaling through cannabinoid 2 receptors part of a protective system? Progress in lipid research. 2011;50(2):193-211.

100.   Guaricci AI, Bulzis G, Pontone G, Scicchitano P, Carbonara R, Rabbat M, et al. Current interpretation of myocardial stunning. Trends in cardiovascular medicine. 2018;28(4):263-71.

101.   Sun Y, Alexander SP, Garle MJ, Gibson CL, Hewitt K, Murphy SP, et al. Cannabinoid activation of PPAR alpha; a novel neuroprotective mechanism. Br J Pharmacol. 2007;152(5):734-43.

102.   Kienzl M, Storr M, Schicho R. Cannabinoids and Opioids in the Treatment of Inflammatory Bowel Diseases. Clin Transl Gastroenterol. 2020;11(1):e00120-e.

130

103.   Schurman LD, Lu D, Kendall DA, Howlett AC, Lichtman AH. Molecular Mechanism and Cannabinoid Pharmacology. Handb Exp Pharmacol. 2020;258:323-53.

104.   Wilhelmsen K, Khakpour S, Tran A, Sheehan K, Schumacher M, Xu F, et al. The endocannabinoid/endovanilloid N-arachidonoyl dopamine (NADA) and synthetic cannabinoid WIN55,212-2 abate the inflammatory activation of human endothelial cells. J Biol Chem. 2014;289(19):13079-100.

105.   Kytikova OY, Perelman JM, Novgorodtseva TP, Denisenko YK, Kolosov VP, Antonyuk MV, et al. Peroxisome Proliferator-Activated Receptors as a Therapeutic Target in Asthma. PPAR Research. 2020;2020:8906968.

106.   Zhong C-B, Chen X, Zhou X-Y, Wang X-B. The Role of Peroxisome Proliferator-Activated Receptor γ in Mediating Cardioprotection Against Ischemia/Reperfusion Injury. J Cardiovasc Pharmacol Ther. 2018;23(1):46-56.

107.   Pacher P, Kunos G. Modulating the endocannabinoid system in human health and disease--successes and failures. The FEBS journal. 2013;280(9):1918-43.

108.   Dhopeshwarkar A, Mackie K. CB(2) Cannabinoid Receptors as a Therapeutic Target—What Does the Future Hold? Molecular Pharmacology. 2014;86(4):430-7.

109.   Chen DJ, Gao M, Gao FF, Su QX, Wu J. Brain cannabinoid receptor 2: expression, function and modulation. Acta Pharmacol Sin. 2017;38(3):312-6.

110.   Montecucco F, Di Marzo V. At the heart of the matter: the endocannabinoid system in cardiovascular function and dysfunction. Trends in pharmacological sciences. 2012;33(6):331-40.

111.   Cabral GA, Griffin-Thomas L. Emerging Role of the CB(2) Cannabinoid Receptor in Immune Regulation and Therapeutic Prospects. Expert reviews in molecular medicine. 2009;11:e3-e.

112.   Nagarkatti P, Pandey R, Rieder SA, Hegde VL, Nagarkatti M. Cannabinoids as novel anti-inflammatory drugs. Future medicinal chemistry. 2009;1(7):1333-49.

113.   Bro-Jeppesen J, Johansson PI, Kjaergaard J, Wanscher M, Ostrowski SR, Bjerre M, et al. Level of systemic inflammation and endothelial injury is associated with cardiovascular dysfunction and vasopressor support in post-cardiac arrest patients. Resuscitation. 2017;121:179-86.

131

114.   Weng Y, Sun S, Park J, Ye S, Weil MH, Tang W. Cannabinoid 1 (CB1) receptor mediates WIN55, 212-2 induced hypothermia and improved survival in a rat post-cardiac arrest model. Resuscitation. 2012;83(9):1145-51.

115.   Rawls SM, Schroeder JA, Ding Z, Rodriguez T, Zaveri N. NOP receptor antagonist, JTC-801, blocks cannabinoid-evoked hypothermia in rats. Neuropeptides. 2007;41(4):239-47.

116.   Rawls SM, Cabassa J, Geller EB, Adler MW. CB1 receptors in the preoptic anterior hypothalamus regulate WIN 55212-2 [(4,5-dihydro-2-methyl-4(4-morpholinylmethyl)-1-(1-naphthalenyl-carbonyl)-6H-pyrr olo[3,2,1ij]quinolin-6-one]-induced hypothermia. The Journal of pharmacology and experimental therapeutics. 2002;301(3):963-8.

117.   Reggio PH. Endocannabinoid Binding to the Cannabinoid Receptors: What Is Known and What Remains Unknown. Current medicinal chemistry. 2010;17(14):1468-86.

118.   Jansen EM, Haycock DA, Ward SJ, Seybold VS. Distribution of cannabinoid receptors in rat brain determined with aminoalkylindoles. Brain Res. 1992;575(1):93-102.

119.   Rodriguez de Fonseca F, Del Arco I, Bermudez-Silva FJ, Bilbao A, Cippitelli A, Navarro M. The endocannabinoid system: physiology and pharmacology. Alcohol Alcohol. 2005;40(1):2-14.

120.   McKinney DL, Cassidy MP, Collier LM, Martin BR, Wiley JL, Selley DE, et al. Dose-related differences in the regional pattern of cannabinoid receptor adaptation and in vivo tolerance development to delta9-tetrahydrocannabinol. J Pharmacol Exp Ther. 2008;324(2):664-73.

121.   Smith SR, Terminelli C, Denhardt G. Effects of cannabinoid receptor agonist and antagonist ligands on production of inflammatory cytokines and anti-inflammatory interleukin-10 in endotoxemic mice. J Pharmacol Exp Ther. 2000;293(1):136-50.

122.   Di Filippo C, Rossi F, Rossi S, D'Amico M. Cannabinoid CB2 receptor activation reduces mouse myocardial ischemia-reperfusion injury: involvement of cytokine/chemokines and PMN. J Leukoc Biol. 2004;75(3):453-9.

123.   Facchinetti F, Del Giudice E, Furegato S, Passarotto M, Leon A. Cannabinoids ablate release of TNFalpha in rat microglial cells stimulated with lypopolysaccharide. Glia. 2003;41(2):161-8.

124.   Tanaka-Esposito C, Chen Q, Lesnefsky EJ. Blockade of electron transport before ischemia protects mitochondria and decreases myocardial injury during reperfusion in aged rat hearts. Transl Res. 2012;160(3):207-16.

132

125.   Chen Q, Moghaddas S, Hoppel CL, Lesnefsky EJ. Reversible blockade of electron transport during ischemia protects mitochondria and decreases myocardial injury following reperfusion. The Journal of pharmacology and experimental therapeutics. 2006;319(3):1405-12.

126.   Moreira PI, Santos MS, Moreno A, Oliveira C. Amyloid beta-peptide promotes permeability transition pore in brain mitochondria. Biosci Rep. 2001;21(6):789-800.

127.   Lesnefsky EJ, Tandler B, Ye J, Slabe TJ, Turkaly J, Hoppel CL. Myocardial ischemia decreases oxidative phosphorylation through cytochrome oxidase in subsarcolemmal mitochondria. Am J Physiol. 1997;273(3 Pt 2):H1544-54.

128.   Thompson J, Hu Y, Lesnefsky EJ, Chen Q. Activation of mitochondrial calpain and increased cardiac injury: beyond AIF release. Am J Physiol Heart Circ Physiol. 2016;310(3):H376-84.

129.   Chen Q, Moghaddas S, Hoppel CL, Lesnefsky EJ. Ischemic defects in the electron transport chain increase the production of reactive oxygen species from isolated rat heart mitochondria. American journal of physiology Cell physiology. 2008;294(2):C460-6.

130.   Szczepanek K, Chen Q, Derecka M, Salloum FN, Zhang Q, Szelag M, et al. Mitochondrial-targeted Signal transducer and activator of transcription 3 (STAT3) protects against ischemia-induced changes in the electron transport chain and the generation of reactive oxygen species. J Biol Chem. 2011;286(34):29610-20.

131.   Paillard M, Gomez L, Augeul L, Loufouat J, Lesnefsky EJ, Ovize M. Postconditioning inhibits mPTP opening independent of oxidative phosphorylation and membrane potential. J Mol Cell Cardiol. 2009;46(6):902-9.

132.   Li Y, Chen B, Yang X, Zhang C, Jiao Y, Li P, et al. S100a8/a9 Signaling Causes Mitochondrial Dysfunction and Cardiomyocyte Death in Response to Ischemic/Reperfusion Injury. Circulation. 2019;140(9):751-64.

133.   Boukens BJD, Christoffels VM, Coronel R, Moorman AFM. Developmental Basis for Electrophysiological Heterogeneity in the Ventricular and Outflow Tract Myocardium As a Substrate for Life-Threatening Ventricular Arrhythmias. Circ Res. 2009;104(1):19-31.

134.   Biotech E. Tissue Lysate preparation - general protocol 2010 [updated 09/24/2010. Available from: https://everestbiotech.com/client_media/protocol_pdfs/Tissue_Lysate_preparation.pdf.

135.   BCA Assay and Lowry Assays [Available from: https://www.thermofisher.com/us/en/home/life-science/protein-biology/protein-assays-analysis/protein-assays/bca-protein-

assays.html?ef_id=EAIaIQobChMIkvbF9sHD7QIViaCGCh0f_gEOEAAYASAAEgIy4vD_Bw
E:G:s&s_kwcid=AL!3652!3!436793334953!p!!g!!bca%20assays&cid=bid_pca_sbu_r01_co_cp
1359_pjt0000_bid00000_0se_gaw_nt_pur_con&gclid=EAIaIQobChMIkvbF9sHD7QIViaCGCh
0f_gEOEAAYASAAEgIy4vD_BwE.

136.   2017 [Available from: https://www.ncbi.nlm.nih.gov/genbank/sequenceids/.

137.   KEGG Mapper – Convert ID 2016 [Available from:
https://www.genome.jp/kegg/tool/conv_id.html.

138.   KEGG Mapper – Search Pathway 2019 [Available from:
https://www.genome.jp/kegg/tool/map_pathway1.html.

139.   Supek F, Bošnjak M, Škunca N, Šmuc T. REVIGO summarizes and visualizes long lists
of gene ontology terms. PLoS One. 2011;6(7):e21800.

140.   Wang Y, Zhou X, Zhao D, Wang X, Gurley EC, Liu R, et al. Berberine inhibits free fatty
acid and LPS-induced inflammation via modulating ER stress response in macrophages and
hepatocytes. PloS one. 2020;15(5):e0232630-e.

141.   Zha W, Wang G, Xu W, Liu X, Wang Y, Zha BS, et al. Inhibition of P-glycoprotein by
HIV protease inhibitors increases intracellular accumulation of berberine in murine and human
macrophages. PLoS One. 2013;8(1):e54349.

142.   Jiang L-s, Pu J, Han Z-h, Hu L-h, He B. Role of activated endocannabinoid system in
regulation of cellular cholesterol metabolism in macrophages. Cardiovascular research.
2009;81(4):805-13.

143.   Zha W, Liang G, Xiao J, Studer EJ, Hylemon PB, Pandak WM, Jr., et al. Berberine
inhibits HIV protease inhibitor-induced inflammatory response by modulating ER stress
signaling pathways in murine macrophages. PLoS One. 2010;5(2):e9069.

144.   Bradley J, Yanyan W, Jankovic L, Huang I, Sharma E, Moore C, et al. 571:
ANTIINFLAMMATORY ACTIVITY OF WIN55,212-2, A NONSELECTIVE
CANNABINOID CB1/CB2 RECEPTOR AGONIST. Critical Care Medicine. 2020;48(1):266.

145.   Xiao Y, Contaifer D, Huang W, Yang J, Hu Z, Guo Q, et al. Cannabinoid Receptor
Agonist WIN55, 212-2 Adjusts Lipid Metabolism in a Rat Model of Cardiac Arrest. Therapeutic
hypothermia and temperature management. 2020: 192-203.

146.   Lee G, Goosens KA. Sampling blood from the lateral tail vein of the rat. J Vis Exp.
2015(99):e52766.

134

147.   Borutaite V, Budriunaite A, Morkuniene R, Brown GC. Release of mitochondrial cytochrome c and activation of cytosolic caspases induced by myocardial ischaemia. Biochim Biophys Acta. 2001;1537(2):101-9.

148.   Peoples JN, Saraf A, Ghazal N, Pham TT, Kwong JQ. Mitochondrial dysfunction and oxidative stress in heart disease. Exp Mol Med. 2019;51(12):1-13.

149.   Paradies G, Paradies V, Ruggiero FM, Petrosillo G. Role of Cardiolipin in Mitochondrial Function and Dynamics in Health and Disease: Molecular and Pharmacological Aspects. Cells. 2019;8(7):728.

150.   Lesnefsky EJ, Chen Q, Tandler B, Hoppel CL. Mitochondrial Dysfunction and Myocardial Ischemia-Reperfusion: Implications for Novel Therapies. Annual review of pharmacology and toxicology. 2017;57:535-65.

151.   Briston T, Roberts M, Lewis S, Powney B, M. Staddon J, Szabadkai G, et al. Mitochondrial permeability transition pore: sensitivity to opening and mechanistic dependence on substrate availability. Scientific reports. 2017;7(1):10492.

152.   Javadov S. The calcium-ROS-pH triangle and mitochondrial permeability transition: challenges to mimic cardiac ischemia-reperfusion. Frontiers in physiology. 2015;6:83-.

153.   Zorov DB, Juhaszova M, Sollott SJ. Mitochondrial reactive oxygen species (ROS) and ROS-induced ROS release. Physiological reviews. 2014;94(3):909-50.

154.   Kalogeris T, Bao Y, Korthuis RJ. Mitochondrial reactive oxygen species: a double edged sword in ischemia/reperfusion vs preconditioning. Redox Biol. 2014;2:702-14.

155.   Gustafsson AB, Gottlieb RA. Heart mitochondria: gates of life and death. Cardiovascular research. 2008;77(2):334-43.

156.   Rouslin W. Mitochondrial complexes I, II, III, IV, and V in myocardial ischemia and autolysis. Am J Physiol. 1983;244(6):H743-8.

157.   Chen Q, Hoppel CL, Lesnefsky EJ. Blockade of electron transport before cardiac ischemia with the reversible inhibitor amobarbital protects rat heart mitochondria. The Journal of pharmacology and experimental therapeutics. 2006;316(1):200-7.

158.   Lesnefsky EJ, Gudz TI, Migita CT, Ikeda-Saito M, Hassan MO, Turkaly PJ, et al. Ischemic injury to mitochondrial electron transport in the aging heart: damage to the iron-sulfur protein subunit of electron transport complex III. Arch Biochem Biophys. 2001;385(1):117-28.

135

159. Tam J, Hong A, Naranjo PM, Yin T, Shinozaki K, Lampe JW, et al. The role of decreased cardiolipin and impaired electron transport chain in brain damage due to cardiac arrest. Neurochemistry international. 2018;120:200-5.

160. Holmuhamedov EL, Oberlin A, Short K, Terzic A, Jahangir A. Cardiac subsarcolemmal and interfibrillar mitochondria display distinct responsiveness to protection by diazoxide. PloS one. 2012;7(9):e44667-e.

161. Borutaite V, Toleikis A, Brown GC. In the eye of the storm: mitochondrial damage during heart and brain ischaemia. The FEBS journal. 2013;280(20):4999-5014.

162. Yang J, Xiao Y, Quan EY, Hu Z, Guo Q, Miao C, et al. Effects of Polyethylene Glycol-20k on Postresuscitation Myocardial and Cerebral Function in a Rat Model of Cardiopulmonary Resuscitation. Crit Care Med. 2018;46(12):e1190-e5.

163. Li H, Hua T, Wang W, Wu X, Miao C, Huang W, et al. The Effects of Pharmacological Hypothermia Induced by Neurotensin Receptor Agonist ABS 201 on Outcomes of CPR. Shock. 2019;51(5):667-73.

164. Flameng W, Andres J, Ferdinande P, Mattheussen M, Van Belle H. Mitochondrial function in myocardial stunning. J Mol Cell Cardiol. 1991;23(1):1-11.

165. Birrell JA, Yakovlev G, Hirst J. Reactions of the Flavin Mononucleotide in Complex I: A Combined Mechanism Describes NADH Oxidation Coupled to the Reduction of APAD+, Ferricyanide, or Molecular Oxygen. Biochemistry. 2009;48(50):12005-13.

166. Kahl A, Stepanova A, Konrad C, Anderson C, Manfredi G, Zhou P, et al. Critical Role of Flavin and Glutathione in Complex I-Mediated Bioenergetic Failure in Brain Ischemia/Reperfusion Injury. Stroke. 2018;49(5):1223-31.

167. Turrens JF, Boveris A. Generation of superoxide anion by the NADH dehydrogenase of bovine heart mitochondria. Biochem J. 1980;191(2):421-7.

168. Stepanova A SS NZ, Konrad C, Starkov A, Manfredi G,Wittig I, Ten V, Galkin A. . Redox-Dependent Loss of Flavin by Mitochondrial Complex I in Brain Ischemia/Reperfusion Injury. Antioxidants & Redox Signaling. 2019;31(9):608-22.

169. Kilbaugh TJ, Sutton RM, Karlsson M, Hansson MJ, Naim MY, Morgan RW, et al. Persistently Altered Brain Mitochondrial Bioenergetics After Apparently Successful Resuscitation From Cardiac Arrest. Journal of the American Heart Association. 2015;4(9):e002232.

170.	Babot M, Birch A, Labarbuta P, Galkin A. Characterisation of the active/de-active transition of mitochondrial complex I. Biochimica et biophysica acta. 2014;1837(7):1083-92.

171.	Chen Q, Thompson J, Hu Y, Dean J, Lesnefsky EJ. Inhibition of the ubiquitous calpains protects complex I activity and enables improved mitophagy in the heart following ischemia-reperfusion. American journal of physiology Cell physiology. 2019;317(5):C910-c21.

172.	Weiss JN, Korge P, Honda HM, Ping P. Role of the mitochondrial permeability transition in myocardial disease. Circ Res. 2003;93(4):292-301.

173.	Murphy E, Steenbergen C. Mechanisms underlying acute protection from cardiac ischemia-reperfusion injury. Physiol Rev. 2008;88(2):581-609.

174.	Kim JS, He L, Lemasters JJ. Mitochondrial permeability transition: a common pathway to necrosis and apoptosis. Biochem Biophys Res Commun. 2003;304(3):463-70.

175.	Kristián T, Bernardi P, Siesjö BK. Acidosis Promotes the Permeability Transition in Energized Mitochondria: Implications for Reperfusion Injury. Journal of neurotrauma. 2001;18(10):1059-74.

176.	Naryzhnaya NV, Maslov LN, Oeltgen PR. Pharmacology of mitochondrial permeability transition pore inhibitors. Drug development research. 2019;80(8):1013-30.

177.	Panel M, Ghaleh B, Morin D. Mitochondria and aging: A role for the mitochondrial transition pore? Aging cell. 2018;17(4):e12793-e.

178.	Pérez MJ, Quintanilla RA. Development or disease: duality of the mitochondrial permeability transition pore. Developmental biology. 2017;426(1):1-7.

179.	Briston T, Roberts M, Lewis S, Powney B, J MS, Szabadkai G, et al. Mitochondrial permeability transition pore: sensitivity to opening and mechanistic dependence on substrate availability. Scientific reports. 2017;7(1):10492.

180.	Kihara Y, Morgan JP. Intracellular calcium and ventricular fibrillation. Studies in the aequorin-loaded isovolumic ferret heart. Circ Res. 1991;68(5):1378-89.

181.	Clements-Jewery H. Mitochondria, the calcium uniporter, and reperfusion-induced ventricular fibrillation. British journal of pharmacology. 2006;149(7):811-3.

182.	Yang L, Youngblood H, Wu C, Zhang Q. Mitochondria as a target for neuroprotection: role of methylene blue and photobiomodulation. Translational neurodegeneration. 2020;9(1):19.

183.   Tissier R, Chenoune M, Pons S, Zini R, Darbera L, Lidouren F, et al. Mild hypothermia reduces per-ischemic reactive oxygen species production and preserves mitochondrial respiratory complexes. Resuscitation. 2013;84(2):249-55.

184.   Dohi K, Miyamoto K, Fukuda K, Nakamura S, Hayashi M, Ohtaki H, et al. Status of systemic oxidative stress during therapeutic hypothermia in patients with post-cardiac arrest syndrome. Oxidative medicine and cellular longevity. 2013;2013:562429.

185.   Mohsin AA, Chen Q, Quan N, Rousselle T, Maceyka MW, Samidurai A, et al. Mitochondrial Complex I Inhibition by Metformin Limits Reperfusion Injury. The Journal of pharmacology and experimental therapeutics. 2019;369(2):282-90.

186.   Stewart S, Lesnefsky EJ, Chen Q. Reversible blockade of electron transport with amobarbital at the onset of reperfusion attenuates cardiac injury. Transl Res. 2009;153(5):224-31.

187.   Aldakkak M, Stowe DF, Lesnefsky EJ, Heisner JS, Chen Q, Camara AK. Modulation of mitochondrial bioenergetics in the isolated Guinea pig beating heart by potassium and lidocaine cardioplegia: implications for cardioprotection. Journal of cardiovascular pharmacology. 2009;54(4):298-309.

188.   Patil K, Halperin HR, Becker LB. Cardiac Arrest: Resuscitation and Reperfusion. Circulation research. 2015;116(12):2041-9.

189.   Mangino M. Fall 2017 PHIS 604 Lecture Notes. 2017.

190.   Kalogeris T, Baines CP, Krenz M, Korthuis RJ. Cell biology of ischemia/reperfusion injury. International review of cell and molecular biology. 2012;298:229-317.

191.   Morrow DA, Wang Y, Croce K, Sakuma M, Sabatine MS, Gao H, et al. Myeloid-related protein 8/14 and the risk of cardiovascular death or myocardial infarction after an acute coronary syndrome in the Pravastatin or Atorvastatin Evaluation and Infection Therapy: Thrombolysis in Myocardial Infarction (PROVE IT-TIMI 22) trial. Am Heart J. 2008;155(1):49-55.

192.   Katashima T, Naruko T, Terasaki F, Fujita M, Otsuka K, Murakami S, et al. Enhanced expression of the S100A8/A9 complex in acute myocardial infarction patients. Circ J. 2010;74(4):741-8.

193.   Altwegg LA, Neidhart M, Hersberger M, Müller S, Eberli FR, Corti R, et al. Myeloid-related protein 8/14 complex is released by monocytes and granulocytes at the site of coronary occlusion: a novel, early, and sensitive marker of acute coronary syndromes. Eur Heart J. 2007;28(8):941-8.

194.   UniProtKB - P02679 (FIBG_HUMAN) 2021 [Available from: https://www.uniprot.org/uniprot/P02679.

195.   UniProtKB - P20472 (PRVA_HUMAN) 2021 [Available from: https://www.uniprot.org/uniprot/P20472.

196.   UniProtKB - Q9H0I9 (TKTL2_HUMAN). 2021.

197.   Donato R. S100: a multigenic family of calcium-modulated proteins of the EF-hand type with intracellular and extracellular functional roles. Int J Biochem Cell Biol. 2001;33(7):637-68.

198.   Du CQ, Yang L, Han J, Yang J, Yao XY, Hu XS, et al. The elevated serum S100A8/A9 during acute myocardial infarction is not of cardiac myocyte origin. Inflammation. 2012;35(3):787-96.

199.   Zhou H, Lutterodt H, Cheng Z, Yu LL. Anti-Inflammatory and antiproliferative activities of trifolirhizin, a flavonoid from Sophora flavescens roots. Journal of agricultural and food chemistry. 2009;57(11):4580-5.

200.   Hao M-x, Jiang L-s, Fang N-y, Pu J, Hu L-h, Shen L-H, et al. The cannabinoid WIN55,212-2 protects against oxidized LDL-induced inflammatory response in murine macrophages. Journal of Lipid Research. 2010;51(8):2181-90.

201.   Liang G, Zhou H, Wang Y, Gurley EC, Feng B, Chen L, et al. Inhibition of LPS-induced production of inflammatory factors in the macrophages by mono-carbonyl analogues of curcumin. Journal of cellular and molecular medicine. 2009;13(9b):3370-9.

202.   Zhang X, Wang G, Gurley EC, Zhou H. Flavonoid apigenin inhibits lipopolysaccharide-induced inflammatory response through multiple mechanisms in macrophages. PLoS One. 2014;9(9):e107072.

203.   Sekimoto R, Fukuda S, Maeda N, Tsushima Y, Matsuda K, Mori T, et al. Visualized macrophage dynamics and significance of S100A8 in obese fat. Proceedings of the National Academy of Sciences. 2015;112(16):E2058-E66.

204.   Hong Y, Zhou Y, Wang Y, Xiao S, Liao DJ, Zhao Q. PPARγ mediates the effects of WIN55,212-2, an synthetic cannabinoid, on the proliferation and apoptosis of the BEL-7402 hepatocarcinoma cells. Mol Biol Rep. 2013;40(11):6287-93.

205.   Drabek T, Foley LM, Janata A, Stezoski J, Hitchens TK, Manole MD, et al. Global and regional differences in cerebral blood flow after asphyxial versus ventricular fibrillation cardiac arrest in rats using ASL-MRI. Resuscitation. 2014;85(7):964-71.

206.   Lamoureux L, Radhakrishnan J, Gazmuri RJ. A Rat Model of Ventricular Fibrillation and Resuscitation by Conventional Closed-chest Technique. J Vis Exp. 2015(98): 1-14.

207.   Sun S, Tang W, Song F, Chung SP, Weng Y, Yu T, et al. Pharmacologically induced hypothermia with cannabinoid receptor agonist WIN55, 212-2 after cardiopulmonary resuscitation. Crit Care Med. 2010;38(12):2282-6.

208.   McMahon SB, Koltzenburg M, Tracey I, Turk DC. Wall & Melzack's Textbook of Pain,Expert Consult - Online and Print,6: Wall & Melzack's Textbook of Pain: Elsevier/Saunders; 2013.

209.   Aizpurua-Olaizola O, Elezgarai I, Rico-Barrio I, Zarandona I, Etxebarria N, Usobiaga A. Targeting the endocannabinoid system: future therapeutic strategies. Drug Discovery Today. 2017;22(1):105-10.

Jennifer Leigh Bradley was born on December 5, 1983 in Charleston, West Virginia. She graduated from Saint Albans High School, Saint Albans, West Virginia in 2002. In May 2006, she received her Bachelor of Arts in Biology from Berea College, Berea, Kentucky. In December 2016, she received her Masters of Science in Microbiology and Immunology with a concentration in Molecular Biology and Genetics from Virginia Commonwealth University, Richmond, Virginia. In the fall of 2017, she continued her graduate career at Virginia Commonwealth University, School of Medicine, Department of Microbiology and Immunology with a concentration in Molecular Biology and Genetics.

Education

Virginia Commonwealth University   Richmond, Virginia
Doctor of Philosophy in Microbiology and Immunology   *2017-present*
Concentration: Molecular Biology and Genetics
Graduation Spring 2021 Current GPA 3.673

Virginia Commonwealth University   Richmond, Virginia
Master of Science in Microbiology and Immunology   *2016*
Concentration: Molecular Biology and Genetics

Berea College   Berea, Kentucky
Bachelors of Arts in Biology   *2006*

Research Experience

Virginia Commonwealth University, Richmond, VA   **June 2016 – Present**
Laboratory and Research Manager
Weil Institute of Emergency and Critical Care Research at VCU
Director: Dr. Wanchun Tang
Deputy Directors: Dr. Mary Ann Peberdy and Dr. Joseph Ornato
Research Focus: Cardiopulmonary Resuscitation

- Research Management: I have knowledge of the University research rules and policies and the skills necessary for program development and implementation, including developing project budgets and providing guidance in project management. I help the directors with development of plans for studies that include budget, personnel, space, supplies and equipment. I also have the ability to conduct tests, draw conclusions, and record and document findings including statistical analysis (JMP and Prism). I synthesize research data and draft research grant applications and publishable documents. I also maintain the research website and work with the directors to coordinate the Wolf Creek Conference.

- Clinical Research Experience: I possess knowledge and experience with human research subject protection (IRB/WIRB) and HIPAA, including CITI Biomedical, Export Controls, Clinical Research Coordinator, Faculty, Staff, and Students, and GCP certification. I also attended the SOM New Coordinator Training-Nuts and Bolts in August 2016.
- Bench Research: I directly supervise research staff by providing training, direction, guidance, and evaluation of operating instruments. This includes a total of 6 visiting scholars each year. I was able to perform the Weil Institute's small animal cardiac arrest model and maintained complex specialized laboratory instruments this past summer. My responsibilities include delegation of project workloads, providing guidance for project management and adhering to University regulations for inspection.
- Animal Research: I monitor the care of research animals and act as a liaison with the IACUC office to ensure that all procedures are in compliance with IACUC and University regulations. This includes IACUC submission, husbandry management, animal ordering, controlled substances, and all inspections. I am also a member of the ACUPAC for IACUC.

Virginia Commonwealth University, Richmond, VA   February 2014 – June 2016
Laboratory and Research Specialist II- Laboratory Manager
Department of Pediatrics
Principal Investigators: Dr. Bruce Rubin & Dr. Henry Rozycki
Research Focus: Aerosol therapy, Airway clearance for lung disease and Type I Alveolar Epithelial Cells

- Laboratory Management: I provided support and assistance to the Chairman of Pediatrics with the oversight of basic, translational, and clinical research efforts conducted within his laboratory, which required knowledge of the University research rules and policies. I also acted as a liaison with the Associate Administrative Director of Pediatric Research for all budgetary processes and monitoring of the Department Chair's expenditures. I developed plans and trials for studies that included budget, personnel, space, supplies, and equipment. I also generated budgets for Co-Investigators and Sub-Investigators with other departments. I managed the onboarding of postdoctoral fellows and students for the laboratory and handled travel arrangements and reimbursements for conferences for the PI and lab members. I also scheduled international teleconference calls and planned accordingly for grant and abstract deadlines. My role required excellent customer service skills; the ability to effectively communicate and to work with individuals from diverse backgrounds and to work in a team environment. I was skilled in program development and implementation and established study time lines and communicated with sponsors for study updates. My role required me to determine priorities and work in a fast-paced, deadline driven environment. I developed and maintained systematic ways for filing and archiving all study related documents and supervised and/or performed data processing

142

and data analysis. I oversaw quality assurance of data, assisted with the development of collection methods, and created and revised study materials, forms, and manuals as needed. I prepared detailed reports for sponsors of experiments, progress reports, informed consent, etc. This required me to review scientific journals, abstracts, and other related literature for information concerning experimental procedures and supplemental support. I also performed troubleshooting on laboratory equipment and acted as the primary contact for vendors, compliance officers, and sponsoring agencies. I worked with post-award monitoring grant expenditures, ordering supplies (Pcard, EVA, Banner and supply center) and organized lab meetings to maintain dialog among co-investigators regarding progress. I maintained the research website, trained students, and conducted laboratory tours for elementary to high school-aged children.

- Statistical Analysis: I supervised and/or performed data processing, coordinated data analysis, and oversaw quality assurance of data. I became proficient in JMP and Microsoft Excel.

- Clinical Research Experience: I maintained the Rubin laboratory webpage, patient registry, and airway sample bank and ensured all were in compliance with IRB/WIRB and University regulations. I consented/enrolled research subjects, conducted study visits, processed clinical samples, and maintained REDCap databases. My duties required experience in clinical trial management, international registries, patient enrollment, sputum collection and processing. I possessed knowledge and experience with human research subject protection (IRB/WIRB) and HIPAA, including CITI Biomedical, Export Controls, Clinical Research Coordinator, Faculty, Staff, and Students, and GCP certification. I also trained in CERNER, OnCore, MERCK ICH GCP, Adverse Experience Reporting, and InForm v4.6 for sponsored clinical trials.

- Bench Research: I directly supervised research staff and provided training, direction, guidance, and evaluation of operating instruments. I operated and maintained complex specialized laboratory instruments and was responsible for delegating project workloads and providing guidance in project management. I performed Sputum Biophysical Analysis (rheology, sputum hydration, and cough clearance), ELLA/ELISAs, RT-PCR, DNA/RNA isolation, tissue culture models: submerged and air-liquid interface of NHBE and Type I Alveolar Epithelial Cells, western blots, FACS, confocal, and immunohistochemistry. I possessed the ability to conduct tests, draw conclusions, record, and document findings.

- Animal Research: I monitored the care of research animals and acted as a liaison with the IACUC office to ensure that all procedures were in compliance with IACUC and University regulations. This included IACUC submission, husbandry management, animal ordering, controlled substances, and all inspections. I also taught rodent non-survival surgery techniques such as tracheostomy and isolation of lungs after bronchoalveolar lavage, mouse breeding and colony management, and sputum mucociliary transportability analysis on an upper frog palate.

143

Virginia Commonwealth University, Richmond, VA   **March 2013 – February 2014**
Laboratory and Research Specialist II- Senior Technician
Department of Pediatrics
Principal Investigators: Dr. Bruce Rubin & Dr. Henry Rozycki
Research Focus: Aerosol therapy, Airway clearance for lung disease and Type I Alveolar
Epithelial Cells

- <u>Laboratory Management:</u> I reviewed scientific journals, abstracts, and other related
  literature for information concerning experimental procedures and supplemental support.
  I performed troubleshooting on laboratory equipment and assisted the research manager
  with monitoring grant expenditures, ordering supplies (Pcard, EVA, Banner and supply
  center) and organizing lab meetings. I also helped maintain the Rubin lab website,
  trained students, and conducted laboratory tours for elementary to high school-aged
  children.
- <u>Statistical Analysis:</u> I became proficient in JMP and Microsoft Excel, which helped with
  presentation of data during weekly laboratory meetings and preparation of industry
  reports.
- <u>Clinical Research Experience:</u> I consented/enrolled research subjects, conducted study
  visits, processed clinical samples, and maintained REDCap databases.
- <u>Bench Research:</u> I performed Sputum Biophysical Analysis (rheology, sputum hydration,
  and cough clearance), ELLA/ELISAs, RT-PCR, DNA/RNA isolation, tissue culture
  models: submerged and air-liquid interface of NHBE and Type I Alveolar Epithelial
  Cells, western blots, FACS, confocal, and immunohistochemistry.
- <u>Animal Research:</u> I taught rodent non-survival surgery techniques such as tracheostomy
  and isolation of lungs after bronchoalveolar lavage, mouse breeding and colony
  management, and sputum mucociliary transportability analysis on an upper frog palate.

Virginia Commonwealth University, Richmond, VA   **February 2012 – March 2013**
Laboratory and Research Specialist I- Lab Manager
Department of Microbiology and Immunology
Principal Investigator: Dr. Daniel Conrad
Research Focus: Immunology, cancer biology, and immunotoxicology

- <u>Laboratory Management:</u> I facilitated the radiation safety inspections and all applicable
  paperwork involved including monitoring of radioisotope levels and use and disposal of
  hazardous waste. I also acted as the Chemical Hygiene Officer. I managed laboratory
  post award grant reconciliation between the Microbiology and Immunology Office,
  ordered supplies, maintained and performed troubleshooting on all laboratory equipment
  and supervised graduate students/hourly workers.
- <u>Bench Research:</u> I observed and assisted with flow cytometry, western blotting, and real
  time PCR. I also performed ELISAs and collected tissues and specimens for laboratory
  analysis.

- Animal Research: I monitored the care of research animals and acted as a liaison with the IACUC office to ensure that all procedures were in compliance with IACUC and University regulations. I also managed the mouse breeding colony of a myriad of knockout and transgenic strains. I conducted Flexivent procedures: non-survival surgery to investigate the effects of the house dust mite on various transgenic mouse models.

Virginia Commonwealth University, Richmond, VA   **July 2008 – February 2012**
Laboratory and Research Specialist I- Laboratory Specialist
Department of Periodontics
Principal Investigator: Dr. Harvey Schenkein
Research Focus: Immunopathology of periodontal disease
- Bench Research: I developed and modified protocols and carried out research independently- including tissue culture to isolate human blood cells for culture. I ensured sterility, maintained and grew cell lines, and maintained anaerobic bacterial cultures without contamination. I also performed standard immunological assays such as separation of immune cells, prepared solutions, sterilized reagents and apparatus, and disposed of radioisotope equipment.
- Animal Research: I gained extensive knowledge of breeding techniques and pregnant mouse/pup anatomy.

Office of Laboratory Services, **South Charleston, WV**   **March 2007-July 2008**
Microbiologist I
- Performed standardized bacteriologic and serologic examinations along with QC procedures for the state public health laboratory.
- Carried out primary isolation techniques of microorganisms; prepared media, solutions, and reagents.
- Operated laboratory equipment and/or scientific instrumentation for use in conducting diagnostic procedures, which included sterilization of apparatus.
- Compiled and maintained records on the characteristics of the organisms identified.
- Performed bacterial identification from patient cultures.
- Operated gen probe (transcription-based amplification system).
- Serotyped salmonella, shigella, e. coli, and meningitis isolated cultures.
- Identified parasites using microscopy techniques on patient stool samples**.**
- Processed sputum cultures to isolate tuberculosis.
- Ensured proper immunohistochemistry-monoclonal antibody staining for the detection of rabies virus.
- Examined animal cranial necropsy for the identification of rabies.

145

West Virginia State Police, South Charleston, WV   **December 2006-March 2007**
Evidence Technician I
Forensic Laboratory
- Provided for the custody of all evidence submitted by various law enforcement agencies in West Virginia.
- Maintained detailed records and integrity of evidence according to established laws, regulations, and standards.

Publications

Cheng C, Li H, Liang L, Jin T, Zhang G, **Bradley JL**, Peberdy MA, Ornato JP, Wijesinghe DS, Tang W. Effects of ω-3 PUFA and ascorbic acid combination on post-resuscitation myocardial function. Biomedicine and Pharmacotherapy. 2021;133:110970.

Xiao, Y., Contaifer, D., Huang, W., Yang, J., Hu, Z., Guo, Q., **Bradley, JL**, Peberdy, M.A., Ornato JP, Wijesinghe, D., and Tang, W. Cannabinoid Receptor Agonist WIN55m212-2 Adjusts Lipid Metabolism in a Rat Model of Cardiac Arrest. Therapeutic Hypothermia and Temperature Management. 2020; doi: 10.1089/ther.2019.0038

Ge, W., Zheng, G., Ji, X., He F., Hu, J., **Bradley, JL**, Moore C., Peberdy, MA, Ornato, JP, Mangino MJ, and Tang, W. Effects of Polyethylene Glycol-20k on Coronary Perfusion Pressure and Postresuscitation Myocardial and Cerebral Function in a Rat Model of Cardiac Arrest. J Am Heart Assoc. 2020;9:e014232

Li H, Hua T, Wang W, Wu X, Miao C, Huang W, Xiao Y, Yang J, **Bradley JL**, Peberdy MA, Ornato J, Dix TA, Beck T, Tang W. The Effects of Pharmacological Hypothermia Induced by Neurotensin Receptor Agonist ABS 201 on Outcomes of CPR. Shock. 2019 May;51(5):667-673. doi: 10.1097/SHK.0000000000001178.

Yang J, Xiao Y, Quan EY, Hu Z, Guo Q, Miao C, **Bradley J**, Peberdy MA, Ornato JP, and Tang W. Effects of Polyethylene Glycol-20k on Postresuscitation Myocardial and Cerebral Function in a Rat Model of Cardiopulmonary Resuscitation. Crit Care Med. 2018 Dec; 46(12):e1190-e1195

Wang W, Hua T, Li H, Wu X, **Bradley J**, Peberdy MA, Ornato JP, and Tang W. Decreased cyclic adenosine monophosphate level and decreased downregulation of β1-adrenoceptor expression in therapeutic hypothermia resuscitated myocardium are associated with improved post-resuscitation myocardial function. J Am Heart Assoc. 2018 Mar 20;7(6):e006573

Lu X, Fries M, Ravindra N, **Bradley J**, Peberdy MA, Ornato JP, Zhu CQ and Tang W. The Individual Role of Sarcolemmal and Mitochondrial KATP Channels Opening During Cardiopulmonary Resuscitation in a Porcine Model Treated with Levosimendan. Heart Circ 2017; 1:017.

Sun P, Wang J, Zhao S, Yang Z, Tang Z, Ravindra N, **Bradley J**, Ornato JP, Peberdy MA, Tang W. Improved Outcomes of Cardiopulmonary Resuscitation in Rats Treated with Vagus Nerve Stimulation and its Potential Mechanism. Shock 2017 Aug 9. [epub ahead of print]

Miao C, Yang Z, Wen C, Yu T, Ravindra N, **Bradley J**, Peberdy MA, Ornato JP, and Tang W. Nitroglycerin Improves Microcirculation During and After Cardiopulmonary Resuscitation in a Porcine Model of Cardiac Arrest. Ann Cardiol Cardiovasc Dis. 2017.2(2):1011

Hua T, Wu X, Wang W, Li H, **Bradley J**, Peberdy MA, Ornato JP, Tang W. Micro-and Macro Circulatory Changes During Sepsis and Septic Shock in a Rat Model. Shock 2017 Jul 20. [epub ahead of print]

Rozycki HJ, **Bradley J**, KaramS. sRAGE is Elevated in the Lungs of Premature Infants Receiving Mechanical Ventilation. Am J Perinatol. March 2017

Wang J, Wu X, Yan Z, Zhao S, QianJ, Yin L, Yu H, Gong P, Cahoon J, **Bradley J**, and Tang W. Protective Effects of Progesterone on Neurological outcomes in a Rat Model of Cardiac Arrest. Arch Emerg Med Crit Care December 2016 1 (3):1016

Schenkein H.A, **Bradley JL** and Purkall D.B. Anticardiolipin in Porphyromonas gingivalis Antisera Causes Fetal Loss in Mice. Journal of Dental Research July 2013 92: 814-818

Conferences
Society of Critical Care Medicine Annual Congress 2020
Wolf Creek Conference 2017, 2019, 2021
American Thoracic Society International Conference 2013, 2014, 2015, and 2016
American Association for Respiratory Care Conference 2013

Grants and Scholarships

2020-VCU Staff Senate Integrity Award $500
2020-Graduate School Travel Grant $300
2020-MPG CPC Travel Award $1,500
2019-VCU Graduate School Hibbs/Waller Scholarship $1,000.
2019-Jennifer Bradley, Mentor: Dr. Wanchun Tang, Measurement of systemic inflammatory response after administration of WIN55, 212-2. Zoll Foundation. $30,000.
2018-MBG CPC Travel Award $180
2018 Fall LabRoots Scholarship $2,000
2017-2017-B Love of Learning Award from Phi Kappa Phi $500
2015-Jennifer Bradley, Mentor: Dr. Bruce Rubin, Mature adipocytes from obese individuals release IL-13, which increases inflammation and induces a goblet cell phenotype in normal human bronchial epithelial (NHBE) cells at air-liquid interface (ALI). Children's Hospital Foundation Research Fund. $5,000.

Additional Training & Recognition

VCU Training
- Grace E Harris Leadership Institute 2020 class of the HIGHER Ground Women's Leadership Development Program
- Wright Center Grant Writing Course
- Multiple Manager Training courses from Human Resources

- Multiple Corporate Education Training courses (Leading Effective Teams, Maximizing Productivity and Managing and Leading Change)
- SOM New Clinical Research Coordinator Boot Camp
- Records Management 101

Collaborative Institutional Training Initiative Course:

- Faculty, Staff, and Students
- Biomedical Responsible Conduct of Research
- Good Clinical Practice
- CITI Export Controls
- Clinical Research Coordinator (CRC)

American Association for Laboratory Animal Science:

- Aseptic Technique for Rodent Survival Surgery
- Introduction to Amphibians
- Introduction to Ferrets
- Introduction to Mice
- Introduction to Rabbits
- Introduction to Rats
- Introduction to Swine
- Mouse Breeding Colony Management
- Post-procedure Care of Mice and Rats in Research Minimizing Pain and Distress
- VCU Animal Research Facility Orientation Course
- Working with the VCU IACUC for staff and students

Other
- Write Now Summer Session National Center for Faculty Development & Diversity 2020
- Grantsmanship for Research Professionals 2020
- RAMS Forum 2018, 2019, 2020
- NCURA Sponsored Project Administration Workshop April and September 2019
- Building Inclusive Communities June 2018
- Bioinformatics 102 June 2018
- Writing and Designing NIH Proposals Webinar February 2017
- SBIR Webinar January 2017
- NIH Grantsmanship Workshop January 2017
- VCU Professional Development Certificate Program September 2016 to present
- Virginia Grants Summit September 2016

- Dangerous Goods Shipping

Student spotlight for VCU Graduate School website Fall 2019:
https://graduate.vcu.edu/welcome/graduate-school-news/student-spotlights/student-spotlight---jennifer-bradley/

Member, Society of Critical Care Medicine 2018-present
Member, American Association for the Advancement of Science 2018
Member, The Honor Society of Phi Kappa Phi November 2014-present

Mentorship

- Summer 2020. Mentor Karen Lo. VCU Medical Student Volunteer.
- Summer 2020. Mentor Matthew Olocco. VCU Medical Student Volunteer.
- Summer 2020. Mentor Hunter Hewlett. VCU Medical Student Volunteer.
- 2019-2020. Mentor Chengli Su, MD, PhD. Weil Institute of Emergency and Critical Care Research Visiting Fellow.
- 2019-2020. Mentor Yan Xiao, MD, PhD. Weil Institute of Emergency and Critical Care Research Post-doctoral Scholar.
- 2019-2020. Mentor Guozhen Zhang, MD. Weil Institute of Emergency and Critical Care Research Visiting Fellow.
- 2019-2020. Mentor Jin Tao, MD. Weil Institute of Emergency and Critical Care Research Visiting Fellow.
- 2019-2020. Mentor Cheng Cheng, MD, PhD. Weil Institute of Emergency and Critical Care Research Visiting Fellow.
- 2019-2020. Mentor Hui Li, MD. Weil Institute of Emergency and Critical Care Research Visiting Fellow.
- 2019-2020. Mentor Lian Liang, MD, PhD. Weil Institute of Emergency and Critical Care Research Visiting Fellow.
- Summer 2019. Mentor Iris Huang. High School Student Volunteer.
- Summer 2019. Mentor Liuzhi Zhang. VCU Medical Student Volunteer.
- Summer 2019. Mentor Lazar Jankovic. VCU Medical Student Volunteer.
- Summer 2019. Mentor Helen Mai. VCU Undergraduate Student Volunteer.
- Summer 2019. Mentor Esha Sharma. Godwin High School Student Volunteer Intern.
- Summer 2019. Mentor Devi Veeramgari. Godwin High School Student Volunteer Intern.
- Summer 2019. Mentor Aaron Yuan. Godwin High School Student Volunteer.
- 2018-2019. Mentor Fenglian He, MD, PhD. Weil Institute of Emergency and Critical Care Research Visiting Fellow.
- 2018-2019. Mentor Juntao Hu, MD. Weil Institute of Emergency and Critical Care Research Visiting Fellow.

149

- 2018-2019. Mentor Xianfei Ji, MD, PhD. Weil Institute of Emergency and Critical Care Research Visiting Fellow.
- 2018-2019. Mentor Weiwei Ge, MD. Weil Institute of Emergency and Critical Care Research Visiting Fellow.
- 2018-2019. Mentor Guanghui Zheng, MD. Weil Institute of Emergency and Critical Care Research Visiting Fellow.
- Summer 2018. Clairice Dailey. Weil Institute of Emergency and Critical Care Research Volunteer.
- 2017-2018. Mentor Jing Xu, MD, PhD. Weil Institute of Emergency and Critical Care Research Visiting Fellow.
- 2017-2018 Mentor Chang-Sheng Wang, MD, PhD. Weil Institute of Emergency and Critical Care Research Visiting Fellow.
- 2017-2018. Mentor Qinyue Guo, MD. Weil Institute of Emergency and Critical Care Research Visiting Fellow.
- 2017-2018. Mentor Zhangle Hu, MD. Weil Institute of Emergency and Critical Care Research Visiting Fellow.
- Summer 2017. Nikki Duggal. Weil Institute of Emergency and Critical Care Research Volunteer.
- 2016-2017. Mentor Changqing Miao, MD. Weil Institute of Emergency and Critical Care Research Visiting Fellow.
- 2016-2017. Mentor Jin Yang, MD, PhD. Weil Institute of Emergency and Critical Care Research Visiting Fellow.
- 2016-2017. Mentor Tianfeng Hua, MD. Weil Institute of Emergency and Critical Care Research Visiting Fellow.
- 2016-2017. Mentor Weiping Huang, MD. Weil Institute of Emergency and Critical Care Research Visiting Fellow.
- 2016-2017. Mentor Yan Xiao, MD, PhD. Weil Institute of Emergency and Critical Care Research Visiting Fellow.
- 2014-2017. Navami Ravindra BS Biomedical Engineering. Weil Institute of Emergency and Critical Care Research and Department of Pediatrics Volunteer.
- 2014-2016. Mentor Tomohiro Akaba, MD, PhD. Department of Pediatrics Postdoctoral Scholar.
- 2014-2016. Mentor Kosaku Komiya, MD, PhD. Department of Pediatrics Postdoctoral Scholar.
- 2014-2016. Mentor Jonathan Ma, MD. Department of Pediatrics Pediatric Resident.
- 2014-2016. Mentor Ashleigh McCormick. Department Biomedical Engineering, Undergraduate Researcher.
- 2013-2015. Mentor Isao Suzaki, MD, PhD. Department of Pediatrics Postdoctoral Scholar.

- 2013-2014. Mentor Shuichi Kawano MD, PhD. Department of Pediatrics Postdoctoral Scholar.

Service
Graduate Student Rep, SOM Teaching Awards Selection Committee **Summer 2020 and 2019**
Volunteer Judge, Virginia Junior Sciences and Humanities Symposium (JSHS)   **March 2020**
Volunteer, Medical Reserve Corps   **September 2008-Present**
Volunteer, Emergency Department at MCV   **Spring and Summer 2013**
Mentor, Tutor of Education and Living Skills   **August 2002-May 2006**
Volunteer, Health Clinic in Ayacucho, Peru   **Summer 2004**

151